

Laboratory-Scale Flame-Mode  
Hazardous Waste Thermal  
Destruction Research

Energy and Environmental Research Corp.  
Irvine, CA

Prepared for

Industrial Environmental Research Lab.  
Cincinnati, OH

Apr 84

U.S. DEPARTMENT OF COMMERCE  
National Technical Information Service

**NTIS**<sup>®</sup>

EPA-600/2-84-086

April 1984

LABORATORY-SCALE FLAME-MODE HAZARDOUS WASTE

THERMAL DESTRUCTION RESEARCH

by

J. C. Kramlich  
M. P. Heap  
J. H. Pohl  
E. Poncelet  
G. S. Samuelson  
W. R. Seeker

Energy and Environmental Research Corporation  
18 Mason  
Irvine, CA 92714-4190

EPA Prime Contract No. 68-03-3113

Subcontract Task 24-1

EPA Project Officer: C. C. Lee

INDUSTRIAL ENVIRONMENTAL RESEARCH LABORATORY  
OFFICE OF RESEARCH AND DEVELOPMENT  
U.S. ENVIRONMENTAL PROTECTION AGENCY  
CINCINNATI, OH 45268

| TECHNICAL REPORT DATA<br>(Please read instructions on the reverse before completing)  |  |  |
|---|--|--|
| 1. REPORT NO.<br>EPA-600/2-84-086   | 2.   | 3. RECIPIENT'S ACCESSION NO.<br>PB8 4 184902             |
| 4. TITLE AND SUBTITLE<br>Laboratory-Scale Flame-Mode Hazardous Waste Thermal Destruction Research   |  | 5. REPORT DATE<br>April 1984                             |
|   |  | 6. PERFORMING ORGANIZATION CODE                          |
| 7. AUTHOR(S)<br>J.C. Kramlich, et.al.   |  | 8. PERFORMING ORGANIZATION REPORT NO.                    |
| 9. PERFORMING ORGANIZATION NAME AND ADDRESS<br>J.C. Kramlich, et.al.<br>EERC<br>18 Mason St.<br>Irvine, CA 92714  |  | 10. PROGRAM ELEMENT NO.<br>CBRD1A                        |
|   |  | 11. CONTRACT/GRANT NO.<br>Contract 68-03-3113            |
| 12. SPONSORING AGENCY NAME AND ADDRESS<br>USEPA<br>Industrial Waste Combustion Group<br>Cincinnati, Ohio 45268  |  | 13. TYPE OF REPORT AND PERIOD COVERED<br>Research report |
|   |  | 14. SPONSORING AGENCY CODE<br>EPA/600/12                 |
| 15. SUPPLEMENTARY NOTES   |  |  |
| <p>16. SUMMARY</p> <p>This research is to investigate the flame mode incinerability of hazardous waste compounds. It was also designed to provide a comparison between flame and non-flame destruction of compounds and act as a guideline for future work on the development of an acceptable incinerability ranking methodology.</p> <p>Two flame reactors were used in order to simulate a wide variety of failure conditions for liquid injection incinerators. The first reactor was called a microspray and consisted of droplets injected into a hydrocarbon flat-flame. The second reactor was a turbulent flame reactor which allowed the investigation of failure conditions in spray flames such as mixing, atomization and quench phenomenon. The compounds investigated included: chloroform, 1,2-dichloroethane, benzene, chlorobenzene, and acrylonitrile.</p> <p>The results indicated that flames without long residence time postflame zones were capable of destroying all the compounds investigated to high efficiencies (&gt;99.99%) when operated correctly. However, under failure conditions such as poor atomization, low excess air, low flame temperature, and quenching, the destruction efficiencies were typically 90-99.9%.</p> |  |  |
| 17. KEY WORDS AND DOCUMENT ANALYSIS   |  |  |
| a. DESCRIPTORS  | b. IDENTIFIERS/OPEN ENDED TERMS                  | c. COSATI Field/Group                                    |
| Hazardous compound incinerability<br>mode of combustion failures<br>Flame-mode destruction<br>non-flame thermal decomposition   |  | Hazardous waste disposal.                                |
| 18. DISTRIBUTION STATEMENT<br>Release to Public   | 19. SECURITY CLASS (This Report)<br>Unclassified | 21. NO. OF PAGES<br>160                                  |
|   | 20. SECURITY CLASS (This page)<br>Unclassified   | 22. PRICE  |

#### NOTICE

This document has been reviewed in accordance with U.S. Environmental Protection Agency policy and approved for publication. Mention of trade names or commercial products does not constitute endorsement or recommendation for use.

## FOREWORD

When energy and material resources are extracted, processed, converted, and used, the related pollution impact on our environment and even our health often requires that new and increasingly more efficient pollution control methods be used. The Industrial Environmental Research Laboratory - Cincinnati (IERL-Ci) assists in developing and demonstrating new and improved methodologies that will meet these needs both efficiently and economically.

This report presents the research results from laboratory-scale flame mode combustion of organic compounds. The research objective was to compare compound incinerability ranking methods and to evaluate differences between non-flame and flame combustion of organic compounds. The results indicated that flames without long residence time post-flame zones were capable of destroying all the compounds investigated to high efficiency (greater than 99.999%) when operated correctly. However, under failure conditions such as poor atomization, low excess air, low flame temperature and quenching, the destruction efficiency was only 90-99.9 percent. The data also indicated that exhaust measurements of carbon monoxide and total hydrocarbons could be used as an indication of operation in failure conditions.

The result of this study will be useful to regulatory programs responsible for implementation of Resource Conservation and Recovery Act (1976), to owners and operators of hazardous waste facilities, and to firms anticipating entry into the manufacture of incinerator equipment.

## ABSTRACT

This constitutes the final report of a program to investigate the flame mode incinerability of hazardous waste compounds. The objective of the program was to generate fundamental flame mode data on a series of compounds in order to make a preliminary comparison of proposed incinerability rankings. It was also designed to provide a comparison between flame and non-flame destruction of compounds and act as a guideline for future work on the development of an acceptable incinerability ranking methodology.

Two flame reactors were used in order to simulate a wide variety of failure conditions for liquid injection incinerators. The approach was to burn a mixture of selected hazardous waste compounds in reactors operated under conditions where incomplete destruction was allowed to occur. The first reactor was called a microspray and consisted of droplets injected into a hydrocarbon flat-flame. The failure conditions explored with this reactor were only thermal, since the flame was premixed. The second reactor was a turbulent flame reactor which allowed the investigation of other failure conditions in spray flames such as mixing, atomization and quench phenomenon. The compounds investigated included hazardous compounds that have a wide range of incinerability rankings: chloroform, 1,2-dichloroethane, benzene, chlorobenzene, and acrylonitrile.

The results indicated that flames without long residence time post-flame zones were capable of destroying all the compounds investigated to high efficiencies (>99.999%) when operated correctly. However, under failure conditions such as poor atomization, low excess air, low flame temperature, and quenching, the destruction efficiencies were typically 90-99.9%. The data indicated that exhaust measurements of CO and total hydrocarbons could be used as an indication of operation in a failure condition. The destruction efficiency was dependent on compound type and failure condition, although the differences between compounds was small. When compared to the proposed ranking procedure no one ranking procedure was able to predict the compound ranking for every failure condition. However, some procedures were able to predict the ranking for specific failure conditions. For example, the non-flame temperature requirements correctly identified the compound order for premixed conditions when the flame temperature was insufficient to burn the compounds. These data indicate that incinerability should be tied to likely failure conditions for the incinerator under consideration and that more data is required for a wide range of failure conditions and compounds.

## ACKNOWLEDGEMENTS

This work was performed under subcontract (Task 24-1) from JRB Associates. The U.S. Environmental Protection Agency prime contract number was 68-02-3113. C. C. Lee was the EPA Technical Project Officer and V. S. Engleman was the JRB Associates Task Manager. Other members of the EPA Technical Advisory Committee who assisted in program guidance were: A. F. Sarofim, Massachusetts Institute of Technology; F. W. Marble, California Institute of Technology; R. M. Fristrom, The Johns Hopkins University; B. Dellinger, University of Dayton Research Institute; W. Tsang, National Bureau of Standards; R. A. Carnes, Industrial Environmental Research Laboratory - Cincinnati EPA; and E. P. Crumpler, Office of Solid Waste, EPA.

We wish to acknowledge the contributions of R. K. Nihart and H. D. Crum, who played important roles in the development of the analytical approach and experimental construction and operation.

## TABLE OF CONTENTS

| <u>Section</u>   | <u>Page</u> |
|--|-------------|
| 1.0 EXECUTIVE SUMMARY . . . . .                              | 1-1         |
| 1.1 Introduction . . . . .                                   | 1-1         |
| 1.2 Experimental Approach . . . . .                          | 1-5         |
| 1.3 Microspray Results . . . . .                             | 1-7         |
| 1.4 Turbulent Flame Reactor Results . . . . .                | 1-10        |
| 1.5 Discussion . . . . .                                     | 1-18        |
| 1.6 Conclusions . . . . .                                    | 1-23        |
| 1.7 Executive Summary References . . . . .                   | 1-25        |
| 2.0 INTRODUCTION . . . . .                                   | 2-1         |
| 3.0 EXPERIMENTAL EQUIPMENT . . . . .                         | 3-1         |
| 3.1 Microspray Reactor . . . . .                             | 3-2         |
| 3.2 Turbulent Flame Reactor . . . . .                        | 3-9         |
| 3.3 Laboratory Facility . . . . .                            | 3-14        |
| 3.4 Analytical Systems . . . . .                             | 3-14        |
| 3.1.1 Measurement of Destruction Efficiency (DE) . . . . .   | 3-15        |
| 3.1.2 Other Measurements . . . . .                           | 3-16        |
| 4.0 RESULTS AND DISCUSSION . . . . .                         | 4-1         |
| 4.1 Microspray--Droplet Decomposition in Flames . . . . .    | 4-1         |
| 4.1.1 Droplets of Mixtures in an Oxygen-Rich Flame . . . . . | 4-2         |
| 4.1.2 Pure Compounds in an Oxygen-Rich Flame . . . . .       | 4-5         |
| 4.1.3 Compound Mixtures with Low Oxygen . . . . .            | 4-8         |
| 4.1.4 Summary of Microspray Rankings and Data . . . . .      | 4-13        |
| 4.2 Turbulent Flame Reactor Results . . . . .                | 4-16        |
| 4.2.1 Influence of Stoichiometry and Load . . . . .          | 4-19        |
| 4.2.2 Influence of Theoretical Air . . . . .                 | 4-25        |
| 4.2.3 Influence of Air Velocity . . . . .                    | 4-28        |
| 4.2.4 Influence of Compound Concentration . . . . .          | 4-30        |



## TABLE OF CONTENTS (Concluded)

| <u>Section</u>  | <u>Page</u> |
|---|-------------|
| 4.2.5 Effect of Quench Coil . . . . .                           | 4-33        |
| 4.2.6 Effect of Nozzle Performance . . . . .                    | 4-36        |
| 4.2.7 Effect of Auxiliary Fuel . . . . .                        | 4-38        |
| 4.2.8 Turbulent Flow Reactor Data Summary . . . . .             | 4-41        |
| 5.0 SUMMARY OF RANKINGS, CONCLUSIONS, AND RECOMMENDATIONS . . . | 5-1         |
| 5.1 Summary and Discussion of Rankings . . . . .                | 5-1         |
| 5.2 Conclusions . . . . .                                       | 5-6         |
| 5.3 Recommendations . . . . .                                   | 5-7         |
| 6.0 REFERENCES . . . . .  | 6-1         |
| APPENDIX A--EXPERIMENTAL FLOW CALIBRATIONS . . . . .            | A-1         |
| APPENDIX B--ANALYTICAL TECHNIQUE FOR TEST COMPOUNDS . . . . .   | B-1         |
| APPENDIX C--THERMAL DECOMPOSITION MODEL . . . . .               | C-1         |
| APPENDIX D--RAW DATA . . . . .                                  | D-1         |

## LIST OF FIGURES

| <u>Figure</u>   | <u>Page</u> |
|---|-------------|
| 1-1   | 1-8         |
| Fraction of test compound remaining in exhaust when 38 $\mu$ m droplets of mixtures of compounds were injected into lean (10 percent excess oxygen) H <sub>2</sub> /air flames as function of flame temperature . . . . .   |             |
| 1-2   | 1-11        |
| Fraction of test compound remaining in exhaust when 38 $\mu$ m droplets of mixtures of compounds were injected into rich (stoichiometric ratio = 0.83) H <sub>2</sub> /air flame as function of flame temperature. Incinerability order at 1050 K is chlorobenzene, benzene, acrylonitrile, and chloroform . . . .                      |             |
| 1-3   | 1-13        |
| Exhaust CO and total hydrocarbons and fraction of test compound remaining in exhaust as a function of theoretical air (constant air velocity, variable load, equal molar mixture of chloroform, benzene, chlorobenzene, and acrylonitrile added 3 percent by weight to heptane . . .  |             |
| 1-4   | 1-14        |
| Impact of theoretical air on CO and DRE from turbulent flame reactor. Incinerability order at 150 percent theoretical air is chloroform, acrylonitrile, benzene, and chlorobenzene (constant load = 48 kW; variable air flow rate and burner velocity; equal molar mixture of compounds added 3 percent by weight to heptane) . . . . . |             |
| 1-5   | 1-16        |
| Impact of theoretical air and load on fraction of test compounds remaining in exhaust of turbulent flame reactor (constant air velocity, variable load 42-24 kW; equal molar mixture of compounds added 3 percent by weight to heptane) . . . . .   |             |
| 1-6   | 1-7         |
| Impact of atomization quality on CO and fraction of test compounds remaining in exhaust of turbulent flame reactor (constant air velocity, variable load: 42-16 kW; equal molar mixture of compounds added 3 percent by weight to heptane . . . . .   |             |
| 1-7   | 1-19        |
| Impact of cooling coil placed in flame on CO and fraction of test compound remaining in exhaust of turbulent flame reactor. (Constant air velocity; load = 32 kW equal molar mixture of compounds added 3 percent by weight to heptane) . . . . .   |             |
| 1-8   | 1-22        |
| Comparison of proposed ranking techniques and concentration measured in the experiments under flame failure conditions normalized so most predominant compound shows full scale . . . . .   |             |

## LIST OF FIGURES (Continued)

| <u>Figure</u>  | <u>Page</u> |
|--|-------------|
| 3-1 Microspray reactor . . . . .   | 3-3         |
| 3-2 Details of microspray reactor . . . . .  | 3-5         |
| 3-3 Schematic diagram of the droplet generator . . . . .   | 3-6         |
| 3-4 Gas temperature measurements in microspray reactor . . . . .   | 3-8         |
| 3-5 Turbulent flame reactor . . . . .  | 3-10        |
| 3-6 Turbulent flow reactor burner detail . . . . .   | 3-12        |
| 4-1 Fraction of test compound remaining in exhaust when 38 $\mu$ m droplets of mixtures of compounds were injected into lean (10 percent postflame oxygen) H <sub>2</sub> /air flames as function of flame temperature . . . . .                                       | 4-3         |
| 4-2 Fraction of test compound remaining in exhaust when 38 $\mu$ m droplets of pure compounds were injected into lean (10 percent postflame oxygen) H <sub>2</sub> /air flames as function of flame temperature . . . . .  | 4-6         |
| 4-3 Fraction of test compound remaining in exhaust when 38 $\mu$ m droplets of mixtures of compounds were injected into rich stoichiometric ratio = 0.83) H <sub>2</sub> /air flames as function of flame temperature . . . . .  | 4-9         |
| 4-4 Model results: fraction of test compound remaining in exhaust when 38 $\mu$ m droplets were exposed to the temperature profiles shown in Figure 3-4a and allowed to react by nonflame thermal decomposition kinetics . . . . .                                     | 4-11        |
| 4-5 Model results: effect of oxygen concentration on thermal decomposition for benzene at isothermal conditions . . . . .  | 4-14        |
| 4-6 Comparison of calculated reactor performance assuming 1) droplet evaporation controls DE, 2) droplet ignition controls DE, and 3) thermal decomposition kinetics control DE; with microspray oxidation mixture data and microspray low oxygen data . . . . .       | 4-15        |
| 4-7 Microspray incinerability rankings . . . . .   | 4-17        |
| 4-8 Exhaust CO, total hydrocarbons, and relative heptane as a function of theoretical air (constant air velocity, variable load: 42-24 kW, equal molar mixture of chloroform, benzene, chlorobenzene, and acrylonitrile added 3 percent by weight to heptane . . . . . | 4-22        |

## LIST OF FIGURES (Continued)

| <u>Figure</u>   | <u>Page</u> |
|---|-------------|
| 4-9      Impact of theoretical air and load on fraction of test compounds remaining in exhaust of turbulent flame reactor (constant air velocity, variable load: 42-24 kW; equal molar mixture of compounds added 3 percent by weight to heptane) . . . . .   | 4-24        |
| 4-10     Impact of theoretical air on CO and DRE from turbulent flame reactor (constant load: 48 kW; variable air flow rate and burner velocity; equal molar mixture of compounds added 3 percent by weight to heptane . . . . .  | 4-27        |
| 4-11     Impact of burner air velocity on fraction of test compounds remaining in exhaust of turbulent flow reactor (156 percent theoretical air; 0.72 gm/sec fuel flow; 3-weight-percent equimolar mixture of test compounds in heptane; 32.3 kW load) . . . . .   | 4-29        |
| 4-12     Impact of compound concentration on fraction of test compound remaining in exhaust of turbulent flow reactor (constant air velocity, variable load: 39-26 kW; variable weight concentration of an equimolar mixture of test compounds in heptane) . . . . .  | 4-31/32     |
| 4-13     Influence of quench-coil on CO in exhaust of turbulent flame reactor as a function of load and theoretical air (constant air velocity, variable load: 42-16 kW; equimolar mixture of compounds added 3 percent by weight to heptane) . . . . .   | 4-34        |
| 4-14     Influence of quench-coil on fraction of test compound remaining in exhaust of turbulent flame reactor as a function of load and theoretical air (constant air velocity, variable load: 42-24 kW; equimolar mixture of compounds added 3 percent by weight to heptane . . . . .   | 4-35        |
| 4-15     Influence of atomization quality on CO in exhaust of turbulent flame reactor as a function of load and theoretical air (constant air velocity, variable load: 42-16 kW; equimolar mixture of compounds added 3 percent by weight to heptane). Also, atomization pressure as a function of theoretical air for each of the nozzles (parameter is nozzle capacity in gal/hr) . . . . . | 4-37        |
| 4-16     Impact of atomizer performance on fraction of test compound remaining in exhaust as a function of percent theoretical air (constant air velocity, variable load: 42-16 kW; equimolar mixture of compounds added 3 percent by weight to heptane) . . . . .  | 4-39        |

## LIST OF FIGURES (Concluded)

| <u>Figure</u> |   | <u>Page</u> |
|---------------|---|-------------|
| 4-17          | Impact of auxiliary fuel type on fraction of test compound remaining in exhaust as a function of percent theoretical air (constant air velocity, variable load: 42-24 kW; equimolar mixture of compounds added 3 percent by weight to No. 2 fuel oil) . . . . . | 4-40        |
| 5-1           | Comparison of proposed ranking techniques and relative compound decomposition of compounds under flame failure conditions . . . . .   | 5-4         |

## LIST OF TABLES

| <u>Table</u> |   | <u>Page</u> |
|--------------|---|-------------|
| 2-1          | Test Compounds and Properties . . . . .                       | 2-6         |
| 3-1          | Normal Operating Conditions for Turbulent Flame Reactor . . . | 3-13        |
| 3-2          | Experimental Measurements . . . . .                           | 3-17        |
| 3-3          | Chlorine Mass Closure . . . . .                               | 3-18        |
| 4-1          | Turbulent Flame Experimental Conditions . . . . .             | 4-20        |
| 4-2          | Atomization Parameters . . . . .                              | 4-21        |

## 1.0 EXECUTIVE SUMMARY

### 1.1 Introduction

Permitting procedures for hazardous waste incinerators are defined by the Resource Conservation and Recovery Act (RCRA). A permit to operate is issued after a trial burn has been executed or other appropriate test data obtained which demonstrate that the incinerator satisfactorily converts hazardous waste into non-hazardous compounds when operated under specified conditions. Satisfactory conversion is defined in terms of destruction and removal efficiency (DRE). However, since most hazardous waste streams contain many compounds, a trial burn which involves the measurement of all of them would be prohibitively expensive. Consequently, the trial burn involves the measurement of a subset of compounds (the principal organic hazardous constituents--POHCs) which are present in the input stream. If the DRE of these POHCs is 99.99 percent or greater, and certain other conditions met (e.g., chlorine and particulate matter removal and emissions standards) then a permit to operate is granted. Thus, the burden of responsibility rests with the permit writer who must select the subset of compounds (POHCs) based upon concentration and incinerability. This constitutes the final report of a project which was carried out to examine methods of ranking incinerability, and to compare flame vs non-flame waste destruction.

Several procedures have been proposed to rank incinerability (Cudahy et al., 1981) namely:

- The heat of combustion.
- The autoignition temperature (AIT).
- A computational approach based upon AIT, compound structure, and other compound-dependent parameters (Lee et al., 1979, 1982).
- The temperature necessary for a given destruction level within a given time under dilute premixed conditions ( $T_{99.99}$ ) (Dellinger et al., 1982; Duvall and Rubey, 1976, 1977; Lee et al., 1979, 1982).
- Susceptibility of the compound bond structure to attack by flame radicals (Tsang and Shaub, 1981).

These procedures have their merits but fail to take into account all the conditions which may exist in actual incinerators. The heat of combustion for example, of a particular compound may be insignificant if it is present in small quantities and is mixed with an auxiliary fuel. In addition, some of these procedures do not consider processes and reactions that occur in flames. The times and temperatures which exist under non-flame experimental conditions may be inappropriate for large-scale diffusion flames.

The concept of incinerability is used to describe the relative degree of difficulty of incineration of the various hazardous organic constituents present in a given waste stream. If during the trial burner it is demonstrated that these compounds which are most difficult to destroy have a DRE greater than 99.99 percent, then it is assumed that compounds ranked more incinerable under the accepted hierarchy will be destroyed at the same or greater DRE than the difficult compounds. Thus, there is a need for some ranking methodology that will aid the permit writer in his selection of difficult compounds. If the ranking methodology is in error, or is not applicable to a particular system, then a condition could exist wherein a POHC was destroyed satisfactorily, but other hazardous compounds in the waste stream were not destroyed sufficiently. Under these circumstances, a trial burn designed to measure only the POHC may have incorrectly demonstrated the satisfactory operation of the incinerator.

Because of the nature of flames, waste compounds which experience a flame environment are rapidly and completely destroyed. This can be demonstrated by considering non-flame thermal decomposition data obtained under dilute pre-mixed conditions (Dellinger et al., 1982; Duvall and Rubey, 1976, 1977; Lee et al., 1979, 1982). As an example, non-flame data indicates that chlorobenzene would decompose to 99.99 percent of its original concentration in 1 sec. at 1038°K (Lee, et al., 1982). At typical flame temperatures (approximately 2000°K), the time required to obtain the same destruction level is much smaller ( $< 10^{-13}$  sec. using the same thermal decomposition data) than the typical 0.10 sec. flame residence time (Perry, et al., 1963).

Thus, non-flame thermal decomposition data obtained under dilute pre-mixed conditions indicate that temperatures much lower than those encountered



in typical incinerator flames will destroy all the organic hazardous waste compounds which have been tested to date. Also, because of high reactant concentrations in flames, free radicals which must be present to propagate the flame will contribute to destruction of the compounds in the flame (Seeker et al., 1981 a). These free radicals will increase the rate of decomposition above those predicted from dilute decomposition kinetics. Under ideal flame conditions, in which all of the waste is exposed to flame temperatures, the concept of incinerability has little significance since all hazardous compounds would be expected to be completely destroyed.

Incomplete destruction of a hazardous waste compound in an actual incinerator must be caused by conditions which allow some of the material to escape or bypass the flame since organic compounds are destroyed rapidly in a flame environment. Most incinerators include long residence time hold-up zones or after-burners to destroy material which is not completely reacted in the flame zone. Thus, incinerability would be expected to be influenced not only by the chemical properties of the compound but also by its physical properties and their interaction with the incinerator operating conditions because these may influence the failure mode. The term failure mode is used to describe those conditions which might occur in a practical incinerator which preclude complete processing of the waste material by a high-temperature turbulent diffusion flame. Thus, the term in the present context does not include conditions which may affect other parts of an incinerator (e.g., after-burner or scrubber). It is important to evaluate incinerability under conditions which simulate those failure modes which could occur in practice.

Various phenomena account for the failure of turbulent diffusion flames, typical of those used in liquid injection incinerators, to completely destroy a liquid waste. The destruction efficiency in the flame may be less than quantitative (100 percent) because of any of the following reasons:

1. Atomization Parameters. When the waste material is injected as a liquid which must be atomized, poor destruction efficiency can result from inappropriate atomization. (a) Droplets which are too large may be produced. (b) Their trajectory may be such

that they penetrate the flame zone and ignition does not occur. (c) Droplets which are too small may promote concentrated evaporation zones which produce fuel-rich pockets.

2. Mixing Parameters. In a turbulent diffusion flame the reactants are supplied separately and reactant contacting takes place via turbulent mixing. Poor mixing can result in low destruction efficiencies because the waste material may not be mixed with oxygen before it escapes from the flame region.
3. Thermal Parameters. The destruction efficiency may be low because flame temperatures are too low. This can occur if the calorific value of the waste/auxiliary-fuel mixture is low or heat removal rates are high.
4. Quenching Parameters. The reactants can be quenched before destruction is complete by heterogeneous or homogenous phenomena. Quench rates are high due to mixing with excessive excess air levels in dual injection systems in which the flame impinges on an aqueous jet, or the flame may contact a relatively cool surface.

Consequently, it is essential to investigate the concept of incinerability in flames under conditions which could account for a failure to completely destroy the waste compound and are typical of real systems.

The primary goal of this study was to compare the incinerability ranking procedures which have been proposed with those measured under flame conditions typical of liquid injection incinerators. The approach utilized was to measure the exhaust compound concentration under different simulated failure modes and to compare the ordering of the compounds to those given by several incinerability ranking procedures. Failure conditions were simulated for all the parameters expected to influence incinerator performance; i.e., atomization, mixing, thermal and quenching. To simulate all of them required two reactors. A microspray reactor consisting of a laminar premixed flat flame into which test compounds were injected, was used to investigate thermal parameters. A subscale turbulent diffusion spray-flame was used to investigate

atomization, mixing and quenching parameters. Secondary goals included the generation of fundamental flame mode destruction data necessary to compare flame and non-flame decomposition. The results are primarily a means of guiding future experimental work, since further work is necessary to select a reasonable ranking protocol.

## 1.2 Experimental Approach

Extensive investigations are being carried out at the University of Dayton Research Institute under EPA sponsorship to define the kinetics of waste decomposition in post-flame regions (Dellinger et al., 1982; Duvall and Rubey, 1976, 1977). The emphasis of the present study was on the flame zone itself and the impact of failure conditions associated with mixing, thermal, quenching, and atomization parameters on the relative destruction of five compounds. These compounds were selected because they represented a broad range of incinerability as defined by existing ranking procedures, and because data within each of the procedures were available for the compounds. The study was restricted to conditions typical of liquid injection incinerators. No attempt was made to include phenomena associated with waste destruction in beds such as that exist in fluidized beds, rotary kilns or hearth incinerators. Two flame reactors were used to study destruction efficiency under different conditions:

1. Microspray Reactor. In the microspray reactor, monodisperse waste droplets were injected into a hot, uniform post-flame gas. These experiments investigated the destruction efficiency (DE) behavior and ranking that resulted from individual droplet evaporation and flame decomposition reactions. The experiment was designed to bridge the gap between the non-flame thermal decomposition experiments and the turbulent flame data. As such, it included two processes in addition to the thermal decomposition experiments: droplet vaporization dynamics and flame reactions. The data were used for the following purposes:
  - To determine what portion of the turbulent flame rankings were due to laminar flame and evaporation processes.

- To compare flame (microspray) vs. non-flame (thermal decomposition) destruction on a fundamental level without the complicating influence of turbulence.
2. Turbulent Flame Reactor. A turbulent flame reactor (TFR) was used to investigate DE and ranking in a turbulent spray diffusion flame. The TFR was operated under conditions to simulate many of the processes occurring in the flame zone of a liquid injection incinerator; these could be exaggerated to simulate different failure modes.

Five compounds (chloroform, acrylonitrile, benzene, chlorobenzene, and 1, 2-dichloroethane) were selected as representative of liquid organic hazardous wastes. All the compounds are listed in the 1980 RCRA regulations, Part 261, Appendix VIII (Federal Register: May 19, 1980). The compounds were chosen to represent a broad range of incinerability based on the most commonly proposed ranking procedures. They cover greater than 90 percent of the range in heats of combustion for the listed compounds (.13 to 10.14 kcal/gm). Since a direct comparison between non-flame thermal decomposition rankings and the flame-mode destruction was an objective of this study, compounds were selected for testing for which non-flame data were available. In addition, the selection also took into account the NBS ranking system, a range of auto-ignition temperatures and a variety of molecular structures. Two of the compounds are aromatic, one is a highly chlorinated methane, another is a chlorinated ethane and one contains nitrogen.

Compound DE was measured in the reactor exhaust by adsorption onto Tenax-GC, followed by thermal desorption and flame ionization gas chromatographic analysis. The use of Tenax for concentrating the sample provided the necessary rapid turnover of samples with sufficient separation and sensitivity. The breakthrough volumes of all the test compounds were directly measured and were found to be greater than the utilized sample volumes. Benzene and 1, 2-dichloroethane were not separable by the column and hence mixtures containing both compounds were avoided. Appendix B details the design, operating procedures, and verification/quality assurance work performed on the DE measurement technique.

### 1.3 Microspray Results

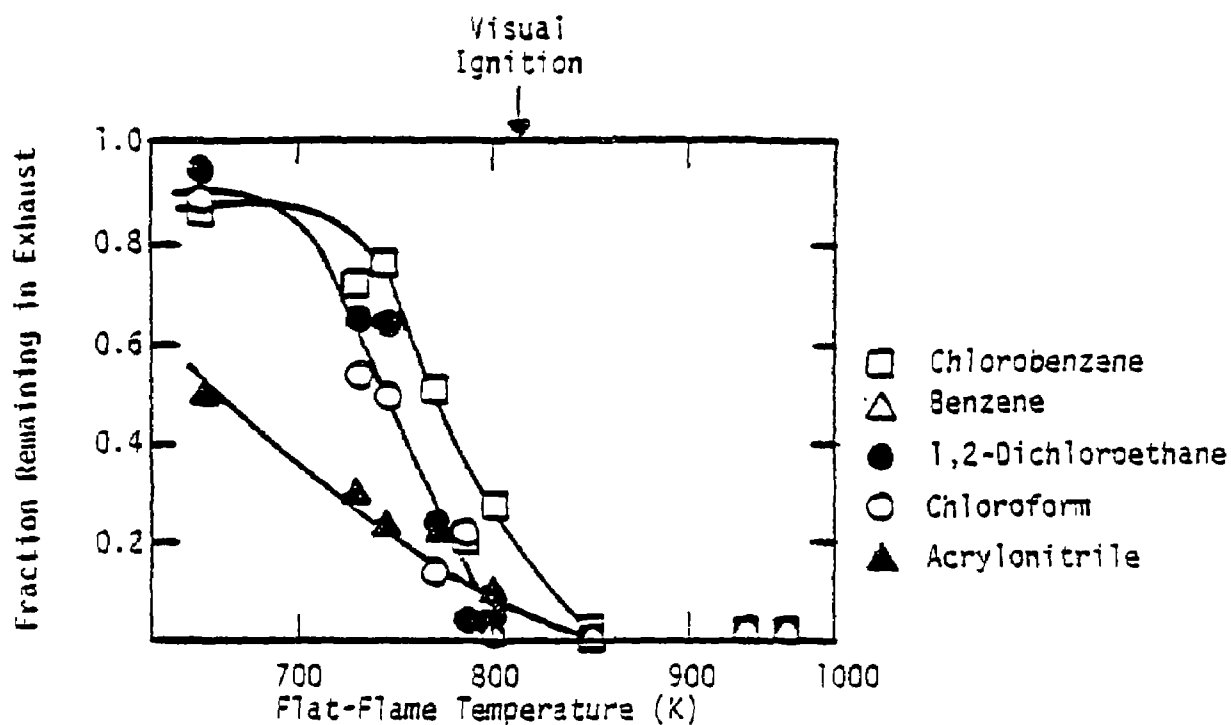
The microspray was used to investigate the impact of thermal parameters for two conditions:

- Fuel-lean - Excess oxygen available to oxidize test compounds.
- Fuel-rich - Insufficient oxygen available to oxidize test compounds.

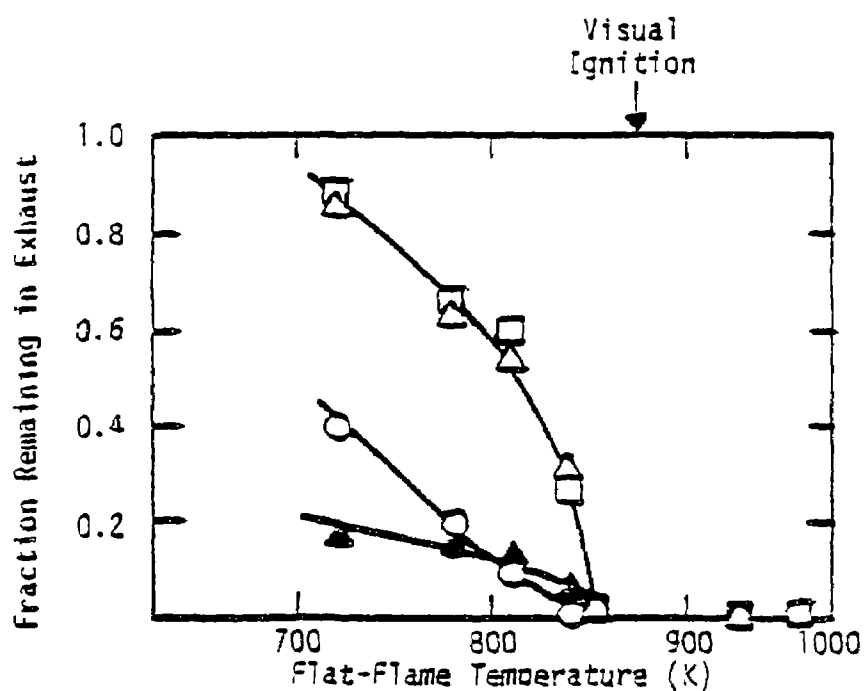
In addition, the effect of using pure compounds was compared with that for mixtures of compounds. The other failure mode parameters (atomization, quenching, and mixing) cannot be effectively investigated in the microspray reactor and were investigated in the turbulent flame reactor.

Figure 1-1 presents data for two mixtures of four compounds shown separately in Figure 1-1a and 1-1b. In these tests, 38  $\mu\text{m}$  droplets of the two mixtures were injected separately into a lean (10 percent excess oxygen)  $\text{H}_2/\text{Air}/\text{N}_2$  flame with different flat-flame temperatures. Exhaust concentrations of the individual test compounds were measured and the data are shown in Figure 1-1 in terms of the fraction of each compound remaining versus the measured flat-flame temperature. This temperature is determined by extrapolating the axial temperature measurements to the burner face and is the highest temperature of the flat flame gas (Appendix D). Under these excess oxygen conditions, flames were observed to surround each individual droplet for both mixtures for flat-flame temperatures in excess of 850 K. However, the minimum droplet ignition temperature was observed at slightly lower temperatures for the 1, 2-dichloroethane mixture, probably due to the substitution of compounds. When the flat-flame temperature is greater than the ignition temperature of the specific compound mixture, the exhaust concentration of the test compounds were below the detection limit of the analytical technique which indicated a destruction level in excess of 99.995 percent.

Calculations using non-flame kinetics indicate that almost no decomposition should occur below 800 K for the residence times ( $\sim 1$  sec.) available in the microspray reactor. However, as shown in Figure 1-1, significant



(a) Mixture containing Dichloroethane, Chlorobenzene, Chloroform and Acrylonitrile



(b) Mixture containing Benzene, Chlorobenzene, Chloroform and Acrylonitrile

Figure 1-1. Fraction of test compound remaining in exhaust when 38  $\mu\text{m}$  droplets of mixtures of compounds were injected into lean (10 percent excess oxygen)  $\text{H}_2/\text{air}$  flames as function of flame temperature.

destruction was measured at flat-flame temperatures below 800 K. This destruction at low flat-flame temperatures is probably due to a local increase in temperature around droplets and flame radical attack. For gas temperatures at and above the point at which the individual droplets were observed to support flames, all the compounds were destroyed, but below the ignition temperature the fraction destroyed depended upon the compound. At low flat-flame temperatures for the dichloroethane mixture, the ranking from highest to lowest concentration was: chlorobenzene, dichloroethane, chloroform, and acrylonitrile. At flat-flame temperatures just below the droplet ignition point, again chlorobenzene was found to be the most difficult compound to be eliminated but the other compounds showed some rearrangement in ranking; however, the effect of compound type is small. When benzene was substituted for dichloroethane (Figure 1-1b), chlorobenzene remained the most prominent compound in the exhaust followed by benzene, chloroform, and acrylonitrile. Again, just below ignition there was some reordering of compounds with chloroform becoming the easiest to eliminate.

These data indicate that for single droplet oxidative conditions where the flame temperature is too low for droplet ignition, a particular order of compounds does exist in terms of the fraction remaining in the exhaust. This order is chlorobenzene, benzene, 1, 2-dichloroethane, chloroform, and acrylonitrile. However, this order changes as the temperatures reach the ignition point. The ordering just below ignition is identical to the ordering suggested by  $T_{99.99}$  and auto-ignition temperature.

When 38  $\mu\text{m}$  droplets of pure compounds were injected into oxygen-rich fuel-lean flame products, the droplets were observed to ignite at different temperatures. For example, visual ignition for chloroform droplets was observed at 860 K, while dichloroethane ignited at 850 K, acrylonitrile at 800 K, and chlorobenzene at 740 K. Benzene had the lowest ignition temperature and was observed to ignite at temperatures below 600 K. For pure compounds, the destruction is controlled by droplet ignition. The observed ignition temperature does not agree with any proposed incinerability ranking procedures although the heat of combustion criteria is almost the same with the exception that acrylonitrile and chlorobenzene are reversed. A potential explanation for this behavior is that the ability to support droplet flames is determined to first order, by the heat release available upon droplet combustion ( $\Delta H_c$ ).

Although second order effects may modify the rankings, for pure droplets the ranking appears to be dominated by heat of combustion.

The absence of oxygen was the third failure mode investigated with the microspray reactor. Droplets of equal molar mixtures of compounds were injected into fuel-rich (stoichiometric ratio = 0.83)  $H_2$ /air/ $N_2$  flames of different temperatures. In these tests, the oxygen was rapidly and completely consumed by the hydrogen in the flat-flame so that no oxygen was available to oxidize the test compounds. The fraction of each compound remaining in the exhaust as a function of the flat-flame temperature is shown in Figure 1-2. Even with mixtures, the temperature required to destroy the compounds, 1050 K, was found to be very similar to the  $T_{99.99}$  temperatures of the individual compounds (920 to 1037 K; see Table 2-1) and were much higher than those required if droplet ignition occurred (Figure 1-1). The fractional destruction was strongly dependent upon flame temperature. In fact, the data show that a very small change in flame temperature above 1050 K produced a substantial change in the compound concentrations, particularly for benzene. A difference between the compounds was observed only at a temperature just below the flat-flame temperature required for complete destruction. At that temperature, the compound that was most predominant was chlorobenzene, followed by benzene, chloroform, and acrylonitrile. This ranking was identical to that measured for the low temperature oxidation data (Figure 1-1). The non-flame  $T_{99.99}$  did identify the temperature range required for complete destruction and the most predominant compounds (chlorobenzene and benzene); however, acrylonitrile and chloroform are reversed from the  $T_{99.99}$  ranking.

#### 1.4 Turbulent Flame Reactor Results

The turbulent flame reactor was operated and tested under a number of conditions. However, many of these conditions resulted in high destruction efficiency of all the test compounds. Only those parameters resulting in significant deterioration of destruction efficiency are presented. Data on high destruction levels are presented elsewhere (Section 4). The conditions investigated in the turbulent flame reactor which had a strong influence on destruction efficiency were primarily associated with three failure parameters:

- Atomization parameter - poor atomization quality



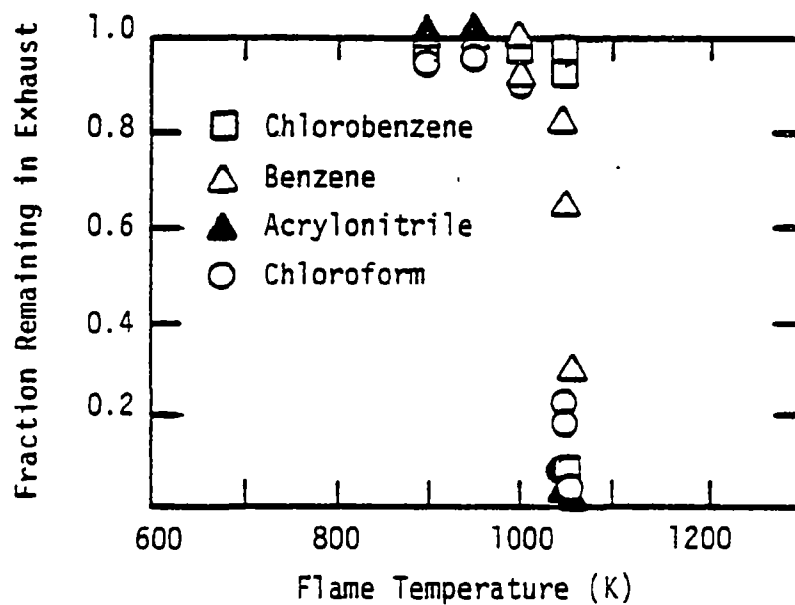


Figure 1-2. Fraction of test compound remaining in exhaust when 38  $\mu\text{m}$  droplets of mixtures of compounds were injected into rich (stoichiometric ratio = 0.83)  $\text{H}_2$ /air flame as a function of flame temperature. Incinerability order at 1050°K (highest to lowest concentration) is chlorobenzene, benzene, acrylonitrile, and chloroform.

- Combustion parameters - high excess air
  - low excess air
  - low heat release
- Mixing (or turbulence) - swirl
  - air velocity

Those parameters found to be of less importance included burner velocity, fuel type (No. 2 fuel oil) and concentration of hazardous waste compounds (from 3 to 25 percent).

It was generally found that exhaust concentration measurements of carbon monoxide and total hydrocarbons were good indicators of flame performance and compound destruction efficiency. The exhaust CO level in particular appeared to be well correlated with the exhaust concentration of the test compounds. This result was expected since the high heat removal rates in the TFR emphasize flame performance over postflame reaction. Since CO is an intermediate in the oxidation of hydrocarbons to CO<sub>2</sub> (Seeker et al., 1981a), it is directly linked with combustion efficiency. Therefore, an examination of the relative CO levels for each failure condition indicates the overall combustion efficiency which can be compared to the destruction efficiency of the hazardous waste compounds. The relationship between exhaust CO, total hydrocarbons measured by the flame ionization detector, and destruction efficiency measured for a mixture of compounds is shown in Figure 1-3. The maximum DRE (>99.995 percent) was measured at 30-40 percent excess air, which corresponded to the minimum in both exhaust CO and hydrocarbon.

Figure 1-4 presents data obtained with the TFR at high heat-release rates (44 kW). Very high destruction levels (>99.995 percent) were measured for all compounds at 20 percent excess air at this heat-release rate with the exception of benzene. It is possible that benzene was a product of incomplete combustion of either the auxiliary fuel or one of the test compounds (e.g., chlorobenzene). The actual source of the benzene whether it is a product of incomplete combustion or an indication of incomplete benzene destruction, has not been determined. Benzene is a possible intermediate in the formation of soot which was observed in the flame in the form of luminosity especially at low excess air levels. Because of the relatively large amounts of heptane present (97 percent) only a small conversion of heptane to benzene is required to account for the exhaust levels

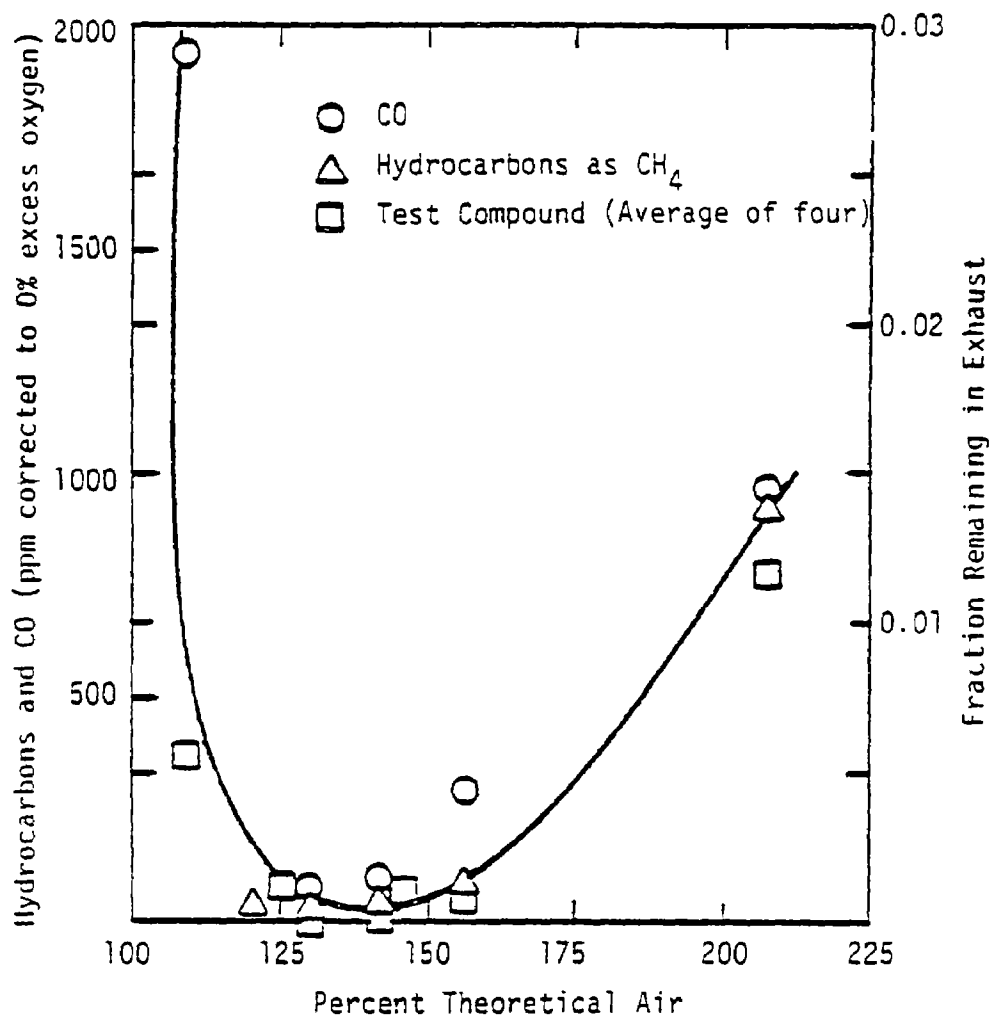
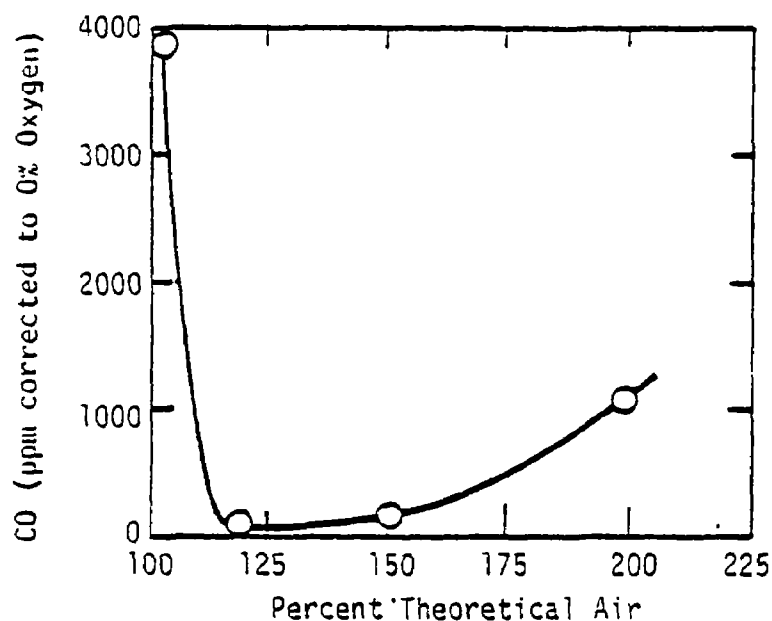
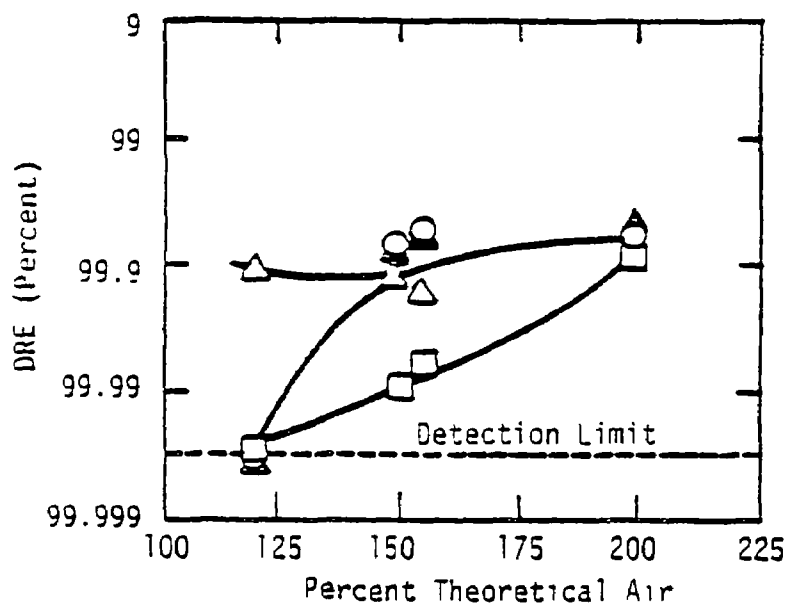


Figure 1-3. Exhaust CO and total hydrocarbons and fraction of test compound remaining in exhaust as a function of theoretical air (constant air velocity, variable load, equal molar mixture of chloroform, benzene, chlorobenzene, and acrylonitrile added 3 percent by weight to heptane).



(a) Exhaust CO Concentration



(b) Destruction and Removal Efficiency

Figure 1-4. Impact of theoretical air on CO and DRE from turbulent flame reactor. Incinerability order at 150 percent T.A. is chloroform, acrylonitrile, benzene, and chlorobenzene (constant load = 48 kW; variable air flow rate and burner velocity; equal molar mixture of compounds added 3 percent by weight to heptane).

of benzene measured at this low excess air condition. However, the benzene could also be the result of a chlorobenzene reaction.

At higher excess air levels (>150 percent theoretical air) the exhaust concentrations of CO and the test compounds increased. This is probably due to lower flame temperatures and increased quenching which can occur when large amounts of unheated air are present. The lowest DRE level obtained for these high heat-release rates (44 kW) was 99.9 percent. The compound differences were small but measureable at 150 percent theoretical air. The ranking from highest to lowest concentration was: chloroform, acrylonitrile, benzene, and chlorobenzene. This particular order, which was found to exist for a number of failure conditions tested with the turbulent flame reactor does not agree with any of the proposed rankings, although the heat of combustion did identify the most predominant compound (chloroform).

The data obtained at low heat-release rates (24-42 kW) are shown in Figure 1-5. This data set was achieved by lowering the fuel flow rate from the nominal operating conditions while maintaining the air flow constant. This drop in load and increase in theoretical air resulted in significant increase in the fraction of the waste compounds in the exhaust. Under this failure condition, chloroform and benzene had similar high exhaust concentrations followed by 1,2-dichloroethane and similar low exhaust concentrations for acrylonitrile and chlorobenzene.

The data presented in Figure 1-6 indicate that atomization parameters had significant impact upon compound destruction. In these tests, a nozzle designed for 1.5 gal/min was operated at .75 gal/min dropping the pressure from 161 psig to 40 psig. This increases the mean droplet size, affects fuel air mixing, and may cause some of the large droplets to escape the flame. The highest compound exhaust concentrations were measured under these poor atomization conditions. However, the order of compounds was found to be identical to other failure conditions for the TFR such as high excess air at high loads, low excess air at low loads, and quench coils. The chloroform was found to be the most predominant compound followed by benzene, acrylonitrile, and chlorobenzene.

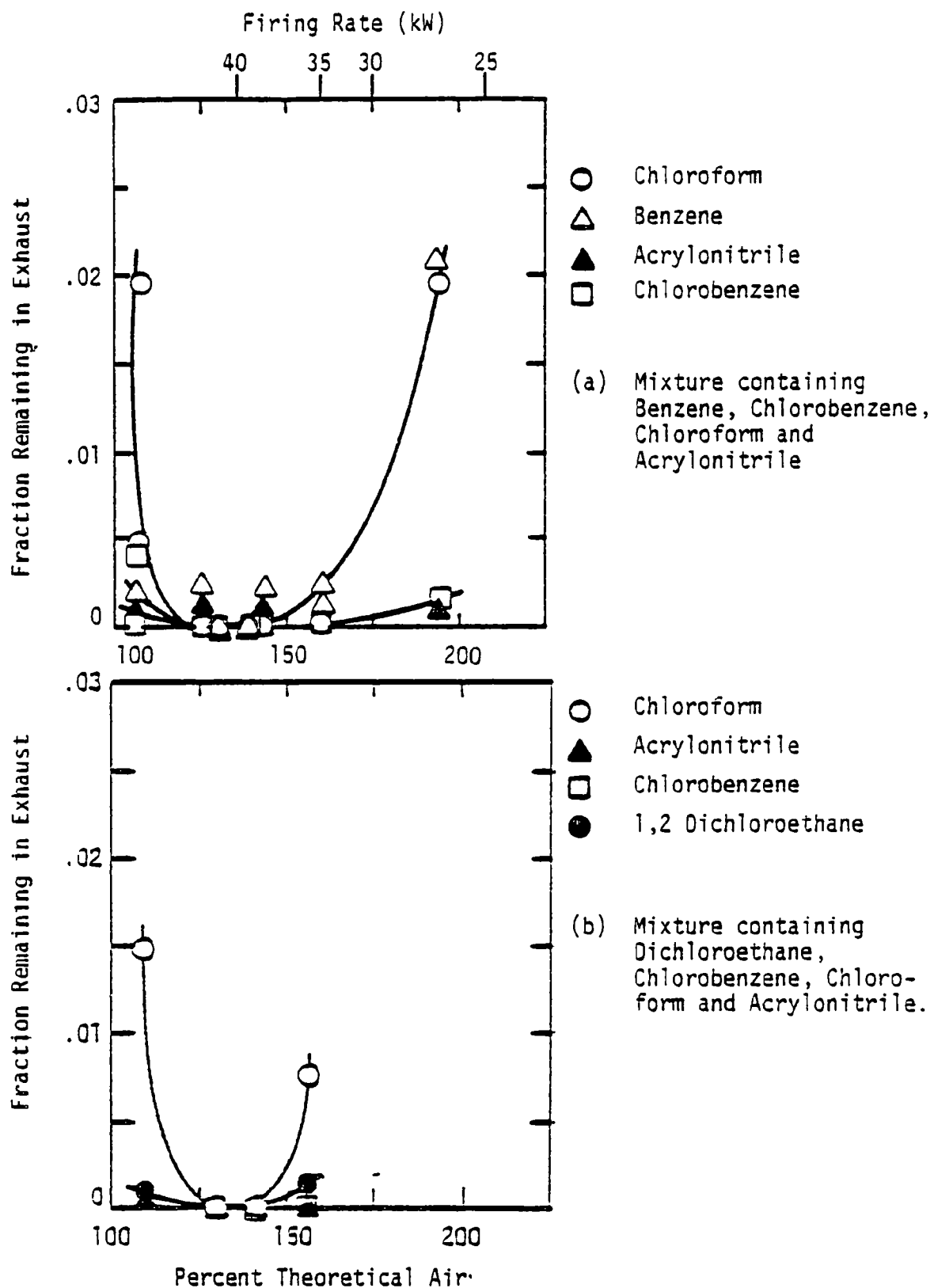
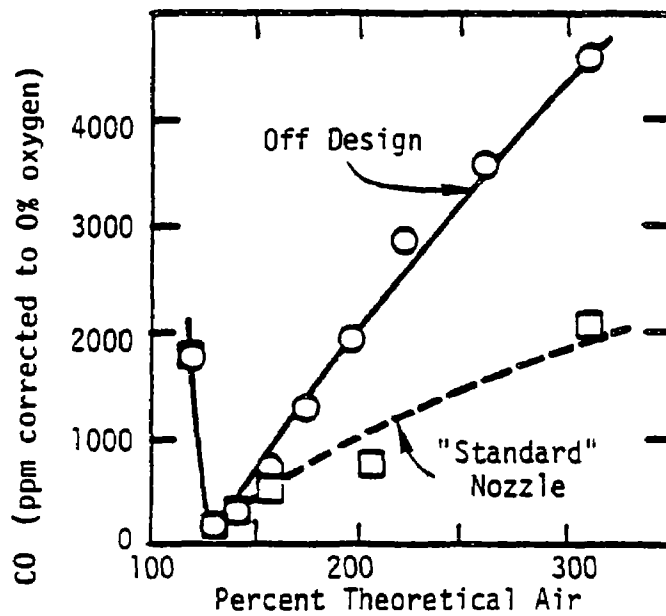
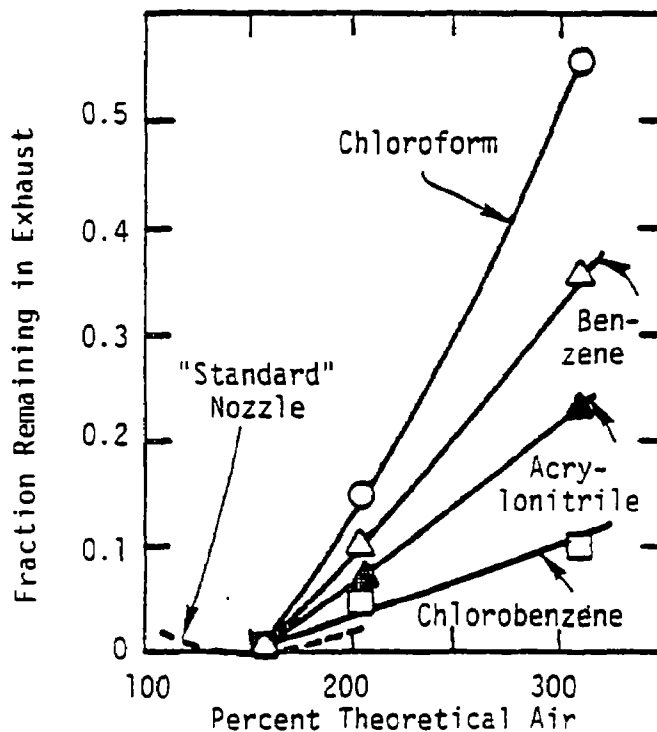


Figure 1-5. Impact of theoretical air and load on fraction of test compounds remaining in exhaust of turbulent flame reactor (constant air velocity, variable load 42-24 kW; equal molar mixture of compounds added 3 percent by weight to heptane).



(a) Carbon Monoxide



(b) Test Compound Data with Standard Nozzle and Off Design Nozzle

Figure 1-6. Impact of atomization quality on CO and fraction of test compounds remaining in exhaust of turbulent flame reactor (constant air velocity, variable load: 42-16 kW; equal molar mixture of compounds added 3 percent by weight to heptane).

A water-cooled copper coil was placed directly within the flame in the TFR to provide an extreme case of flame-quenching in order to investigate destruction efficiencies under this mode of foilure. In this failure condition test, the coil acted to cool the flame and supplied a surface area for reactants to quench. The presence of the quench surface increased both CO and the test compound concentration (see Figure 1-7). The dashed line for the uncooled data was derived from Figure 1-5. The order of the compounds was similar to other failure conditions with chloroform being the most predominant and chlorobenzene the least predominant compound in the exhaust. However, the positions of acrylonitrile and benzene were reversed from the order found in other failure modes.

### 1.5 Discussion

The combustion of hydrocarbon fuels in turbulent diffusion flames results in relatively high flame-zone temperatures (between 1600-2000 K) and residence times are on the order of 0.1 seconds. If the waste compounds investigated in this study experience these conditions, then they would be quantitatively destroyed. The results of this study agree with this hypothesis. Turbulent diffusion spray flame and a laminar reactor burning single droplets were capable of destruction efficiencies greater than 99.995 percent. In the case of the turbulent flame reactor under optimized conditions (stable flame, low CO and total hydrocarbon) the compounds were destroyed mainly in the flame because post-flame decomposition was minimized due to the fact that the flame was contained by cold walls. Consequently, it can be concluded that a flame is an extremely efficient mode of destroying waste compounds and the concept of incinerability under these conditions has little value. If everything is destroyed it is not possible to rank compounds in terms of difficulty or ease of destruction. Consequently, a series of experiments were designed to assess incinerability under several limiting conditions which might typify the failure modes of practical liquid injection incinerators.

The microspray reactor investigated those conditions associated with single droplet combustion in the absence of complications due to turbulent



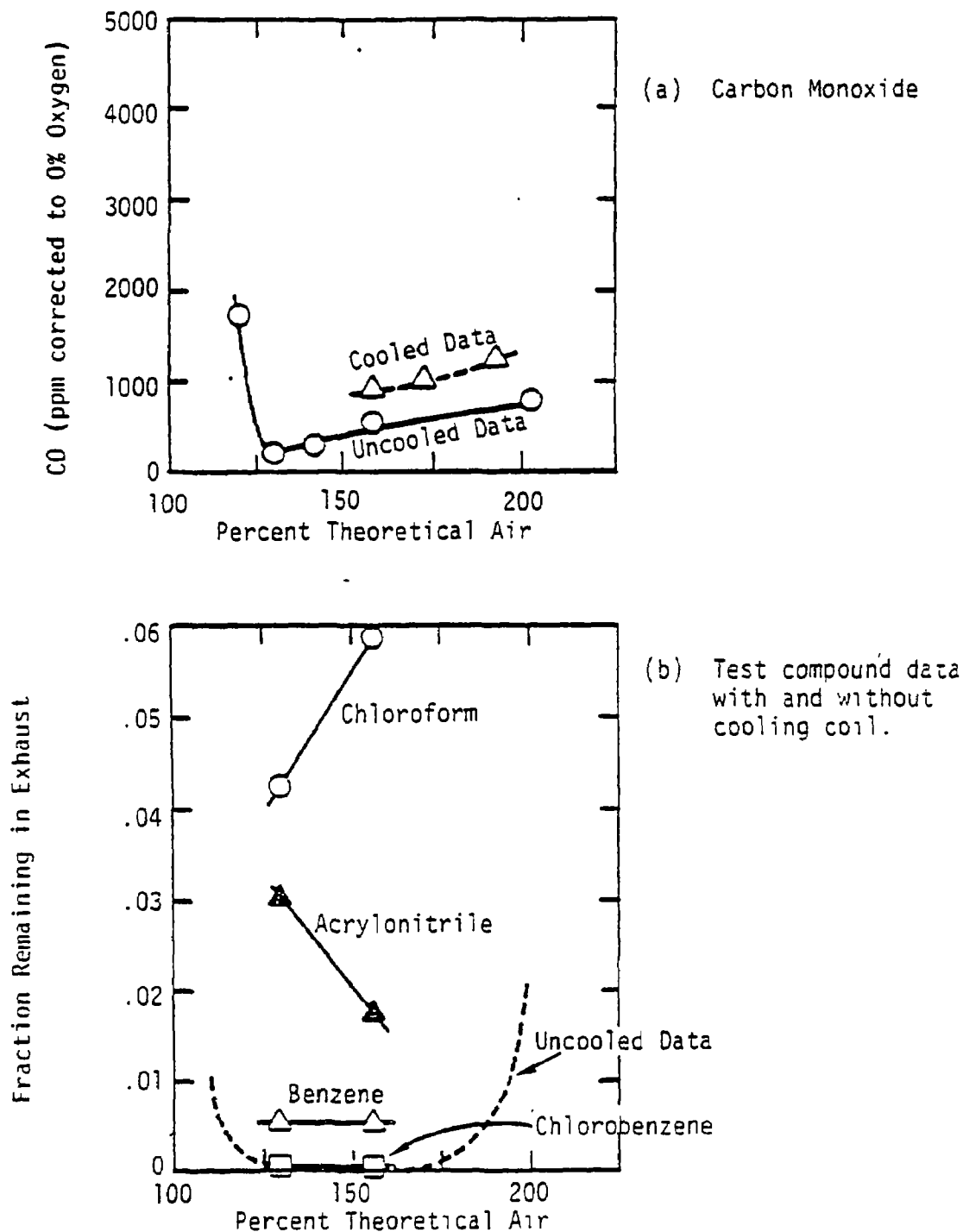


Figure 1-7. Impact of cooling coil placed in flame on CO and fraction of test compound remaining in exhaust of turbulent flame reactor. (Constant air velocity; load = 32 kW equal molar mixture of compounds added 3 percent by weight to heptane).

mixing. It was selected in order to study thermal effects separated from turbulent mixing and atomization. The temperature required to ignite droplets of hazardous waste under oxygen-rich conditions in the laminar premixed flat-flame reactor was found to be low (850°K) in comparison to typical flame temperatures (1500-2000°K). Above the ignition temperature, the droplets were visually observed to ignite and the compounds tested were quantitatively (> 99.995 percent) destroyed. Even in the absence of oxygen, the microspray data were consistent with the high destruction efficiencies achievable in a turbulent diffusion spray flame environment.

The TFR was operated at high heat removal rates by operating with water-cooled walls in order to minimize post-flame reactions and mixtures up to 25 percent by weight of the test compounds were investigated. Even in the absence of significant post-flame decomposition, destruction efficiencies which corresponded to the detection limits of the analytical systems (99.995 percent) were achieved for all the compounds tested. In the turbulent flame reactor, a direct relationship was observed between overall combustion efficiency as indicated by exhaust CO and hydrocarbon emissions and the destruction of the test compounds. Conditions which minimized the CO concentration in the exhaust gases also maximized destruction efficiency. Under all failure conditions investigated, exhaust CO concentration increased when the test compound concentration increased. These results suggest the feasibility of using exhaust CO and potentially total hydrocarbons to monitor the performance of liquid injection incinerators once the conditions giving the maximum destruction efficiency have been defined.

The incinerability or ordering of the compounds was found to depend on the actual failure condition which caused the inefficiency. When both the microspray and the turbulent flame reactor were operated under conditions which simulated failure modes of practical incinerators, measureable differences in the destruction efficiency of the five test compounds were obtained. For example, chlorobenzene was the most difficult to eliminate in the microspray when the temperature was too low to ignite the droplets, but was the

least difficult to eliminate for a variety of failure conditions in the TFR such as poor atomization quality.

Figure 1-8 presents a series of bar graphs which allow a comparison between incinerability as defined by the various failure modes and the rankings indicated by procedures based upon  $T_{99.99}$ , heat of combustion, the NBS method and AIT. The bar graph shows the concentrations measured in the experiment normalized so that the most predominant compound shows full-scale and the lesser concentrations are expressed as a percentage of that maximum concentration. This approach gives an indication of the measured magnitude of the difference in destruction efficiency between compounds. A comparison of these relative concentration measurements with proposed incinerability ranking techniques demonstrates that none of the proposed techniques agree with the data for all failure conditions. However, some of the ranking procedures were found to be appropriate for specific failure conditions. For example, the non-flame thermal destruction ( $T_{99.99}$ ) and AIT procedures both agreed with the compound concentration measurements when the temperature was below droplet ignition temperature and under oxygen-deficient conditions. Heat of combustion was found to correlate the pure compound data when the microspray was operated below droplet ignition temperature. In most instance, chloroform was the most difficult compound to incinerate for the failure conditions investigated with the TFR, and this was anticipated by only one of the four ranking techniques - heat of combustion.

Although measureable differences in the destruction efficiency of the five test compounds were obtained, the differences were not large under any of the conditions tested. For the most part, the variation in the concentration (between highest and lowest) of the compounds in the exhaust was typically of the order of five, although variations larger than ten were measured under some circumstances. This suggests that the selection of POHC may not be very critical because the differences between compounds are small. If the permit writer selects three compounds based upon two or more ranking techniques, and it is demonstrated that their DRE is greater than 99.99 percent, then it is very unlikely that any other compounds will be destroyed to a significantly lesser degree.

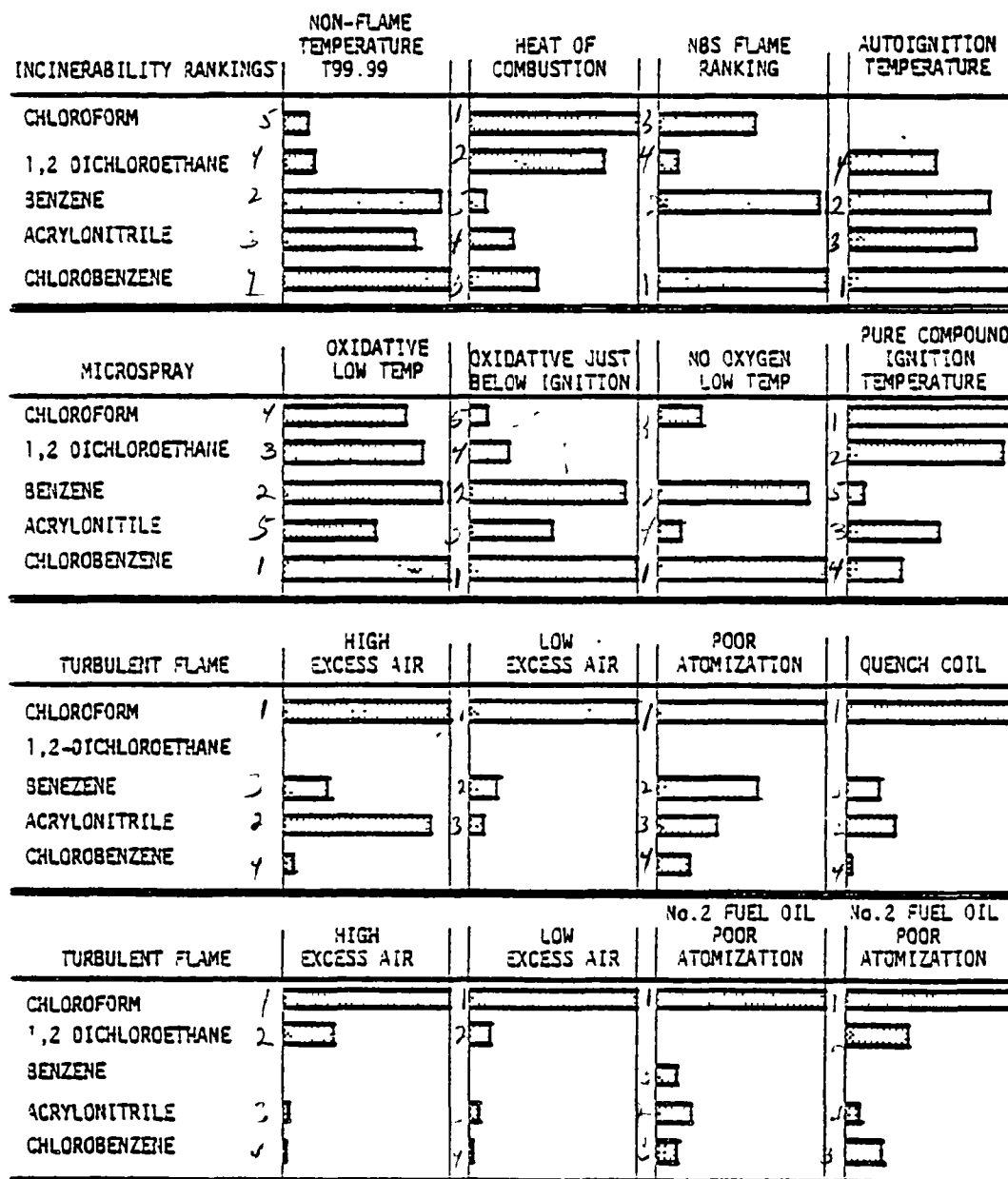


Figure 1-8. Comparison of proposed ranking techniques and concentration measured in the experiments under flame failure conditions normalized so most predominant compound shows full scale.

This study has identified the differences between compound destruction efficiency caused by failure conditions associated with the flame zone. High destruction efficiencies have been demonstrated in the flame alone. However, many incinerators are equipped with post-flame hold-up zones and after-burners in order to achieve additional thermal decomposition of compounds which escape the flame zone. In order for an incinerator to fail to destroy a compound, the material must both escape the flame and the temperature be too low in the post-flame hold-up zone to destroy the compound (less than  $T_{99.99}$ ). The differences in the concentration of compounds in the exhaust of the incinerators is associated with both the flame and non-flame zones. The thermal decomposition which occurs in the post-flame zone can alter the ranking in the exhaust. As an example, consider a flame zone in which the DE of chloroform and chlorobenzene was 95 percent and 99 percent, respectively (a flame ranking consistent with the data of Figures 1-6 or 1-7). Utilizing non-flame kinetics and a 1.0 sec isothermal post-flame zone (kinetics shown in Table 2-1), for post-flame temperatures below about 870 K, the flame zone ranking will persist in the exhaust. Above 1008 K both compounds are destroyed to 99.99 percent DE. Hence, there are potential situations, dependent on incinerator conditions, for either a flame zone or a post-flame ranking to prevail within a given unit.

It was not the purpose of this study to ascertain why destruction efficiency under flame conditions can be compound and failure mode specific. More detailed measurements such as fundamental kinetic flame studies, are necessary to provide a full explanation of the causes of the rankings. It could be associated with flame inhibition due to the presence of halogens which are known to reduce burning rates. Under quenching conditions, these effects could be enhanced. The formation of products of incomplete combustion (PICs) as a consequence of the partial destruction of the waste compound, was not investigated. An alternate method of assessing incinerability could be based upon the potential to form PICs which are themselves hazardous.

## 1.6 Conclusions

1. Under optimum conditions, flames are capable of destroying hazardous waste compounds with very high efficiencies (greater than 99.995 percent) without the need for long residence time high-temperature post-flame zones or after-burners.

2. Reduced flame destruction efficiencies are the result of operation under some failure mode such as poor atomization, poor mixing, or flame quenching.
3. Incinerability, or ordering of compounds in terms of their relative destruction efficiency, is dependent on the actual failure condition which caused the inefficiency.
4. Optimum conditions for destruction of hazardous waste compounds in turbulent diffusion spray flames correspond to minimal exhaust CO and total hydrocarbons.
5. No one incinerability ranking system appears to predict correctly the relative destruction efficiency of the five compounds tested for all failure conditions investigated. However, several rankings did correctly predict relative DE for specific failure conditions.
6. More data is required on other compounds and other failure conditions more appropriate to different types of hazardous waste incinerators to fully determine the limitations of incinerability ranking systems and develop an appropriate incinerability ranking methodology.
7. Future experimental effort should be directed toward extending the compound data base beyond the current five, and in particular, the extension of experimental capabilities to consider additional failure modes (e.g., those associated with post-flame thermal processes of after-burners).

## 1.7 Executive Summary References

- Cudahy, 1981. Incinerability, Thermal Oxidation Characteristics and Thermal Oxidation Stability of RCRA Listed Hazardous Wastes. IT Enviroscience Corp.
- Dellinger, B., D. S. Duvall, D. L. Hall, and W. A. Rubey, 1982. Laboratory Determinations of High Temperature Decomposition Behavior of Industrial Organic Materials. 75th Annual Meeting of the APCA. Paper No. 82-3.5. New Orleans, LA.
- Dietrich, V. E., 1979. Dropsizes Distribution for Various Types of Nozzles. In Proceedings of the 1st International Conference on Liquid Atomization and Spray Systems. The Fuel Society of Japan, Tokyo, Japan. p. 69.
- Duvall, D. S. and W. A. Rubey, 1976. Laboratory Evaluation of High-Temperature Destruction of Kepone and Related Pesticides. Technical Report UDRI-TR-76-w1, University of Dayton Research Institute. EPA 600/2-76-299.
- Duvall, D. S. and W. A. Rubey, 1977. Laboratory Evaluation of High-Temperature Destruction of Poly-chlorinated Biphenyls and Related Compounds. EPA 600/2-77-228.
- Lee, K. C., J. L. Hansen, and D. C. Macauley, 1979. Predictive Model of the Time/Temperature Requirements for Thermal Destruction of Dilute Organic Vapors. 72nd Annual Meeting of the APCA. Cincinnati, OH.
- Lee, K. C., N. Morgan, J. L. Hansen, and G. M. Whipple, 1982. Revised Model for the Prediction of the Time-Temperature Requirements for Thermal Destruction of Dilute Organic Vapors and its Usage for Predicting Compound Destructability. 75th Annual Meeting of the APCA, New Orleans, June 1982.
- Seeker, W. R., M. P. Heap, and T. J. Tyson, 1981a. Gas Phase Chemistry. Volume I of Final Report for EPA 68-02-2631.
- Tsang, W. and W. Shaub, 1981. Chemical Processes in the Incineration of Hazardous Waste. National Bureau of Standards. Paper presented to American Chemical Society Symposium on Detoxification of Hazardous Wastes, New York, NY.

## 2.0 INTRODUCTION

According to the Resource Conservation and Recovery Act regulations, standards for safe operation of hazardous waste incinerators are defined as achieving at least 99.99 percent destruction and removal efficiency (DRE) of the hazardous constituents in the waste feed. The interim final rule (Federal Register: 1/23/81) stipulates that the standard of operation must be demonstrated in a trial burn for only a limited set of compounds in the waste stream or by submission of acceptable data. The permit writer selects one or more compounds, designated as the principal organic hazardous constituents (POHC), based upon the component concentration in the waste stream and the relative ease of incineration. Demonstration of 99.99 percent DRE for the POHC defines safe operating conditions. This approach assumes that destruction of all the remaining more easily incinerated compounds is greater than 99.99 percent DRE at this specified operating condition. The permit operating requirements are then specified based on these trial burn operating conditions.

The procedure assumes the existence of some measure of ranking the relative ease of destruction of individual compounds (i.e., degree of incinerability). At present, a single ranking list is employed and, hence, the ranking must be system-dependent; i.e., it must be applicable to all types of incinerators under all operating conditions. Since the proof of compliance is based solely upon trial burn measurements of the POHC chosen from the ranking, it is critical that the ranking correctly reflect the relative ease of incinerability in the system and operating conditions under consideration. If it does not, the incinerator may be operated under conditions which release hazardous compounds even though it is quantitatively destroying the selected POHC.

An appropriate incinerability ranking could be obtained from extensive trial burn data. Such an approach is advantageous because the resulting ranking would be based on actual incinerator performance. It would also indicate if ranking was a function of incinerator type or operating condition. However, such an approach cannot be adopted because of the expense of measuring each waste during a trial burn. In addition, the measurement techniques required for obtaining complete characterization of incinerator performance are, at least partially, beyond the state-of-the-art.



The quantities of compounds escaping from the incinerator will likely depend on the actual failure condition which allowed the material to escape. The development of an incinerability ranking without extensive trial burn data on all compounds requires consideration of the possible mechanisms of escape. Liquid injection incinerators typically produce the heat necessary to destroy the compounds in large-scale turbulent-diffusion flames burning either an auxiliary fuel or the hazardous waste itself. This is followed by large, well insulated hold-up zones in which wastes that escape the flame are removed by thermal decomposition, after-burners, and gas cleaning equipment such as scrubbers. In such an incinerator, the parameters which control waste destruction efficiency are:

1. Atomization Parameters. When waste material is injected as a liquid which must be atomized, poor destruction efficiency can result from inappropriate atomization. Droplets which are too large may be produced or their trajectory may be such that they pass through the flame zone without completely evaporating.
2. Mixing Parameters. In a turbulent diffusion flame the reactants are supplied in separate streams and reactant contacting takes place via turbulent mixing. Poor mixing can result in low destruction efficiencies because the waste material may not be mixed with oxygen before it escapes from the flame region.
3. Thermal Parameters. The destruction efficiency may be low because flame or post-flame temperatures are low. This can occur if the calorific value of the waste/auxiliary fuel mixture is low, heat removal rates are high, or quench rates are high due to mixing with excessive amounts of air.
4. Quenching Parameters. The reactants can be quenched before destruction is complete by heterogeneous or homogeneous phenomena. Mixing can cause quenching as explained above, or the flame may impinge upon a relatively cool surface.

Consequently, it is essential to investigate the concept of incinerability in flames under conditions which could account for a failure to completely destroy the waste compound and are typical of real systems.

A number of incinerability ranking procedures and tests have been proposed (Cudahy, et al., 1981). These procedures include:

- Heat of combustion per unit mass compound.
- Autoignition temperature (AIT).
- Temperature required to yield a 99.99 percent destruction efficiency in a specified residence time (normally 1-2 sec) derived from dilute first order thermal decomposition kinetics ( $T_{99.99}$ ).
- Correlation of compound specific properties such as AIT, structure, etc., with  $T_{99.99}$ . This approach establishes an estimated  $T_{99.99}$  ranking and thus avoids the necessity of obtaining thermal decomposition data for each compound.
- Susceptibility of bonds to flame radical attack (National Bureau of Standards: NBS).
- Miscellaneous approaches: molar heat of combustion, heat of formation per unit weight, Gibbs free energy per unit weight, ionization potential, flash point, activation energy derived from thermal decomposition kinetics, and heat of formation of ion per unit weight.

Each of these ranking procedures approaches the problem of determining incinerability in a different manner. The advantages and disadvantages, and the relationship of each to the incineration process will be discussed in Sec. 5.

The primary goal of this study was to establish if any of the proposed incinerability rankings were appropriate to account for compound effects that might occur for possible failure conditions for the most common (Keitz, et al., 1983) type of incinerator, liquid injection. The approach utilized in the study was to measure the relative exhaust compound concentration when different modes of failure were allowed to occur and to compare this ordering to proposed incinerability ranking procedures. Secondary goals included generating fundamental flame-mode destruction data necessary to compare flame and non-flame decomposition and to act as a guide for types of experimentation needed for establishing an incinerability ranking that could account for different modes of failure.

Two flame reactors were employed which allowed the relative destruction of compounds to be observed under two limiting mixing conditions. A micro-spray reactor consisting of a laminar premixed flat flame was used to investigate the effect of thermal and stoichiometric parameters on destruction efficiencies of individual droplets where large-scale turbulent mixing was not important. The second flame reactor utilized was the turbulent flame reactor which is similar to a real system in that it consisted of a turbulent diffusion spray flame burning a mixture of hazardous waste and an auxiliary fuel. It was utilized to investigate atomization, mixing, and quenching parameters.

In the subsequent section the details of the experimental approach utilized in this study are discussed. In section 4 the results from both reactors are presented and discussed in terms of the behavior of different test compounds under a variety of incineration failure conditions; the flame data are compared with the proposed incinerability rankings and the conclusions of the study and recommendations for further effort are discussed in section 5.

Five compounds representative of liquid organic hazardous waste listed in the RCRA regulations (Appendix 8; 19 May 1980 Federal Register) were selected for these flame reactor studies. This limited number required that compounds be selected carefully to provide the maximum amount of comparison information.

The following criteria were utilized in the selection of test compounds:

1. Selected Compounds Show Variations in Incinerability Rankings. To provide as thorough a test of each of the incinerability ranking procedures as possible, the test compounds were selected to represent a wide variation within each ranking procedure. Since only five compounds were selected, it was necessary to give precedence to choosing compounds with wide variations in the heat of combustion and thermal decomposition rankings.
2. Nonflame Decomposition Data Exist. A direct comparison between thermal decomposition rankings and the flame-mode destruction rank-

ings requires that nonflame thermal decomposition data are available for all selected compounds.

3. Various Molecular Structures. The structure criteria consisted of two parts: First, the test compounds were selected to be representative of the various organic structures classified by the EPA as hazardous waste (Appendix 8 of the 19 May 1980 Federal Register). Second, an effort was made to select compounds with similar non-flame thermal decomposition data but whose structures were entirely different.
4. Liquid Compounds. Liquids were chosen for this first set of compounds because they represent the largest class of waste generated. Since only five test compounds were considered, it was also necessary to consider only liquids so that the results for the different compounds could be compared directly.

These selection criteria were derived directly from the program objectives. Of first importance was obtaining flame-mode destruction data for comparison with the several proposed ranking procedures; hence, the first criteria required that the proposed ranking procedures be well represented by the test compounds. A second objective required the comparison of flame and nonflame results. This objective dictated that nonflame thermal decomposition data be available. Also, compounds with entirely different molecular structure but similar thermal decomposition data were selected to determine if flame-mode rankings are structure-dependent. Testing of solid, liquid, and gaseous compounds in an experiment where only five compounds were used would have made the comparisons required in the objectives impossible. The rankings resulting from the tests could not be separated into physical and chemical causes with such a narrow data base; thus only liquid compounds were selected.

The list of selected compounds is shown in Table 2-1. All compounds are liquids at room temperature. The first order thermal decomposition parameters (pre-exponential term and activation temperature) are listed, along with the value for  $T_{99.99}$  for 1.0 sec. derived from the kinetic parameters. The time required for a droplet of initial diameter of 100  $\mu\text{m}$  to completely

TABLE 2-1. TEST COMPOUNDS AND PROPERTIES

| Compound and Structure                                   | Boiling Point | A<br>(sec <sup>-1</sup> ) | Activation Temperature Tact (K) | T <sub>99.99</sub> (K) | ΔH <sub>vap</sub> (cal/gm) | Evap. Rate (msec)       | NBS Ranking | ΔH <sub>c</sub> (kcal/gm) | AIT (K)                |
|--|---------------|---------------------------|---------------------------------|------------------------|----------------------------|-------------------------|-------------|---------------------------|------------------------|
|  | (K)           | (1)                       | (1)                             | (2)                    | (3)                        | (4)                     | (5)         | (6)                       | (7)                    |
| Benzene  | 352           | 7.4 x 10 <sup>21</sup>    | 48,300                          | 1,007                  | 103.57                     | 14.4                    | 4           | 10.03                     | 836                    |
| Chlorobenzene  | 405           | 1.3 x 10 <sup>17</sup>    | 38,200                          | 1,038                  | 77.59                      | 10.8                    | 3           | 6.6                       | 911                    |
| Chloroform CHCl <sub>3</sub>                             | 355           | 2.9 x 10 <sup>12</sup>    | 24,500                          | 925                    | 64.75                      | 9.0                     | 18          | 0.75                      | -                      |
| 1,2-Dichloroethane CH <sub>2</sub> Cl-CH <sub>2</sub> Cl | 356           | 4.8 x 10 <sup>11</sup>    | 23,000                          | 931                    | 85.3                       | 11.9                    | 28          | 3.0                       | 686                    |
| Acrylonitrile CH <sub>2</sub> =CH-CN                     | 351           | 2.1 x 10 <sup>12</sup>    | 26,300                          | 1,003                  | 149.84                     | 20.8                    | -           | 7.93                      | 754                    |
| Highest (8)  | NA            | NA                        | 48,300 (Benzene)                | 1,112 (Methane)        | 241 (Methanol)             | 33.5 (Methanol)         | NA          | 10.14 (Toluene)           | 988 (Phenol)           |
| Lowest (8)   | NA            | NA                        | 11,300 (DDT)                    | 754 (DDT)              | 46.42 (CCl <sub>4</sub> )  | 6.4 (CCl <sub>4</sub> ) | NA          | 0.13 (CHBr <sub>3</sub> ) | 363 (CS <sub>2</sub> ) |

(1)  $C/C_0 = \exp(-kt)$ ;  $k = A \exp(-T_{act}/T)$ . (Values are from Lee et al., 1979 and 1982 except chloroform (Dellinger, 1982).)

(2) Temperature for 99.99 percent DE at  $t = 1$  sec. [Values from same sources as (1)].

(3) Latent heat of vaporization.

(4) Time for 100 μm droplet to evaporate at 1000 K.

(5) Rank 1 is most difficult to incinerate. [Adapted from Tsang and Shaub (1981).]

(6) Heat of combustion.

(7) Autoignition temperature.

(8) Highest and lowest values observed in each category.

NA - Not appropriate

evaporate is also shown. A variety of organic structures are represented. Benzene and chlorobenzene are aromatic, chloroform is a chlorinated methane, 1,2-dichloroethane is a chlorinated ethane, and acrylonitrile contains nitrogen. Although AIT data are not available for chloroform, it was included because of its very low heat of combustion. Acrylonitrile was selected because it has almost the same  $T_{99.99}$  as benzene, but has a different structure. For reference, the highest and lowest values for compounds that have been determined in each ranking system are included to indicate the range of values covered by the selected test compounds. The selected compounds represent greater than 90 percent of the range covered by listed compounds for heat of combustion (.13 to 10.14 kcal/gm), and encompassed roughly 70 percent of the compounds tested to data for non-flame decomposition temperature, autoignition temperature, and the NBS incinerability ranking.

### 3.0 EXPERIMENTAL EQUIPMENT

In this section the experimental systems are introduced. Discussion topics include the reasons for selecting two distinct reactor designs, the physical description of the two reactors and their associated equipment, the sampling and analytical systems, and the laboratory facility.

The discussion in the previous section indicated that several potential escape mechanisms exist for the flame zone of liquid injection incinerators. This research program addressed the incinerability rankings that resulted from the laboratory simulation of these failure modes. In order to investigate a variety of realistic failure modes for liquid injection incinerators, considerable experimental flexibility was necessary. This flexibility was obtained through two reactor designs: the microspray reactor and the turbulent flame reactor (TFR).

The microspray experiment was designed to study the rankings that result from individual droplet processes without large-scale turbulent mixing. These processes include:

- Droplet physical processes such as evaporation, liquid phase reactions, etc.
- Flame zone chemistry in the immediate droplet vicinity.
- Nonflame decomposition chemistry away from the immediate droplet vicinity.

The experiment was designed to bridge the gap between the non-flame thermal decomposition experiments and the turbulent flame data. As such, it included two processes in addition to those present in the thermal decomposition experiments : droplet vaporization dynamics and flame reactions. The data were used for the following purposes:

- To determine what portion of the turbulent flame rankings were due to droplet flame and evaporation processes.
- To compare flame (microspray) vs. non-flame (thermal decomposition) destruction on a fundamental level without the complicating influence of turbulence.

The TFR included all of the processes that occur in the microspray, and the following:

- Droplet-droplet interactions in a high number density droplet field.
- Turbulent mixing.
- Thermal quench.

### 3.1 Microspray Reactor

The microspray reactor was employed in this program in order to investigate single droplet reactions without limitations associated with turbulent mixing. Data from this reactor could be easily interpreted in terms of how thermal parameters influenced compound incinerability in the absence of atomization, mixing, or quenching limitations. The microspray reactor (Figure 3-1) is a modification of flame reactors used previously in the study of the thermal decomposition of pulverized coal particles and heavy fuel oil droplets (Seeker et al., 1981b; Kramlich et al., 1981). In these flame reactors, particles or droplets of the material to be studied (in this particular case, droplets of hazardous waste) are injected through a laminar, premixed, hydrocarbon flat flame and thermal decomposition of the material takes place in a flame environment. The reactor was chosen because it can provide a gas-phase environment similar to that experienced by droplets in the near field of spray flames. Badzioch (1967) first specified the criteria necessary to study the decomposition of solid fuels appropriate for a flame environment. For liquid fuels, those criteria can be specified as follows:

- The gas-phase temperature must be in the range of normal flame temperatures (up to 2000 K) and be well-defined and controllable.
- The fuel must be in the form of droplets in the size range (20-200  $\mu\text{m}$ ) representative of commercial fuel injectors.
- The droplets should be well-dispersed in a gas-phase environment which is similar to the recirculated products in the near-field of the flame in order to simulate the contacting between liquid and gas.

Previous work with this reactor has shown that it meets these criteria and the data generated on the decomposition of pulverized coal compare favorably



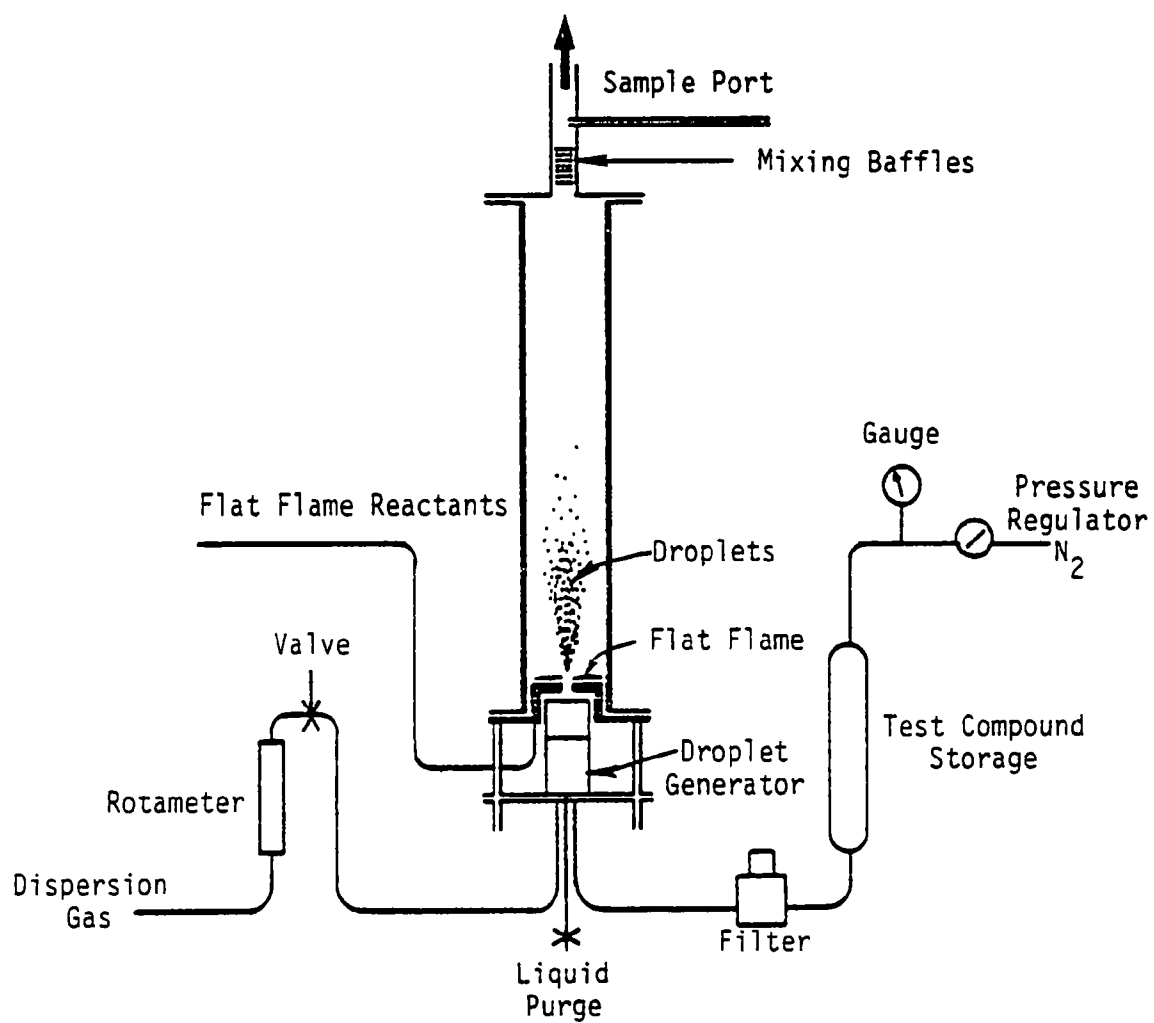


Figure 3-1. Microspray reactor.

with in-flame data from larger scale turbulent diffusion flames (Seeker and Heap, 1982).

In the reactor, monodisperse droplets are injected into hot postflame gases. The droplets are sufficiently dispersed to prevent droplet-droplet interaction. Thus, the reactor behavior is characteristic of an ensemble of individual droplets. This droplet dispersion is accomplished by ballistically injecting droplets through an opening in the center of a flat-flame burner. The burner is shown in Figure 3-2 and consists of an 8.9-cm-square piece of ceramic honeycomb (Corning Celcor Cordierite, 39 cells/cm<sup>2</sup>). The premixed main burner flow enters through the rear of the burner and is distributed to the honeycomb through the porous stainless steel plate. These premixed gases form a flat flame that is stabilized within 2 mm of the face of the honeycomb by heat loss to the burner.

The droplet stream enters the reactor through a 1.3-cm-diameter opening in the burner center. Monodisperse droplets are generated by the Berglund-Liu vibrating orifice technique (TSI Model 3050). In this technique, liquid is forced through a small orifice to form a liquid jet; in this study the orifice diameter was 20  $\mu\text{m}$ . A schematic of the droplet generator is shown as Figure 3-3. The orifice plate is vibrated by a piezoelectric ceramic to induce an extremely regular breakup of the jet into monodisperse droplets (Berglund and Liu, 1973). In the present study, the droplet diameter was 38  $\mu\text{m}$ , although diameters between 20 and 200  $\mu\text{m}$  are possible. This diameter and the droplet spacing were verified by high magnification spark shadow photography.

The droplets emerge from the generator in a single column and agglomerate unless dispersed. Dispersion is accomplished by passing the droplets through a second orifice with a small amount of dispersion gas. The oxygen content of the dispersion gas was adjusted such that the stoichiometry, including the droplets, was constant throughout the burner. The flat flame is located at the inlet end of a 10-cm-square by 100-cm-long chimney (Figure 3-1) within which the droplet reactions occur.

Two chimneys are available. One is fitted with Vycor windows to permit visual observation of the droplet flame. Because of the potential for

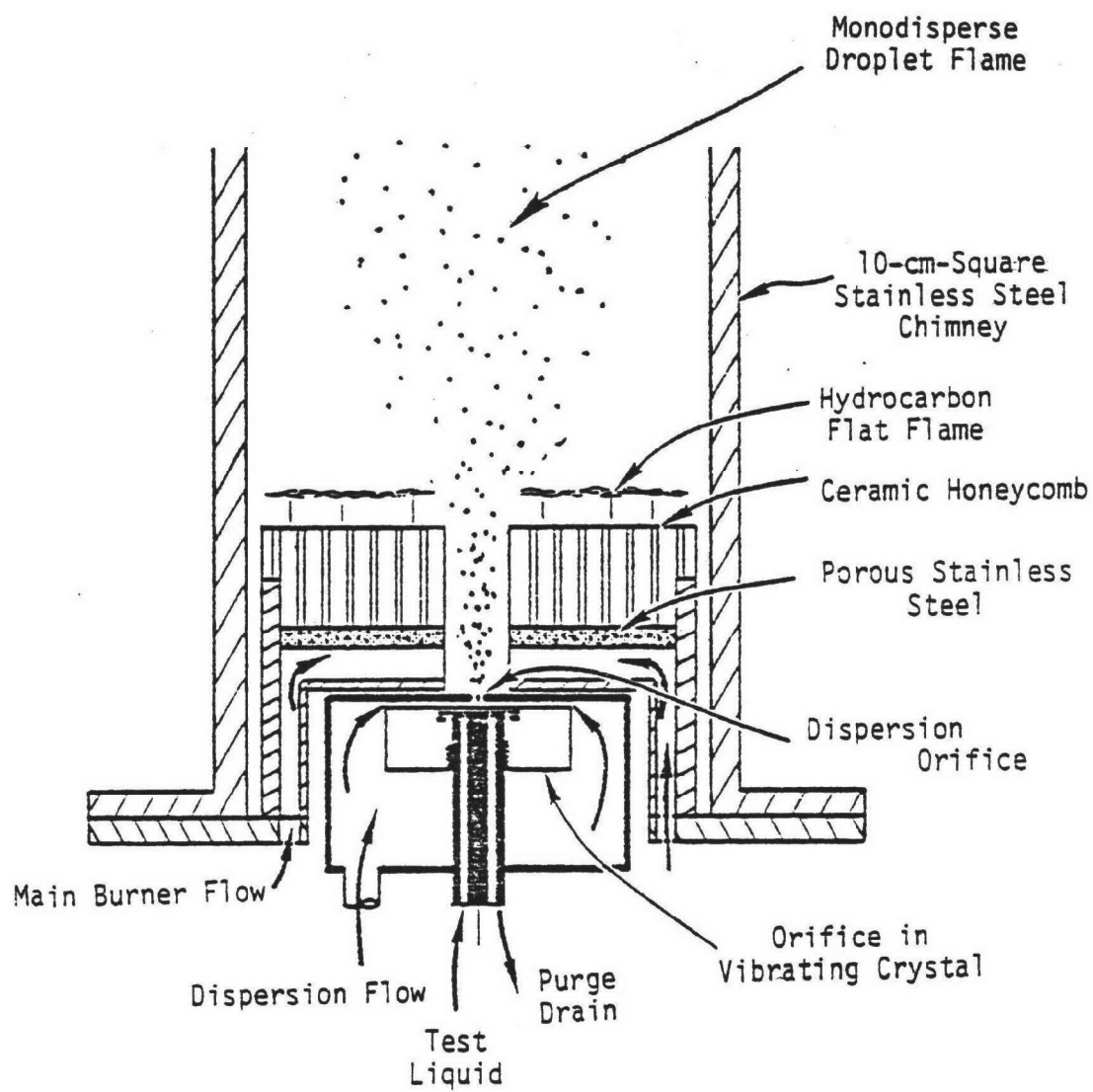


Figure 3-2. Details of microspray reactor.

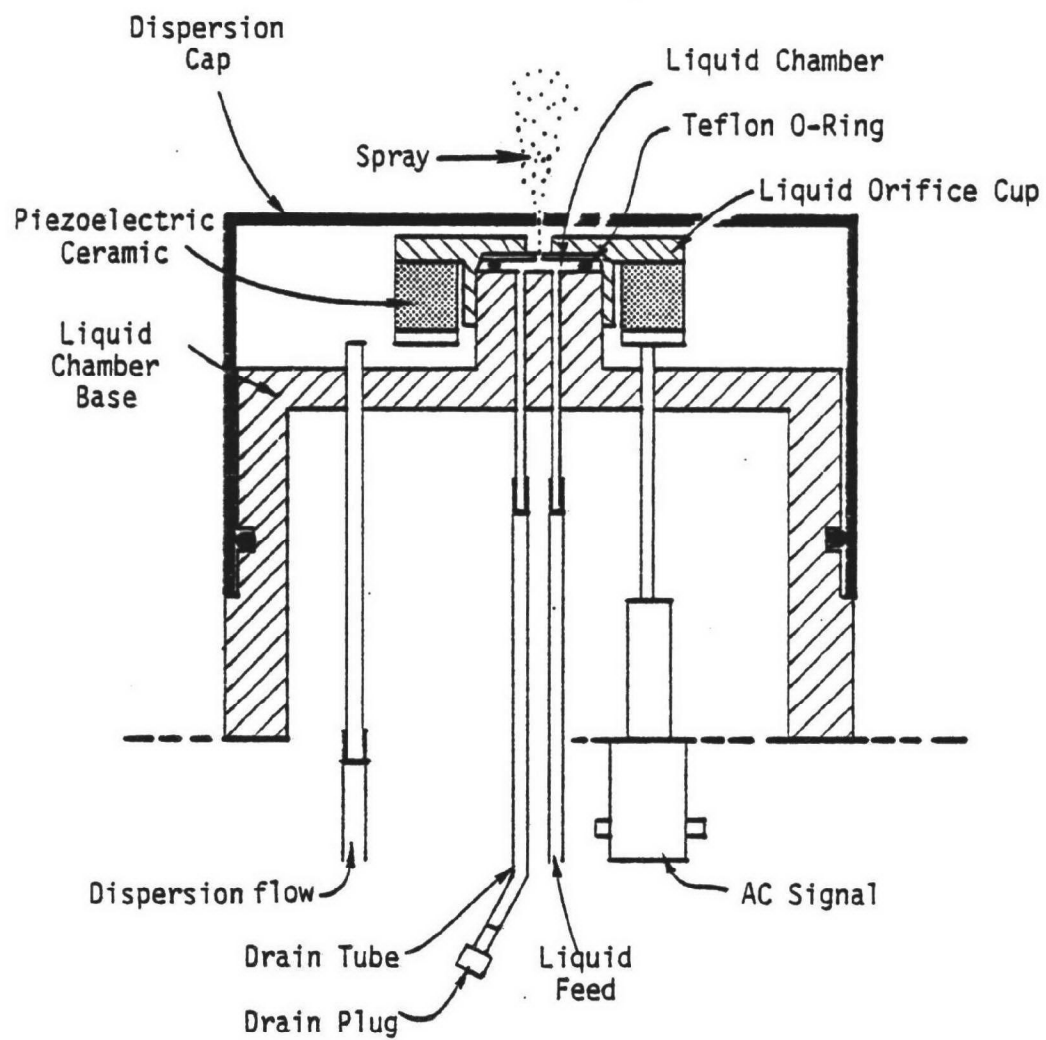


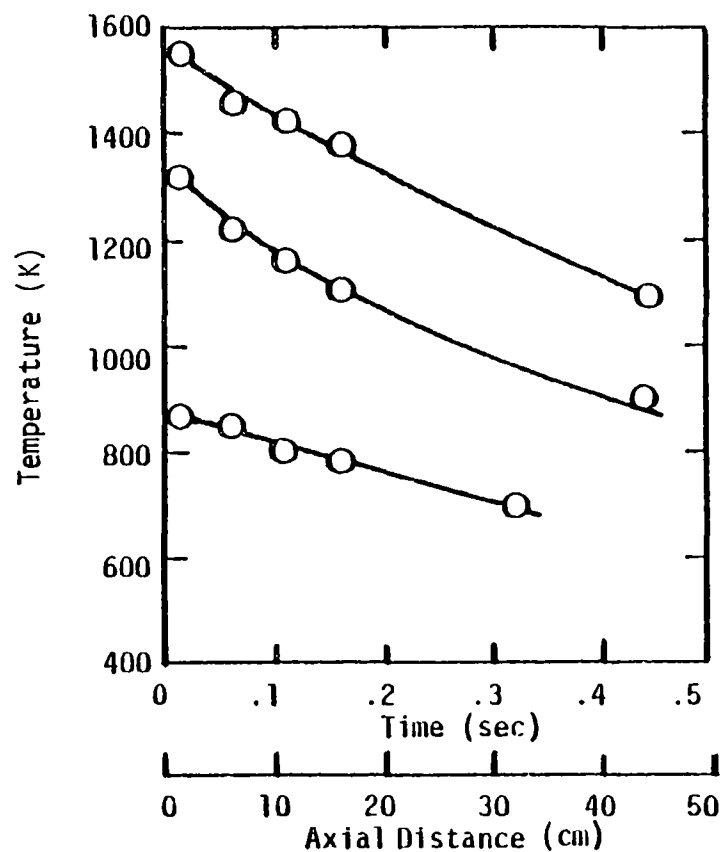
Figure 3-3. Schematic diagram of the droplet generator.

window seal leakage, a second chimney without windows is used for concentration measurements. The exhaust gases pass through a tube containing baffles to mix the gas uniformly prior to sampling.

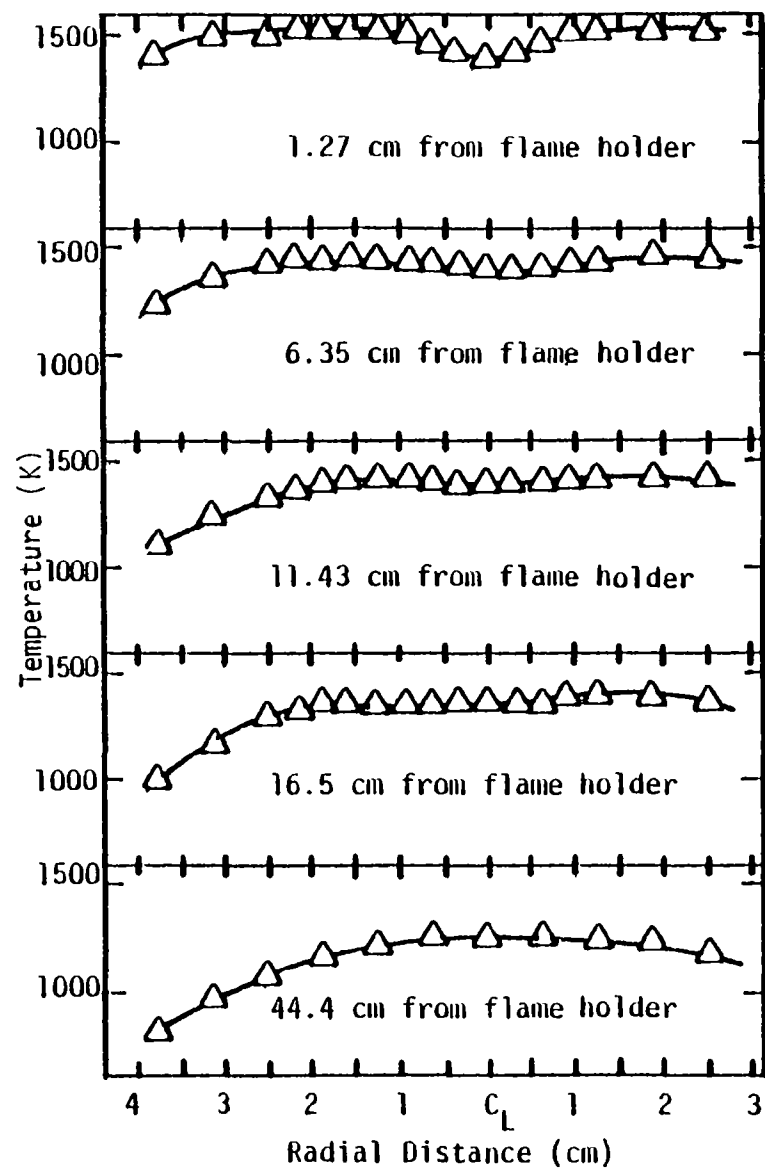
The main burner gas for the microspray consists of an  $H_2/N_2$ /air mixture. The air is obtained from a compressed air supply, two-stage pressure regulated, and double filtered prior to the flow control rotameter. The hydrogen and nitrogen are obtained from vendor-supplied compressed gas bottles. The flow control panel and its calibration are the subject of Appendix A.

In this study, the microspray reactor was used to investigate the impact of two controllable parameters on the relative thermal destruction of hazardous waste compounds: temperature and stoichiometry. In addition, the characteristics of pure waste compounds were compared to those of mixtures of waste compounds. One potential failure mode dealing with the flame condition is too low a flame temperature to destroy the waste constituents. The flat-flame temperature was controlled by varying the amount of diluent nitrogen in the flame reactants. This flat flame temperature was the "ambient" temperature within which the droplet flames occurred. After ignition, however, the droplet flame temperature was expected to exceed the local flat-flame temperature. Typical axial profiles of the gas-phase temperatures as measured with a type-R (Pt/Pt--13 percent Rh) thermocouple on the center line of the chimney are presented in Figure 3-4a. Radial temperature profiles (Figure 3-4b) indicated that the gas-phase temperature across the reactor was relatively uniform except near the edges of the reactor. These measurements were made with droplet dispersion flow but without droplets. Since the droplets were dispersed only around the center of the reactor with a maximum diameter of 3 cm, the individual droplets all were subjected to an identical temperature history which altogether avoided the influence of the walls. The temperature history was controlled by the flame temperature which was implied by extrapolating the axial temperature measurements to the burner face. The destruction data was determined as a function of this extrapolated measured flame temperature.

Compound effects were also investigated for two extremes in stoichiom-



(a) Gas phase temperatures on center line of microspray reactor for different flame conditions.



(b) Gas phase temperature as a function of axial and radial distance for one flame condition.

Figure 3-4. Gas temperature measurements in microspray reactor.

etries, rich and lean. For rich conditions, the flat flame was operated with no excess oxygen ( $SR = .83$ ). Under these conditions the droplets evaporated and thermally decomposed without sufficient oxygen available to support droplet combustion. For lean conditions the burner stoichiometry and nitrogen diluent flow were adjusted to maintain 10 mole percent oxygen in the post-flame gas. In this case, oxygen was available throughout the reactor, allowing the droplets to ignite and burn.

The final parameter investigated in the microspray reactor was mixtures of compounds. The majority of the data were taken on equimolar mixtures of four compounds. The use of mixtures assured that the compounds were initially exposed to the same time/temperature and stoichiometry, and hence any measured differences could be attributed to the compound itself. A limited set of data were obtained on pure compounds for comparison.

### 3.2 Turbulent Flame Reactor

The turbulent flame reactor (TFR) was designed especially for the present program to provide a turbulent liquid spray flame, including swirl, recirculation, broad drop-size distribution, and high variation in droplet number density. It was particularly important that the reactor be capable of simulating the compound escape mechanisms that can occur for flame zones of liquid injection incinerators. Very high heat removal rates were utilized to quench postflame reactions. Thus, the destruction which occurred in the turbulent diffusion flame was emphasized over nonflame decomposition which can occur in the postflame region. The reactor design is based on a configuration for which aerodynamic field data are available (Baker et al., 1975).

The reactor consists of a swirling air/liquid spray burner firing into a 30.5-cm-diameter by 91.5-cm-long water-cooled cylindrical enclosure shown in Figure 3-5. The water-cooled cylinder is made of 304 stainless steel and is formed into three interchangeable segments which are joined by flanges and gasketing. The lowest segment has four sight glass ports, one of which is used for flame ignition. The reactor top plate contains an exhaust fitting which includes the sampling ports, and a Vycor plate/mirror arrangement for obtaining an axial view of the flame.

The burner consists of a pressure-atomized nozzle (Delavan WDA series)

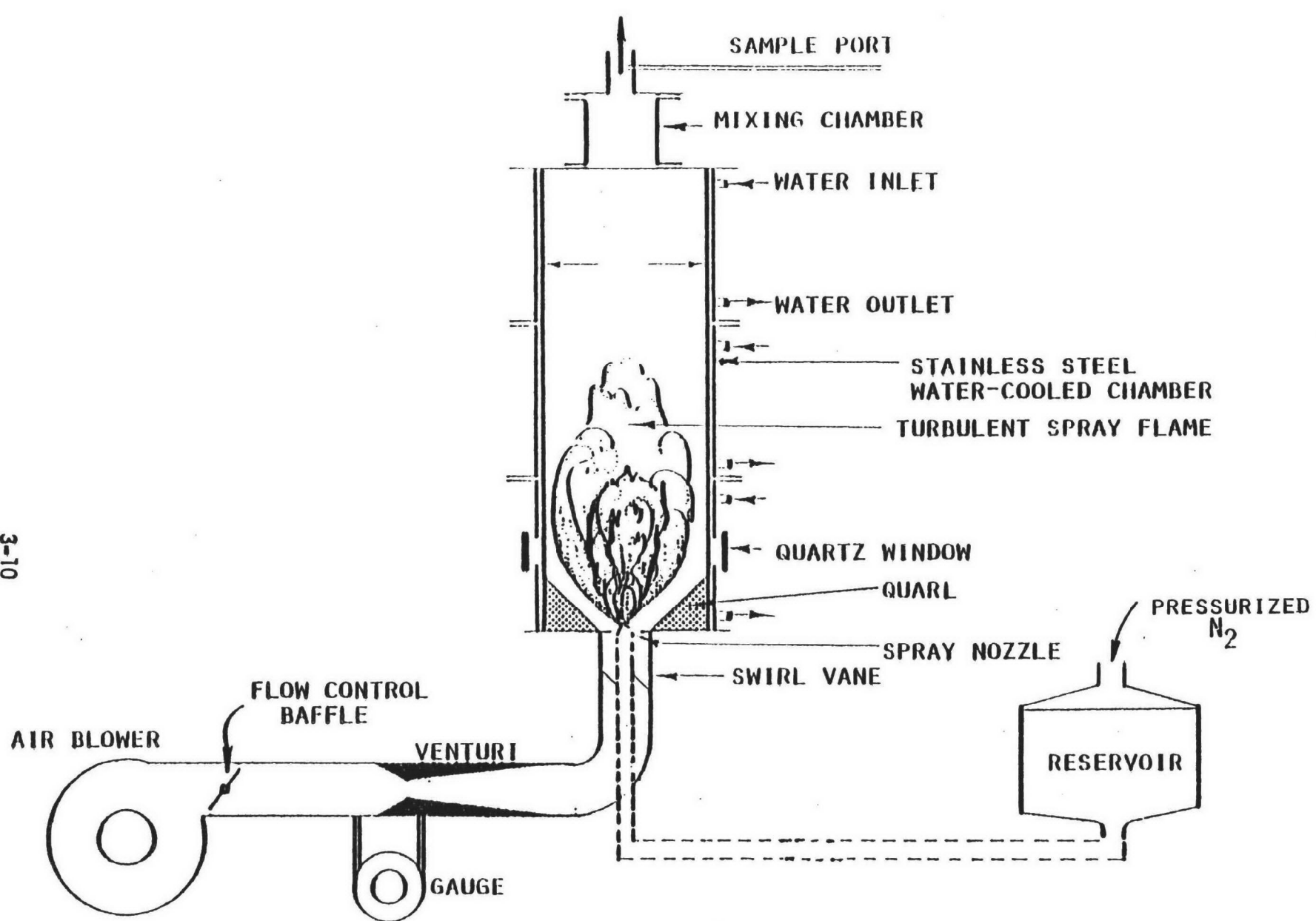


Figure 3-5. Turbulent flame reactor.



located level with the bottom plate of the reactor as shown in Figure 3-6. The main burner air is introduced through the annular space around the nozzle. Variable area flow constrictors were fixed into this space to vary burner air velocity independently of air flow rate. Interchangeable swirl vanes are placed into the gap between the constrictor and the nozzle shaft. The vane angle was set to provide a swirl number of unity for the present study. (Swirl number is defined as the ratio of angular momentum to axial momentum for the swirling air flow.) To provide a smooth entry of air into the burner and to prevent corner recirculation, a castable refractory quarl is placed in the lower water-cooled segment. As shown in the figure, this has the form of a 45-degree cone.

The liquid fuel feed system consists of a pressurized storage tank. The fuel-flow vs. tank-pressure calibration is discussed in Appendix A. The tank is pressurized with bottled nitrogen and the pressure is regulated with a two-stage bottle regulator. The burner air flow is supplied by a high-pressure-head rotary blower and is metered with a venturi flow meter. The calibration is discussed in Appendix A.

The normal operating conditions for the TFR were selected by considering commercial practice, visual flame stability, low exhaust CO ( $<75$  ppm) and total hydrocarbon measurements ( $<20$  ppm), and high destruction and removal efficiency of hazardous waste compounds. The conditions chosen for this normal operating mode are specified in Table 3-1. Under this condition, extremely high DRE levels of the test compounds were achieved ( $> 99.995$  percent). The actual test conditions investigated for the TFR were selected to allow specified failure conditions to exist. Several variations from the normal operating conditions were investigated which had little influence on the high flame destruction efficiency of the hazardous waste constituents. These included auxiliary fuel type (No. 2 fuel oil), burner throat velocity and test compound concentration (up to 25 percent). Those variations which did result in significant deterioration in flame performance and were thus used to investigate the relative compound destruction under failure conditions included:

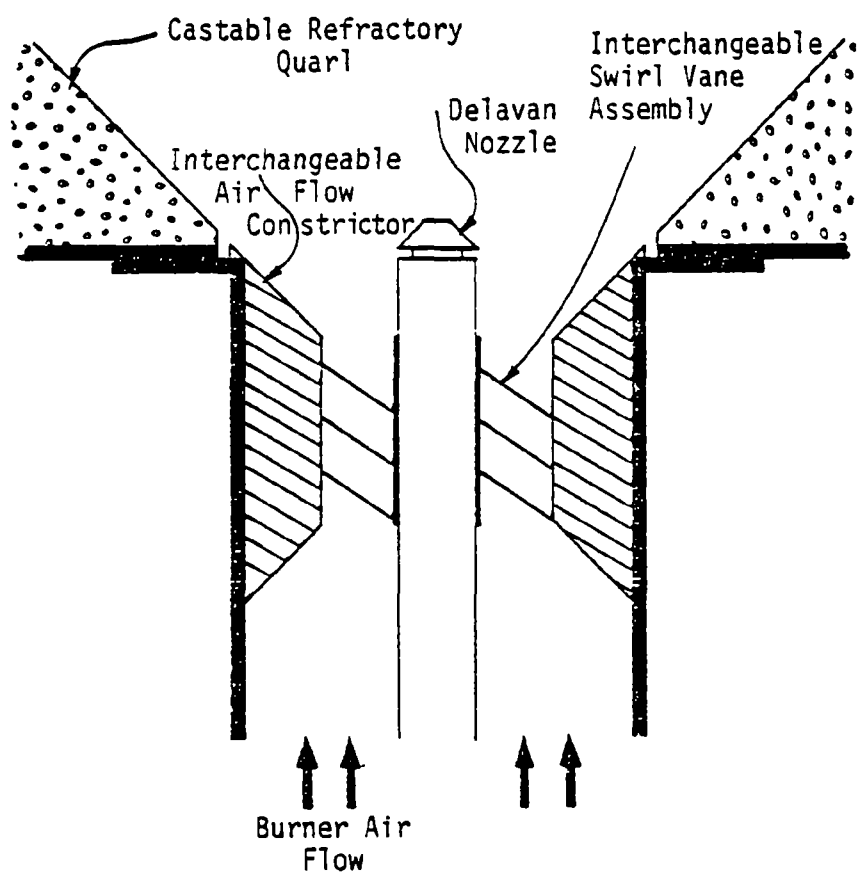


Figure 3-6. Turbulent flow reactor burner detail.

TABLE 3-1. NORMAL OPERATING CONDITIONS FOR TURBULENT FLAME REACTOR

| NOZZLE                                   | Delavan Pressure Jet, Hollow Cone, 60° Spray Angle Model WDA-60 <sup>0</sup> -1.5 |
|--|---|
| NOZZLE PRESSURE                          | 103 psig  |
| AUXILIARY FUEL                           | Heptane   |
| FUEL FLOW RATE                           | 1.4 gm/sec (11 lb/hr)   |
| AIR FLOW RATE                            | 14.3 l/sec (1830 ft <sup>3</sup> /hr)   |
| BURNER THROAT VELOCITY                   | 7.1 m/sec (23.3 ft/sec)   |
| BURNER SWIRL NUMBER                      | 1.0   |
| EXCESS AIR                               | 30%   |
| BURNER HEAT RELEASE RATE                 | 38 kW (131,000 Btu/hr)  |
| TEST COMPOUND CONCENTRATION              | 3% by Mass  |
| EXHAUST CONCENTRATIONS                   | CO: 75 ppm<br>Total Hydrocarbons: 20 ppm  |
| DESTRUCTION EFFICIENCY OF TEST COMPOUNDS | >99.995%  |

- Low excess air
- High excess air
- High excess air and low load
- Poor atomization quality
- Quench coils within flame

The exhaust concentration of test compounds were measured under these failure conditions for mixture of compounds in the auxiliary fuel along with continuous measurements of CO and hydrocarbon to indicate overall flame performance.

### 3.3 Laboratory Facility

The laboratory facility is designed to:

- Facilitate ease of operation
- Prevent laboratory air contamination during routine operation.
- Physically separate working personnel and experiments from incidental workers and bystanders.
- Minimize the hazards associated with equipment malfunctions and accidents such as spills, broken lines, fires, and utility outages.

To meet these design objectives, the laboratory is divided into a reactor room and a control room. The reactor room contains all of the facilities for handling the test compounds, including storage, preparation, and waste handling. The reactor room is isolated from the general building air flow system and is independently ventilated. Both reactors were located within ventilated enclosures. The systems were designed so that both reactors could be shut down from the control room without entering the reactor room.

### 3.4 Analytical Systems

The test compound destruction measurements are performed by adsorption onto Tenax resin followed by thermal desorption and gas-chromatograph/flame-ionization detector analysis. The details of the system design, calibration, determination of compound breakthrough volumes, and minimum sensitivity tests are discussed in Appendix B.

In addition to the destruction efficiency tests, measurements of CO, CO<sub>2</sub>, O<sub>2</sub>, and unburned hydrocarbons are performed.

### 3.4.1 Measurement of Destruction Efficiency (DE)

The equipment and techniques of the DE measurements are discussed in detail in Appendix B and are similar to those of Parsons and Mitzner (1975), and Dellinger et al. (1982). The technique, in summary consists of the adsorption of waste compound from a known quantity of sample gas onto Tenax-GC. This is accomplished by passing sample gas through an externally water-cooled Pyrex cartridge packed with Tenax. At the conclusion of sampling, the cartridge is thermally desorbed and the contents are analyzed by flame ionization gas chromatography (GC-FID). The procedure is to insert the cartridge into the helium carrier gas line so that the helium flows sequentially through the cartridge, the Porapak-Q column and the FID. The cartridge is placed within an aluminum block heater which heats the cartridge to 120 C for a sufficient time to desorb the test compounds and deposit them on the inlet of the room temperature GC column. Following desorption the column oven is temperature programmed, the compounds separated, and the compound concentration measured.

The analytical technique is calibrated by sampling and analysis of known gas-phase concentrations of the test compounds. The sampling flow rate was optimized and the breakthrough volumes for each compound were determined to be greater than the sampling volume; these tests are detailed in Appendix B.

One limitation with the present analytical system is that two of the test compounds, benzene and 1,2-dichloroethane, could not be resolved by the Porapak column. To avoid this problem two sets of compound mixtures are used to prevent the simultaneous use of these two compounds. The mixtures are: 1) containing chlorobenzene, benzene, acrylonitrile, and chloroform; and 2) containing chlorobenzene, acrylonitrile, 1,2-dichloroethane, and chloroform.

The Tenax-GC technique was selected because of its high sensitivity (1.5 ppb or 99.995 percent DE in the TFR) and the relatively rapid sample turnaround time (1.5 hr). The technique is compatible with both the TFR and microspray in that test compounds, auxiliary fuel, and products of incomplete combustion encountered in this study were adequately separated. Repetitive calibration tests have indicated an inherent experimental scatter that corresponds to  $\pm 5$  percent at the 90 percent confidence level (See Appendix D).

The regulations require that trial burn POHC Destruction and Removal Efficiency (DRE) be 99.99 percent. DRE is based on the efficiency of both the incinerator and any stack gas cleaning system. In the present experiment there is no stack gas cleaning equipment before the measurement point, so experimental destruction performance is reported as Destruction Efficiency (DE) in this report rather than as DRE.

#### 3.4.2 Other Measurements

In addition to the DE tests, the measurements shown in Table 3-2 were performed. In any fuel-lean hydrocarbon flame, the overall efficiency is defined in terms of fuel utilization. Fuel is fully utilized when all fuel and fuel fragments are oxidized into  $\text{CO}_2$  and water. Any CO, fuel, or fuel fragments that exist in the exhaust represent lost efficiency. Thus, the CO and unburned hydrocarbon measurements are used as an indication of flame efficiency. The  $\text{CO}_2$  and  $\text{O}_2$  measurements are used to calculate the burner stoichiometry. This calculated burner stoichiometry is compared with the stoichiometry based on the fuel and air flow rates to detect any operational flow problems.

A means of independently verifying the DE calculation procedure is to utilize a tracer whose concentration is not changed by the flame. If the tracer does not appear at the concentration expected from the fuel flow, then the DE calculation is being improperly done or uncontrolled loss of tracer is occurring within the reactor or sampling system. One such tracer is the chlorine present in three of the test compounds. In the flame, chlorine is quantitatively converted to hydrochloric acid, HCl. Stack gas HCl concentrations are measured and compared with the flow of chlorine entering with the fuel. A closed chlorine mass balance is a check for uncontrolled compound losses and, in particular, a cross-check on the DE calculation procedures.

An HCl measurement technique ( $\text{Cl}_2$  was not expected nor observed at the experimental conditions) was utilized which involved collection in midget impingers containing 0.1 normal NaOH. At the conclusion of sampling, the liquid is titrated against 0.01 normal mercuric nitrate. A normal acid-base titration cannot be used because of dissolved  $\text{CO}_2$  interference; mercuric nitrate is chlorine-specific.

TABLE 3-2. EXPERIMENTAL MEASUREMENTS

| Species or Variable   | Measurement Technique  |
|-----------------------|--|
| CO                    | Anarad nondispersive infrared analyzer   |
| CO <sub>2</sub>       | Beckman nondispersive infrared analyzer  |
| Hydrocarbons          | Beckman Model 402 total flame ionization detector  |
| O <sub>2</sub>        | Taylor paramagnetic analyzer   |
| Gas Temperature       | <ol style="list-style-type: none"> <li>1. Microspray flame: Type S (platinum-rhodium) uncoated fine-wire thermocouple</li> <li>2. Turbulent flame exhaust: Type S thermocouple</li> <li>3. Microspray exhaust: Type B (copper-constantan) uncoated thermocouple</li> </ol> |
| Compound Mass Closure | Stack gas HCl measurement  |

A limited series of measurements were performed in the TFR to assure closure of Cl mass balance. Table 3-3 shows the expected ppm of HCl against the measured stack HCl. The results indicate that within the experimental error of HCl measurement the chlorine mass balance is closed. These data were obtained at a high DE ( 99.995 percent) condition in the TFR.

TABLE 3-3. CHLORINE MASS CLOSURE

| HCl Expected<br>(ppm) | HCl Measured<br>(ppm) |
|-----------------------|-----------------------|
| 340                   | 339.6                 |
| 350                   | 336.9                 |



#### 4.0 RESULTS AND DISCUSSION

Through the use of two flame reactors, the impact of a number of possible incinerator failure modes on relative compound destruction has been explored. The microspray reactor provided information on the behavior of droplets in a laminar environment without turbulent mixing limitations. The impact of thermal parameters were investigated for the following conditions for pure test compounds and test compound mixtures:

- Fuel-rich flat-flame: insufficient oxygen available to support droplet flames.
- Fuel-lean flat-flame: post-flat-flame gas contains 10 mole percent oxygen which is available for reaction with test compounds.

Other failure conditions (i.e., those caused by poor atomization, solid surface quenching, and turbulent mixing limitations) cannot be effectively investigated in the microspray reactor and were investigated in the turbulent flame reactor.

##### 4.1 Microspray--Droplet Decomposition in Flames

In the microspray flame reactor, droplets of test compounds were injected through a flat-flame. The droplets were widely dispersed in the laminar plug flow region of the reactor to prevent interactions between individual droplets or the flamelets around individual droplets. The impact of several parameters on the relative decomposition of test compounds were investigated. The parameters were controlled primarily by the conditions established by the support flat flame and included the flat-flame temperature, the availability of oxygen for oxidation of test compounds, and the effect of using droplets of pure compounds compared with droplets of compound mixtures.

The major emphasis of this study was the relative behavior of different compounds to flame conditions in order to determine if one compound was more likely to escape destruction than another. The majority of the data were obtained using mixtures of compounds. In that way, the test compounds were assured of experiencing the same time/temperature history. Exhaust measurements of the test compound concentration were made for each compound in the mixture and compared. These measurements were made at each condition

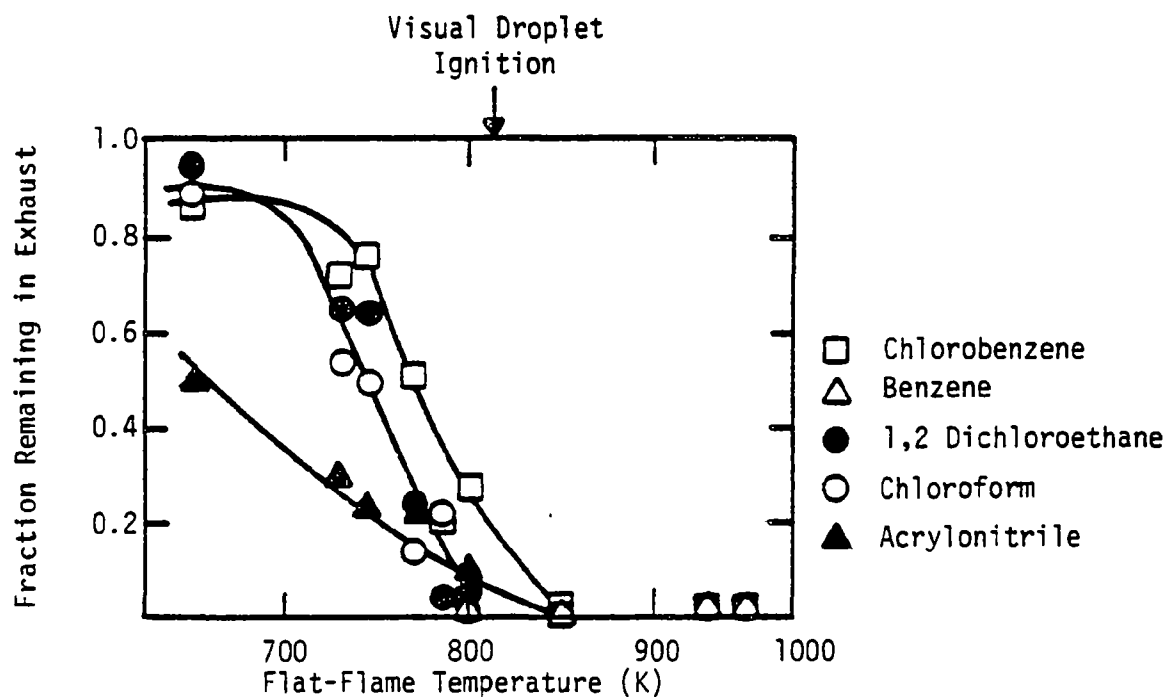
established by the support flat flame in order to examine if changes in the relative compound destruction would occur for different conditions. The relative order of test compounds measured in the microspray flame environment will later be compared to proposed incinerability ranking techniques (section 5).

#### 4.1.1 Droplets of Mixtures in an Oxygen-Rich Flame

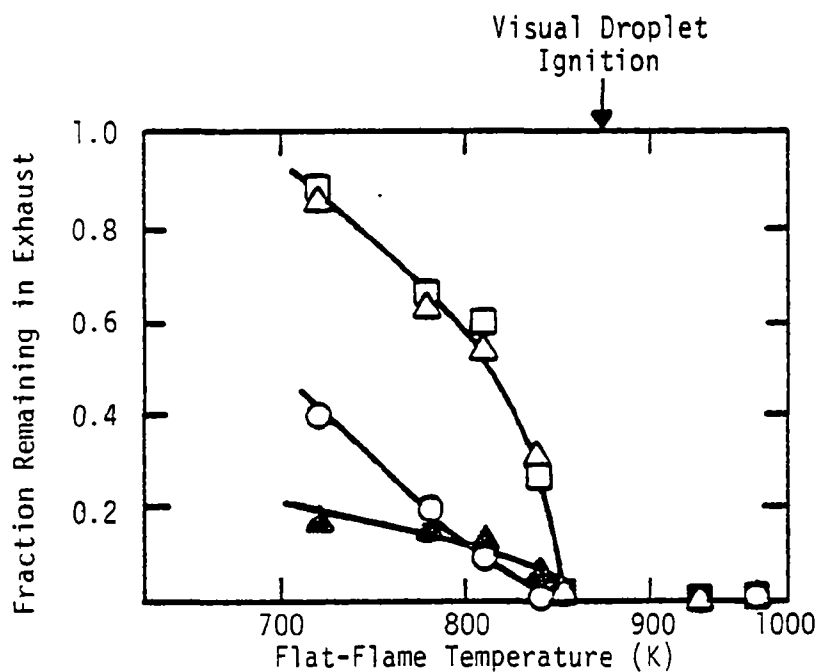
In these tests, 38  $\mu\text{m}$  droplets of two mixtures were separately injected into a lean  $\text{H}_2/\text{air}/\text{N}_2$  flame. Exhaust plane concentrations of the test compounds were measured for different flat-flame temperatures. The flat-flame burner flow rates were adjusted to provide 10 mole percent oxygen in the post-flame gas and to hold the (cold) gas velocity through the flat-flame burner at 25 cm/sec. Gas temperature was the only variable; it was controlled through the use of reactant flow rates while maintaining 10 percent excess oxygen and 25 cm/sec flame velocity. The flat-flame temperature range was selected to encompass complete compound destruction at high temperatures and small destruction levels at low temperatures (i.e., 600-1100 K).

The results for the mixture of chlorobenzene, acrylonitrile, chloroform, and 1,2-dichloroethane are shown in Figure 4-1a. The fraction of each of the test compounds that escaped the reactor unreacted is plotted against the flat-flame temperature. The plot indicates that at low flat-flame temperatures (650 K) all of the compounds except acrylonitrile passed through the reactor with essentially no reaction. As the flame temperature was increased the fraction of the compound that reacted increased up to a flame temperature of 850 K, above which destruction of all compounds became complete. At 850 K and above no trace of compound was analytically indicated which demonstrated that DE was at least 99.995 percent.

These DE measurements were supported by visual observation of the droplet behavior in the reactor. For temperatures at and above 825 K the droplets supported individual flamelets; the minimum droplet ignition temperature is indicated on the figure. Below the ignition temperature a very faint form of chemiluminescence was observed in the area of the droplet stream. This indicated that some form of radical reaction not associated with individual droplet flames occurred below the droplet ignition temperature.



(a) Mixture containing Dichloroethane, Chlorobenzene, Chloroform and Acrylonitrile



(b) Mixture containing Benzene, Chlorobenzene, Chloroform and Acrylonitrile

Figure 4-1. Fraction of test compound remaining in microspray exhaust when 38  $\mu\text{m}$  droplets of mixtures of compounds were injected into lean (10 % post-flame oxygen)  $\text{H}_2/\text{air}$  flames as a function of flame temperature.

In Figure 4-1b, similar results are presented for the mixture in which benzene replaced 1,2-dichloroethane. The qualitative features are identical to those of Figure 4-1a; i.e., well-defined droplet ignition point, high DE above droplet ignition, slow destruction reaction below droplet ignition. The data indicated that the ignition point had shifted from 825 K for 1,2-dichloroethane mixture to 875 K for the benzene mixture. This was probably due to the effect of the substitution of benzene for 1,2-dichloroethane on the droplet ignition temperature. These results indicated that:

- If a droplet flame was observed to be present, then destruction efficiency was greater than 99.99 percent.
- The composition of the mixture determined the actual ignition temperature of the droplet; however, if the droplet was ignited, the destruction efficiency was sufficiently high that no compound differences were measured (i.e., no ranking could be determined).
- At temperatures below ignition a form of incomplete oxidative, radical-assisted decomposition occurred.

The rankings generated by this experiment were dependent upon the flat-flame temperature:

- Well below ignition (650-750 K), the decomposition ranking in terms of most difficult to easiest to remove was: chlorobenzene, benzene, 1,2-dichloroethane, chloroform, and acrylonitrile.
- Immediately below ignition temperature the ordering changed to: benzene, chlorobenzene, acrylonitrile, 1,2-dichloroethane, and chloroform.
- Temperatures above the ignition point resulted in very high DE, so no ranking was obtained.

The thermal decomposition ( $T_{99.99}$ ) and AIT ranking (Table 2-1) is chlorobenzene, benzene, acrylonitrile, 1,2-dichloroethane, and chloroform. Except for the placement of acrylonitrile the  $T_{99.99}$  ranking predicts the microspray data ranking for temperatures well below ignition and is identical for temperatures just below ignition. However, the flame-mode ignition temperatures measured in the microspray (825-875 K) were considerably below the tempera-

ture typical of nonflame thermal destruction (925-1038 K).

A plausible explanation for the different temperature requirements for destruction is involved with the differences in waste concentration between the microspray experiments and the nonflame thermal destruction experiments. In the latter, the compound concentration is sufficiently low that radicals resulting from the initial attack are recombined in the inert carrier gas. In the microspray experiment, the locally high compound concentrations in the vicinity of individual droplets can lead to the appearance of a droplet flame. The droplet flame temperature can be considerably elevated above the flat-flame temperature (825-875 K). This high droplet flame temperature and the high concentrations of flame radicals act to accelerate the test compound destruction beyond the rate predicted by nonflame thermal destruction data.

#### 4.1.2 Pure Compounds in an Oxygen-Rich Flame

Data were also obtained in which droplets of pure test compound rather than compound mixtures were injected into the microspray reactor. The experiments were designed to ascertain the difference between decomposition of pure droplets and droplets composed of a mixture of waste compounds. The experiments were conducted in exactly the same manner as the mixture experiments just described. Except for chlorobenzene, where a wide range of flame temperatures were examined, the data were obtained as follows:

1. The reactor temperature was adjusted until the point of visual ignition was determined.
2. Destruction efficiency measurements were obtained at the ignition point, and at flame temperatures approximately 100 K above and below the ignition point.

The results are shown in Figure 4-2 as a plot of unreacted compound leaving the reactor versus the flat-flame temperature. The visually observed ignition temperatures for each of the compounds were:

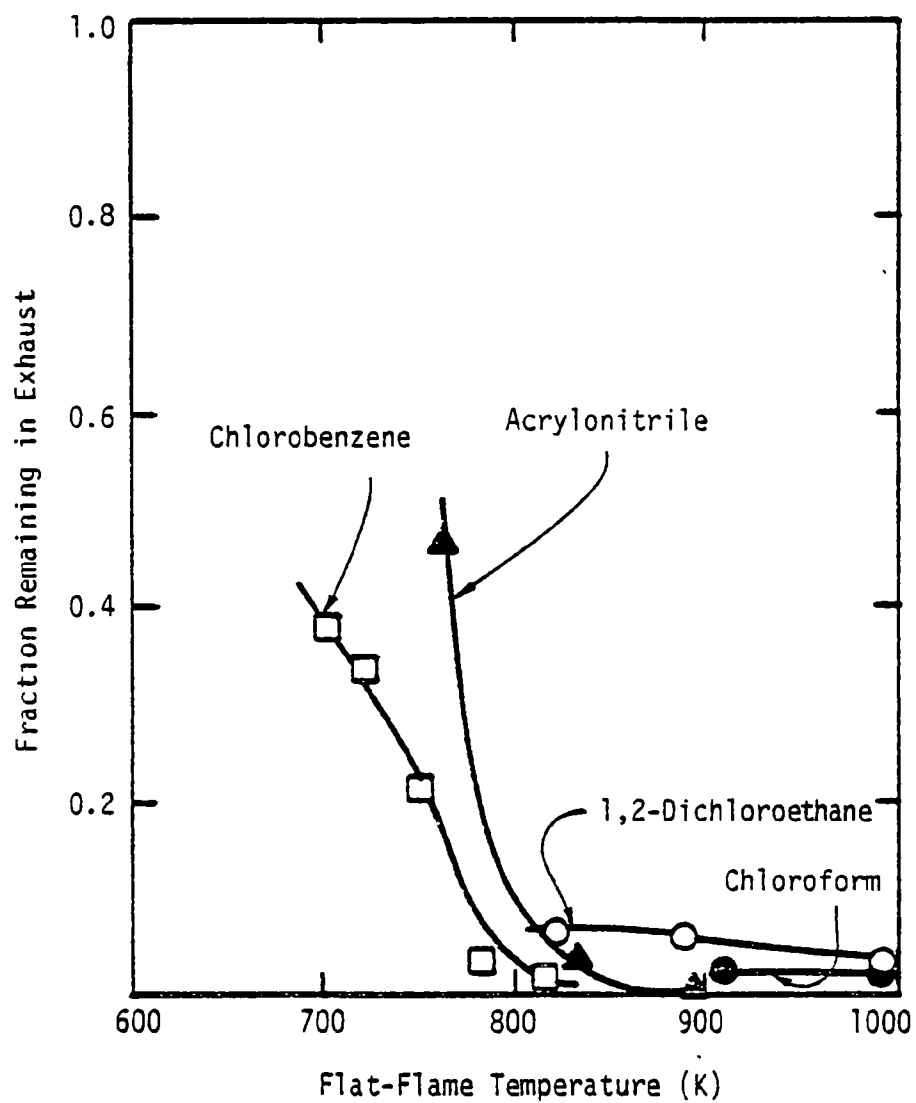


Figure 4-2. Fraction of test compound remaining in exhaust when 38  $\mu\text{m}$  droplets of pure compounds were injected into lean (10 percent post-flame oxygen)  $\text{H}_2$ /air flames as function of flame temperature.

| <u>Compound</u>    | <u>Ignition Temperature (K)</u> |
|--------------------|---------------------------------|
| Chloroform         | 903                             |
| 1,2-Dichloroethane | 888                             |
| Acrylonitrile      | 833                             |
| Chlorobenzene      | 813                             |
| Benzene            | <700                            |

Benzene droplets remained ignited until the flat-flame itself became extinguished. Thus, no benzene data are shown on the figure and the ignition temperature was similar to the heat of combustion (chloroform, 1,2-dichloroethane, chlorobenzene, acrylonitrile, and benzene) ranking except acrylonitrile and chlorobenzene were reversed.

The following summarizes the similarities and differences between the pure compound and mixture microspray data:

- In both experiments, the visual ignition temperature was found to correspond to a shift between low DE at lower temperatures and high DE at higher gas-flame temperatures.
- For pure compound droplets the ignition temperature was compound specific.
- The droplets composed of a mixture experienced a single ignition temperature; this characteristic mixture ignition temperature (825-875 K) was in the same range as that of the pure compounds ( 700-903 K) which made up the mixture.

For pure compound droplets, a plausible explanation for the ranking behavior involves the relative ability of a droplet to maintain a droplet flame. The thermal theory of ignition (Semenov, 1935) holds that ignition will occur when the heat generated by reaction exceeds the heat loss from the droplet region generated by reaction. Heat production is strongly coupled to compound heat of combustion and, thus, heat of combustion may be the best indicator of relative DE among independently burning droplets of pure compounds. However, other processes such as evaporation rate, specific oxidation kinetics, and halogen flame inhibition may act as second order effects to modify rankings. For droplets composed of a mixture of compounds all com-

ponents within the mixture ignite at the same temperature which is characteristic of the mixture and not the individual compounds. Thus, the actual ignition temperature does not influence the relative compound destruction. For temperature below the characteristic ignition temperature of the mixture, the relative rates of oxidative removal kinetics of the individual components determines the relative decomposition of the compounds.

#### 4.1.3 Compound Mixtures With Low Oxygen

Experiments were performed to measure ranking behavior under conditions where oxygen was not available for droplet ignition. The data were obtained by operating the flat-flame at a constant fuel-rich equivalence ratio ( $\phi = 1.2$ ). To obtain lower temperatures, the fuel/air flow was proportionally reduced and the flow of nitrogen increased to maintain a constant cold burner velocity and equivalence ratio. The droplet stream was dispersed with the same mixture which was supplied to the burner to insure that oxygen from the dispersion gas was at the same concentration as that of the burner gas.

The results are shown in Figure 4-3 as unreacted test compound leaving the reactor as a function of flat-flame temperature. The data indicated an abrupt change from zero to complete reaction at a flat-flame temperature of 1050 K. The individual compound behavior was so similar that it was difficult to derive a ranking from the data. However, the data near 1050 K displayed sufficient compound variation to establish the following ranking: chlorobenzene, benzene, chloroform, and acrylonitrile. This ranking was most closely matched by the  $T_{99.99}$  and AIT ranking: chlorobenzene, benzene, acrylonitrile, chloroform. The decomposition behavior showed an abrupt change with temperature at about 1050 K. Only small changes in temperature were necessary to produce a considerable change in DE, as illustrated on the Figure.

These nonflame decomposition data differed from the flame-mode data in two important ways. First, the nonflame reaction above 1050 K, where compound consumption was complete, was not accompanied by droplet flamelets, as were the corresponding oxygen-rich data. Secondly, the decomposition reaction occurred at a much higher flat-flame temperature (1050 K) than the cor-



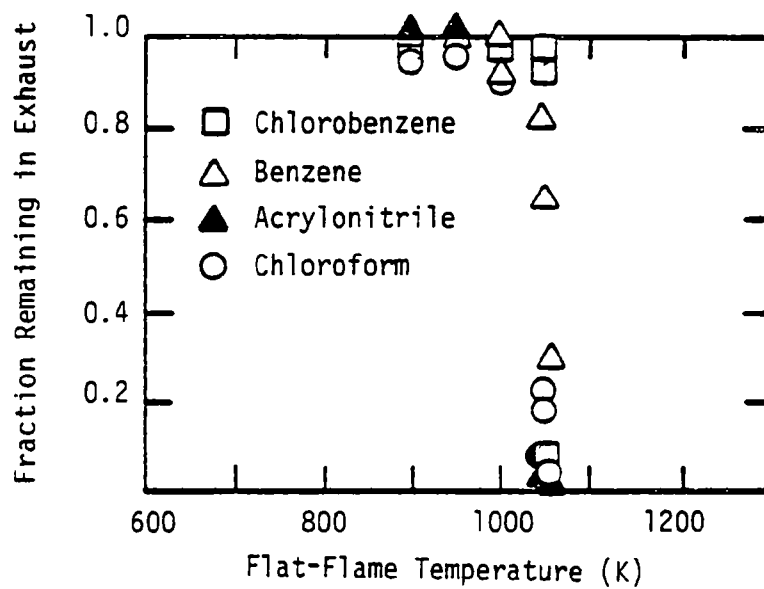


Figure 4-3. Fraction of test compound remaining in exhaust when 38  $\mu\text{m}$  droplets of mixtures of compounds were injected into rich (stoichiometric ratio = 0.83)  $\text{H}_2$ /air flames as function of flame temperature.

responding 10 percent oxygen data (825-875 K).

Since nonflame thermal destruction appeared to control compound removal under low oxygen conditions, the data analysis was aided by a simple analytical model based on combined droplet evaporation and nonflame decomposition behavior. The simple predictive model assumed the following:

- Time/temperature history of the reactor gas is identical to the profiles shown in Figure 3-4a.
- Droplet boiling rate was controlled by the heat transfer rate between the free stream and the droplet surface. Calculations have shown that mass transfer rate of vapor away from the droplet surface is relatively rapid compared to heat transfer; thus, heat transfer is expected to be the controlling step.
- Vapor was chemically removed by first-order nonflame thermal decomposition kinetics.

The model consists of two coupled first-order differential equations. The details of the derivation and the solution technique are reported in Appendix C. The calculation yields (1) a profile of the fraction of liquid evaporated as a function of time, and (2) a profile of the fraction of original feed reacted as a function time. Results for the reactor exit (i.e.,  $t = 1$  sec which corresponds to the experimental sampling point) are shown in Figure 4-4 for the five test compounds and, for reference, DDT and methane which have the lowest and highest thermal decomposition temperatures, respectively, of compounds for which kinetic data are available. The principal conclusions drawn from the model were:

1. For all conditions, droplets were completely evaporated early in the burner (evaporation time of  $38\text{ }\mu\text{m}$  droplets = 5 msec).
2. Predicted exhaust concentrations were unaffected by drop size for  $D < 400\text{ }\mu\text{m}$ . For  $D \leq 200\text{ }\mu\text{m}$ , results were insensitive to changes in  $\Delta H_{\text{vap}}$ , Nu, and boiling temperature for values within the range of values represented by the test compounds, and were sensitive only to time/temperature history and kinetic parameters. However, a large-scale nozzle may have an upper limit of drop size were evap-

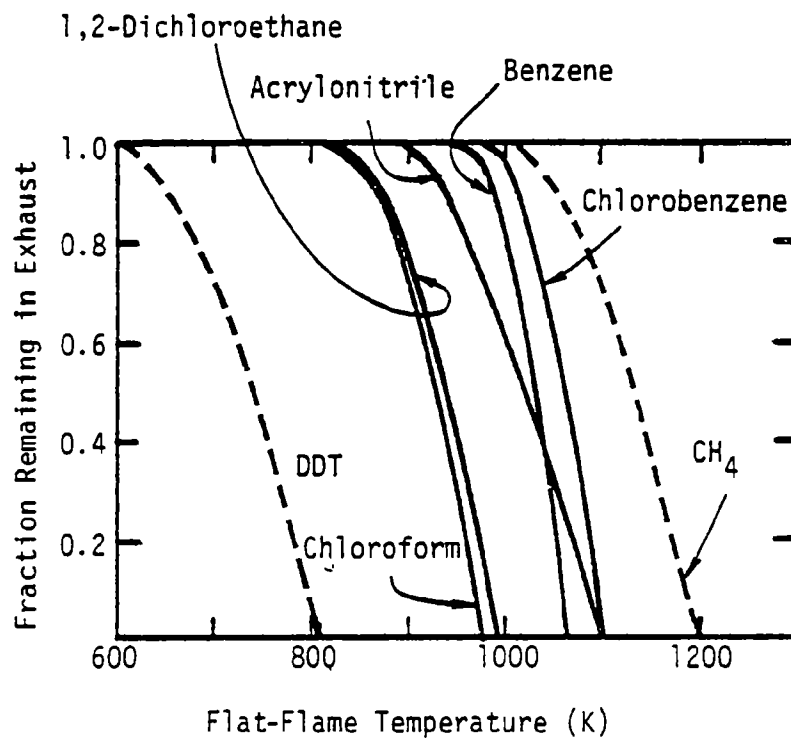


Figure 4-4. Model results: fraction of test compound remaining in exhaust when 38  $\mu\text{m}$  droplets were exposed to the temperature profiles shown in Figure 3-4a and allowed to react by nonflame thermal decomposition kinetics.

oration time becomes a significant fraction of destruction time (Seeker and Samuelsen, 1981).

The main shortcoming of the model was that it did not include flame-zone chemistry (flames about individual droplets or about vapor clouds). However, this did not present a difficulty for the present fuel-rich conditions as droplet flames could not persist due to the lack of sufficient free oxygen in the post-flame gas.

Comparison of the model results (Figure 4-4) with the nonflame droplet decomposition data (Figure 4-3) shows:

- The approximate flat-flame temperature at which compound reaction becomes active in the experiment (1050 K) was well-predicted by the model (970-1070 K).
- The data indicated that there was little difference in the temperature/destruction characteristic for the compounds tested. The model indicated that the data should be spread over a range of 100 K for the compounds tested. A maximum variation of 400 K is expected for all the kinetic data developed to date.

The observed similarity in rates between thermal destruction data and the microspray pyrolysis data was surprising because the thermal destruction results were obtained in 21 percent oxygen while the microspray results were obtained with less than 1 percent oxygen. Thermal decomposition (Dellinger et al., 1982) results for PCB indicated that reaction rate was first order in  $O_2$  between 2.5 and 35 percent  $O_2$  at atmospheric pressure. Assuming the first-order dependence applied to other organic compounds and taking benzene for an example, the rate expression can be written in terms of  $O_2$ :

$$-\frac{dC}{dt} = -k' P_O C$$

where  $C$  = benzene concentration (ppm)

$P_O$  = oxygen partial pressure (atm)

$k'$  = rate constant ( $\text{sec}^{-1} \text{ atm}^{-1}$ ) defined by

$$k' = \frac{k}{P_A}$$

where  $P_A$  = partial pressure of  $O_2$  in atmospheric pressure air (atm).

$k$  = published rate constant based on air.

Thus, the above rate equation expresses both the correct rate for air and the first-order oxygen concentration dependence. This equation was integrated for a constant temperature. Figure 4-5 shows the calculated unreacted fraction as a function of temperature for a one-second residence time. The three curves correspond to 21, 2.5, and 0.25 percent  $O_2$ . These calculations indicated that a two-order of magnitude change in oxygen concentration resulted in less than a 100 K shift in the destruction curve. Thus, the microspray results were relatively insensitive to oxygen concentration and the low  $O_2$  concentration data would be nearly indistinguishable from the nonflame calculations based on 21 percent  $O_2$ .

The results suggest that nonflame thermal decomposition kinetics control both the absolute reaction rate and the ranking. Only a small variation in thermal behavior was observed between the compounds. The nonflame thermal decomposition kinetic data would indicate approximately a 100 K variation between the most and least incinerable test compounds. A plausible explanation is that the actual decomposition kinetics are modified by the high concentration of compounds present and the interactions between the compounds in the mixture.

#### 4.1.4 Summary of Microspray Rankings and Data

Microspray Destruction Process. The overall DE of the microspray reactor was governed primarily by the flat-flame temperature (droplet thermal environment) and the availability of free oxygen in the region surrounding the droplet. When sufficient oxygen was available the absolute destruction was governed by the ability of the droplets, whether they were composed of a pure compound or a mixture, to support a droplet flame. At low flat-flame temperatures the thermal environment of the droplets was too cold to establish a droplet flame and low DE resulted. At sufficiently high flat-flame temperatures the droplets establish flamelets and DE was essentially complete. Figure 4-6 shows a plot of flat-flame temperature versus fraction unreacted compound

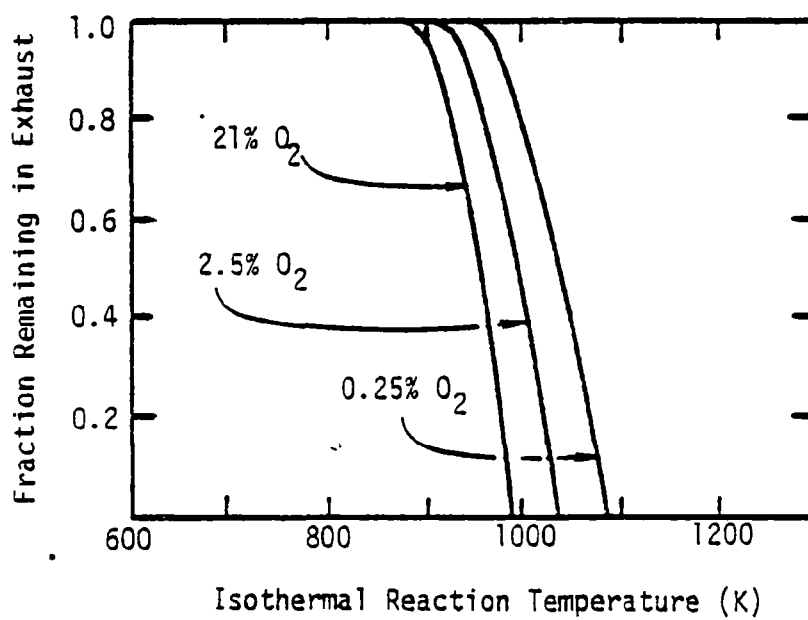


Figure 4-5. Model results: effect of oxygen concentration on thermal decomposition for benzene at isothermal conditions.

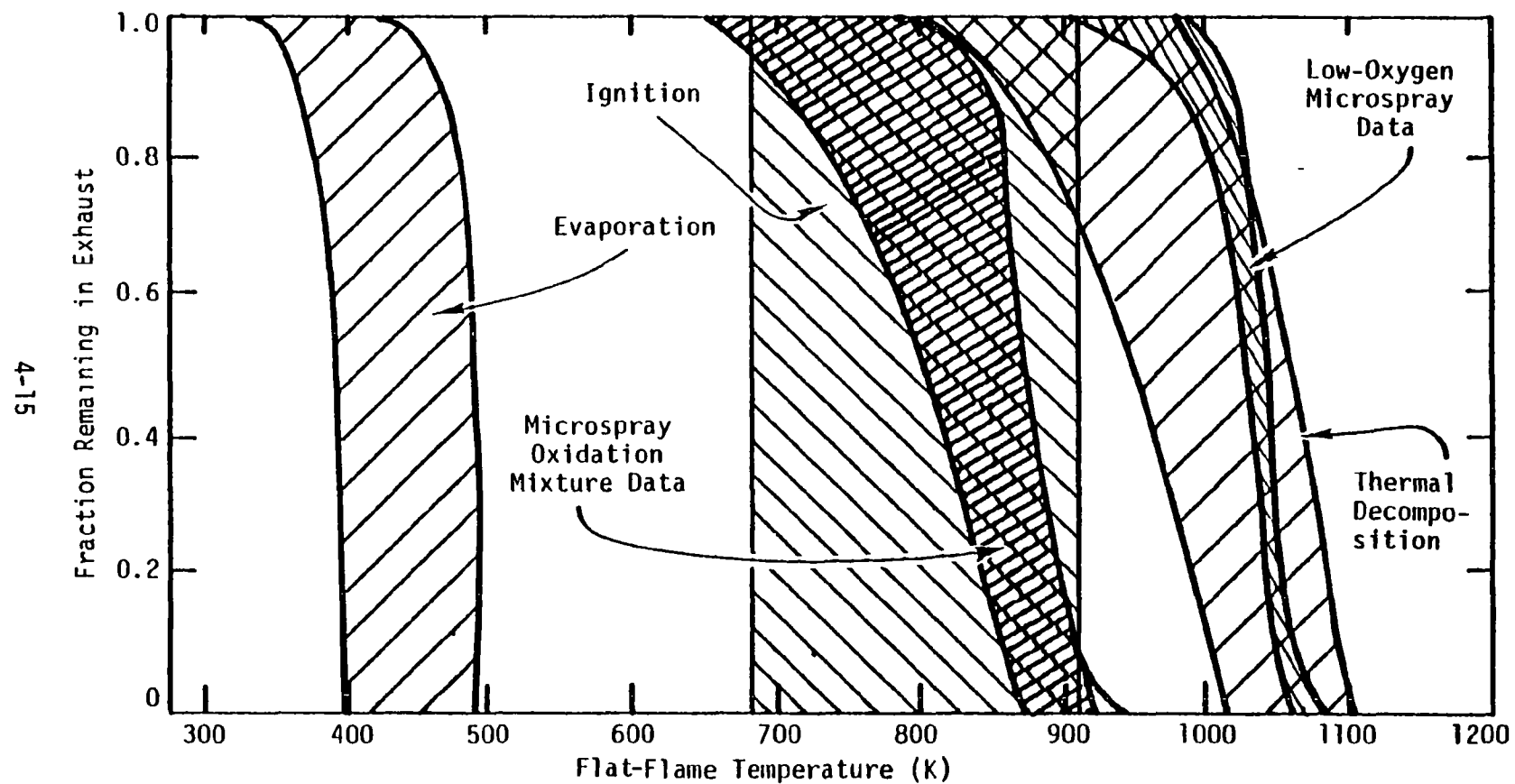


Figure 4-6. Comparison of calculated reactor performance assuming 1) droplet evaporation controls DE, 2) droplet ignition controls DE, and 3) thermal decomposition kinetics control DE; with microspray oxidation mixture data and microspray low oxygen data.

leaving the reactor. Three theoretical regions are shown; each indicates where the microspray data would be expected to fall if evaporation (based on droplet evaporation time), ignition (based on AIT), or thermal decomposition kinetics were the rate-controlling step governing compound release. The microspray oxidation mixture data shown on the figure indicate that the controlling process is an ignition phenomena, which agrees with the interpretation of the visual data discussed above.

When insufficient oxygen was available to support droplet flames the reactor DE appeared to be governed by nonflame thermal destruction kinetics. Figure 4-6 shows that the temperature requirements for complete destruction in the microspray operated fuel-rich was compatible with nonflame thermal decomposition kinetics. In summary, when free oxygen is present, ignition is the rate-controlling process; and when insufficient free oxygen is available thermal decomposition kinetics appear to be rate controlling.

Microspray Rankings. The relative decomposition of the test compounds is shown in Figure 4-7 with values for several of the ranking procedures. The figure was prepared with the concentration of the most prominent compound shown as full scale and the remaining compounds expressed as a percentage of the maximum concentration. None of the ranking procedures exactly predicted any of the microspray rankings. However, the nonflame thermal destruction ( $T_{99.99}$ ) and AIT procedures both closely agreed with the compound concentration measurements when the temperature was below droplet ignition temperature and under oxygen-deficient conditions. Heat of combustion was found to closely correlate the pure compound data when the microspray was operated below droplet ignition temperature.

#### 4.2 Turbulent Flame Reactor Results

A description of the turbulent flame reactor (TFR) and its range of combustion variables was supplied in section 3. The purpose of the turbulent flame experiment was to simulate the modes of escape of waste from the flame zone of liquid injection incinerators. In the flame zone of such a system finite rate mixing between fuel and air is expected to be the controlling mechanism of combustion efficiency. In the TFR, exactly the same processes govern the combustion efficiency because both are recirculation-stabilized



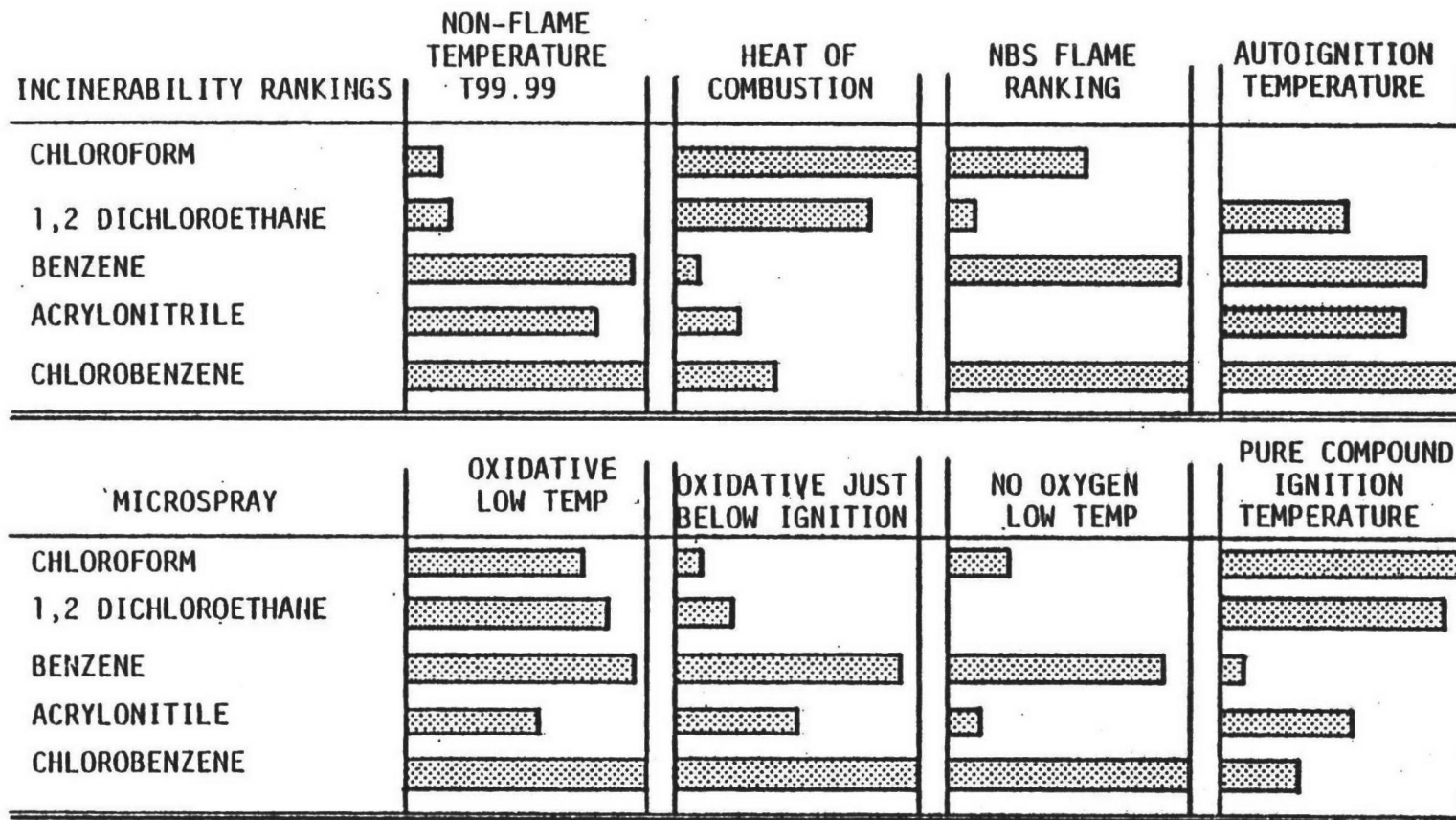


Figure 4-7. Microspray incinerability rankings.

turbulent diffusion liquid spray flames. The use of a high heat removal rate for the TFR insured that the measurements would emphasize flame zone reactions. Flame zone rankings were established for a variety of modes of inefficiency in the TFR. As a result of the similarities between the flame zone of a liquid injection incinerator and the TFR, the rankings established in this series of tests should relate closely to the rankings from the flame zone of real incinerators undergoing the same forms of inefficiencies.

The approach used to specify the turbulent flow experimental conditions was to locate highly efficient combustion conditions characterized by visual stability, high DE, low exhaust carbon monoxide, and low unburned hydrocarbons. There are termed "optimal" conditions. Poor operation was induced by perturbing the highly efficient condition by a variety of means (e.g., changing air velocity, introducing cold surfaces, etc.). These low efficiency conditions are called "nonoptimal." The ranking that resulted from each form of inefficiency was then determined by comparing the relative DE measurements from the five test compounds.

The DE data are, for most of the cases, presented twice in companion plots:

- A linear plot of fraction unreacted compound is provided with a scale of 0.0 to 0.03 to facilitate comparisons between different plots.
- A logarithmic plot is provided to quantify the data points whose DE are too high to be resolved on the linear plots.

For each test condition simultaneous CO, CO<sub>2</sub>, and O<sub>2</sub> measurements were obtained. The CO measurement was taken as a measure of the overall reactor efficiency. The results indicated that the CO measurements correlate with the measured destruction efficiency. For this reason, the CO data are reported along with the DE results for most of the test conditions. The CO<sub>2</sub> and O<sub>2</sub> measurements were used primarily to check stoichiometry and reactor feed rates and are not included in this report.

The conditions investigated in the turbulent flame reactor which had a strong influence on destruction efficiency were primarily associated with three failure conditions:

- Atomization parameters--poor atomization quality.

- Quenching parameters--quenching on cold surface.
- Mixing parameters--low excess air
  - high excess air
  - low heat release rate.

Those parameters found to be of less importance included burner velocity, fuel type (No. 2 fuel oil) and concentration of hazardous waste compounds (from 3 to 25 percent). For all data, the swirl number was unity. The specific experimental conditions are outlined in Table 4-1.

All tests where fuel-flow was varied required the use of several nozzles; this was necessary so that atomization pressure, and therefore atomization quality, was never significantly changed. Table 4-2 shows the flow rate ranges for which particular nozzles were used. Only during the nozzle performance tests were the constraints of this table not followed.

#### 4.2.1 Influence of Stoichiometry and Load

These measurements constituted the baseline condition and were obtained by varying the fuel flow rate at constant air flow and velocity. The atomization quality of the pressure atomized Delavan WDA-series nozzles changed with fuel flow. To maintain consistent atomization quality over the range of fuel flow rates, it was necessary to substitute nozzles of different capacity in accordance with Table 4-2.

Unburned hydrocarbon, CO, and relative heptane measurements were obtained to characterize the relative efficiency of the flame. Heptane demonstrated a significant volumetric breakthrough on the Tenax under the normal analytical procedure (see Appendix B). Despite the fact that the Tenax did not quantitatively capture heptane, the calibration indicated that the analytical response was linear in heptane concentration. Thus, the heptane measurements were relative rather than absolute and were included only to differentiate between high and low heptane destruction conditions. These measurements, shown in Figure 4-8, indicated that a region of high combustion efficiency existed between approximately 120 and 150 percent theoretical air. At higher fuel flows, mixing was not sufficient to eliminate all of the fuel-rich pockets, even though the burner was operated at an overall fuel-lean stoichiometry.

TABLE 4-1. TURBULENT FLAME EXPERIMENTAL CONDITIONS

| Experimental Cases                      | Theoretical Air (percent) | Fuel Flow (gm/sec) | Load (kW) | Velocity (m/sec) | Nozzle Delavan WDA 600 Series (nominal capacity in gallons/hr) | Fuel           | Compound Concentration in Fuel (weight percent) | Text Figures |
|---|---------------------------|--------------------|-----------|------------------|--|----------------|---|--------------|
| Baseline                                | 110-210                   | .93-.54            | 42-24     | 7.1              | (1)  | Hep-tane       | 3   | 4-8,4-9      |
| Theoretical Air Constant Load           | 120-200                   | 1.08               | 48        | 25-15            | 1.5  | B              | B   | 4-10         |
| Air Velocity                            | 156                       | .72                | 32        | 7.1-17           | 1.0  | B              | B   | 4-11         |
| Compound Concentration                  | B                         | B                  | B         | B                | B  | B              | 10,25   | 4-12         |
| Cold Surface <sup>(2)</sup> Impingement | B                         | B                  | B         | B                | B  | B              | B   | 4-13, 4-14   |
| Nozzle Performance                      | 110-320                   | .93-.34            | 42-16     | B                | (3)  | B              | B   | 4-15, 4-16   |
| Auxiliary Fuel                          | B                         | B                  | B         | B                | B  | No. 2 Fuel Oil | B   | 4-17         |

B Variable identical to baseline experiment.

(1) Nozzles selected to maintain operation within capacity limits: see Table 4-2.

(2) Repeat of the baseline experiment with quench coil within the flame.

(3) 1.5-gallon/hr nozzle was operated at flows below design.

TABLE 4-2. ATOMIZATION PARAMETERS

| Heptane Flow |          | Percent Theoretical Air <sup>1</sup> | Nominal Nozzle Flow (gal/hr) <sup>2</sup> | Atomization Pressure (psig) | Load (kW) |
|--------------|----------|--------------------------------------|---|-----------------------------|-----------|
| gm/sec       | (gal/hr) |                                      |   |                             |           |
| .93          | 1.3      | 120                                  | 1.5                                       | 121                         | 42        |
| .86          | 1.2      | 130                                  | 1.5                                       | 103                         | 39        |
| .79          | 1.1      | 142                                  | 1.5                                       | 87                          | 36        |
| .72          | 1.0      | 156                                  | 1.0                                       | 161                         | 32        |
| .65          | 0.9      | 173                                  | 1.0                                       | 130                         | 29        |
| .56          | 0.8      | 195                                  | 1.0                                       | 103                         | 25        |
| .50          | 0.7      | 223                                  | 0.75                                      | 140                         | 23        |
| .43          | 0.6      | 260                                  | 0.75                                      | 103                         | 19        |
| .36          | 0.5      | 312                                  | 0.5                                       | 161                         | 16        |

<sup>1</sup>Based on the nominal air flow of 16.9 gm/sec (30.5 scfh).

<sup>2</sup>Sizing parameter based on design flow rate.

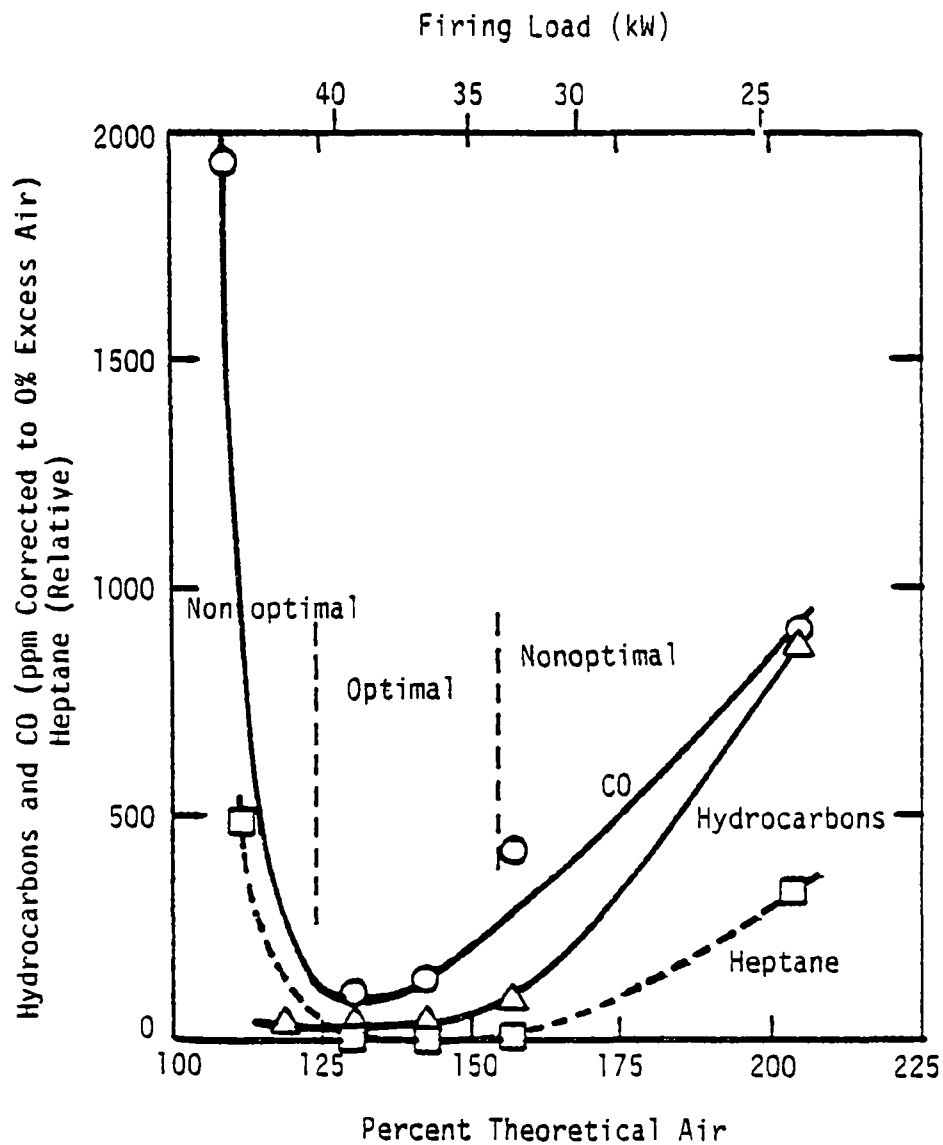


Figure 4-8. Exhaust CO, total hydrocarbons, and relative heptane as a function of theoretical air (constant air velocity, variable load: 42-24 kW, equal molar mixture of chloroform, benzene, chlorobenzene, and acrylonitrile added 3 percent by weight to heptane).

At very fuel-lean conditions the excess air lowered the flame temperature and likely quenched portions of the flame prior to the complete consumption of reactants. These measurements indicated that the burner operated in a manner consistent with practical systems. Under "optimal" conditions, consumption of fuel and fuel fragments was high and the flame efficiency, as defined by fuel consumption, was near unity. Under "nonoptimal" conditions the inefficiency of the flame was characterized by release of unburned fuel and fuel intermediates.

Destruction efficiency data for the corresponding conditions were obtained for both the benzene and the 1,2-dichloroethane test compound mixtures. Figure 4-9a shows the data for the benzene mixture. The results are plotted as fraction of compound remaining in the reactor exhaust as a function of reactor stoichiometry and firing load. The general trends show that DE and overall combustor efficiency are strongly related. The "optimal" and "nonoptimal" conditions defined from Figure 4-8 correspond respectively with the high (120-150 percent theoretical air) and low DE measurements in Figure 4-9. The rankings obtained from these results, and in general all of the following results were divided into optimal and nonoptimal conditions. For optimal conditions the results indicated the following:

- Absolute DE was always greater than 99.99 percent and was generally greater than 99.995 percent.
- No repeatable ranking was observed. Rather, the compounds appeared to be ranked in a random manner.

For nonoptimal conditions the results indicated:

- The DE for individual compounds was normally no worse than 98 percent. When one compound was released in significant quantities, the other compounds tended to be within a factor of ten of the same concentration.

At high DE, neither the absolute DE nor the ranking were repeatable. Instead, the DE for each compound varied in a random manner between 99.98 and 100 percent. Characterization of the measurement system (Appendix D) has shown that this variation was not due to an analytical problem. Rather, it was attributed to the random fluctuations that are inherent in a turbulent flame.

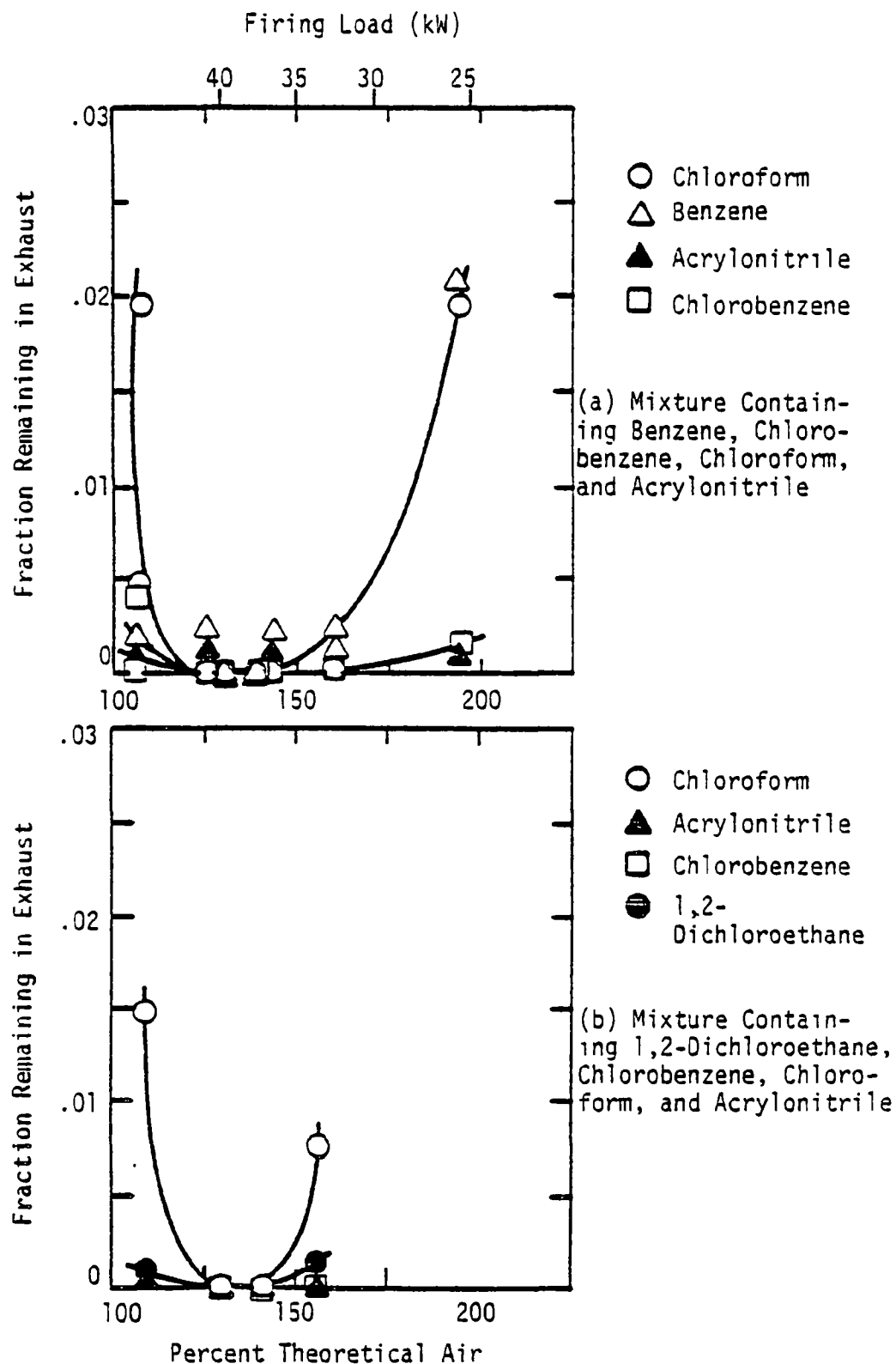


Figure 4-9. Impact of theoretical air and load on fraction of test compounds remaining in exhaust of turbulent flame reactor (constant air velocity, variable load: 42-24 kW; equal molar mixture of compounds added 3 percent by weight to heptane).



Over the 10-minute sampling period, 99.99 percent DE corresponded to 60 msec of zero efficiency operation for an otherwise completely efficient flame. Thus, the absolute DE and the ranking at high-efficiency conditions were subject to individual flame fluctuations and were expected, even over a 10-minute sampling period, to show apparently random fluctuations. At lower DE, conditions release was governed by large-scale escape mechanisms against which the random fluctuations observed for the high-DE conditions were unmeasurable. This result may have serious implications to trial burn data. Practical systems would be expected to behave in a similar manner to the TFR under high efficiency conditions because the turbulent flames in each have similar properties. Extension of these TFR results to a practical incinerator would imply that high-efficiency operation would result in nonrepeatable rankings. Thus, the POHC would not be guaranteed to be the lowest DRE compound during the trial burn.

The corresponding experiment for the 1,2-dichloroethane mixture produced the results illustrated in Figure 4-9b. The trends demonstrated by the benzene mixture data in Figure 4-9a are also apparent here:

- High DE was measured between 120 and 150 percent theoretical air.
- Chloroform tended to be the most predominant compound at non-optimum conditions. Chlorobenzene was normally the most easily destroyed compound, and the remaining compounds showed various rankings between chloroform and chlorobenzene.
- No repeatable ranking was observed for the high-efficiency conditions.

#### 4.2.2 Influence of Theoretical Air

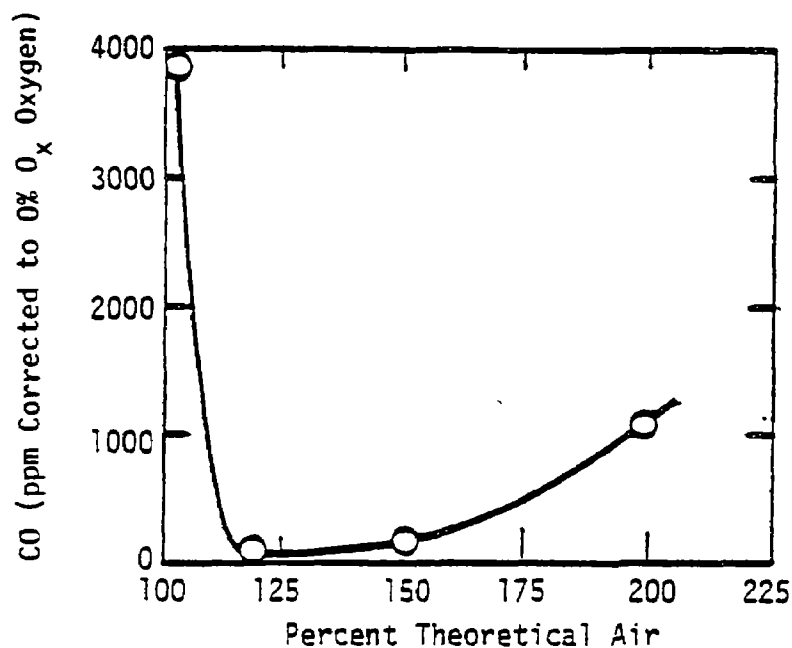
In the data just discussed, the stoichiometry variation was obtained by changing the fuel flow at a constant air flow rate. This procedure caused the burner heat release rate to change (from 42 to 24 kW) simultaneously with stoichiometry. In this section, the effect of stoichiometry on DE and ranking were investigated at a constant burner heat release rate (48 kW) by varying air flow rate at a constant fuel flow rate.

The data in Figure 4-10 were obtained by holding the fuel flow constant and varying the air flow (fuel flow = 1.08 gm/sec; 3-weight-percent test compound in heptane; load = 48 kW). This resulted in a variation of both air velocity and stoichiometry. The results demonstrated that a high-DE condition was obtained at 120 percent theoretical air. The CO data indicated that flame efficiency decreased as theoretical air was both increased and decreased from this value. The DE data decreased from an optimum of greater than 99.995 percent, except for benzene, when air flow was increased, but the measurements were not carried to a sufficiently fuel-rich condition to observe a corresponding degradation in DE.

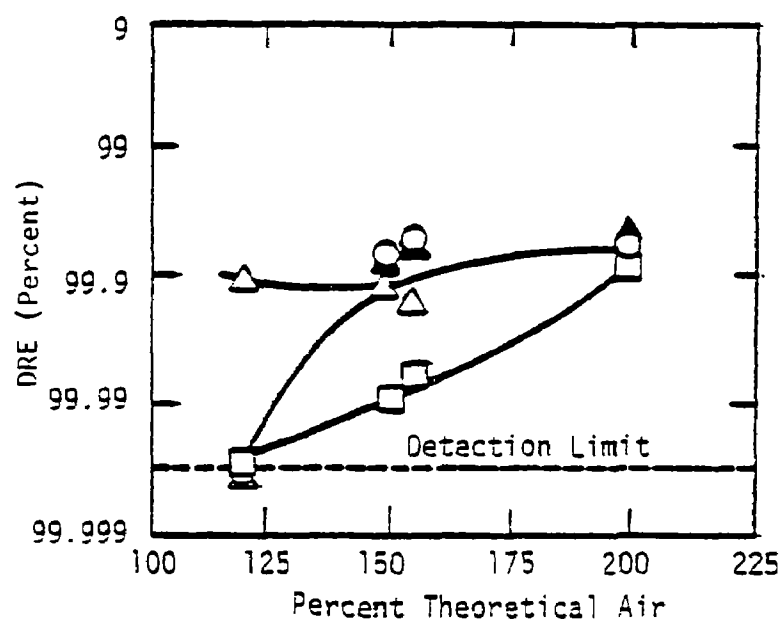
At nonoptimum conditions the ranking (difficult to easiest) was chloroform, acrylonitrile, benzene, and chlorobenzene. This ranking agrees with the variable fuel flow rate data (Figure 4-9) in choosing chloroform and chlorobenzene as the most difficult and most easily destroyed compounds. At the optimum condition, all of the compounds were at unmeasurably low concentrations (>99.995 percent DE) except benzene. This behavior can be interpreted as indicating that benzene was a product of incomplete combustion (PIC) resulting from the parent fuel or from one of the other test compounds (e.g., chlorobenzene). The actual source of the benzene, whether it is a product of incomplete combustion or an indication of incomplete benzene destruction, has not been determined. Benzene is a possible intermediate in the formation of the soot which was observed in the flame in the form of luminosity, especially at low excess air levels. Because of the relatively large levels of heptane present (97 percent) only a small conversion of heptane to benzene is required to account for the exhaust levels of benzene measured at this low excess air condition. However, the benzene could also be the result of a simple transformation of one of the test compounds, e.g., chlorobenzene.

The addition of excess air to turbulent spray flames decreases fuel and fuel-fragment consumption efficiency through a reduction in flame temperature and through thermal quenching. Thermal quenching can occur in a diffusion environment when cold air is rapidly mixed with a burning packet of gas so that the combustion reaction is extinguished prior to completion. The same mechanism is likely to adversely affect DE.

The results of Figure 4-10 for optimum conditions indicated that the



(a) Exhaust CO Concentration



(b) Destruction and Removal Efficiency

Figure 4-10. Impact of theoretical air on CO and DRE from turbulent flame reactor (constant load: 48 kW; variable air flow rate and burner velocity; equal molar mixture of compounds added 3 percent by weight to heptane).

variation in DE between the most- and least-prevalent compound was no greater than a factor of ten. This was a small variation compared to nonflame thermal decomposition kinetics where many orders of magnitude can separate compound concentrations at specific temperatures. For example, the kinetic data in Table 3-4 indicates that at 925 K and one second residence time the DE for benzene is 20 percent and for 1,2-dichloroethane is 99.95 percent, a difference of over 3 orders of magnitude in emission rate. One plausible mechanism of incomplete destruction under high excess air conditions is flame quenching. Flame quenching occurs when burning packets of gas are rapidly mixed with cold air so that the combustion reaction is abruptly stopped. As an example, consider two test compounds A and B. These are present in equal concentration in the center of a fuel-rich packet; they are of equal concentration because 1) A and B entered the reactor in equal concentrations, and 2) the center of the packet has not experienced a combustion reaction. A diffusion flame exists at the packet boundary where free oxygen diffuses into the packet gas. Turbulent quenching occurs when the packet is rapidly diluted with cold air so that the boundary diffusion flame is extinguished and the test compounds are diluted beyond their capacity to support further combustion. Thus, given an equal prequench concentration, an instantaneous quench, and no postflame reaction, the two compounds are released by the flame in equal concentrations. In reality, second-order effects such as relative susceptibility to quench or halogen flame inhibition may be superimposed on the first order quenching phenomena. This would result in a relatively small variation in DE, similar to the factor of ten variation that was experimentally observed.

#### 4.2.3 Influence of Air Velocity

The effect of burner air velocity on DE and ranking was investigated by varying the area of the burner throat while holding fuel flow, total air flow, and atomization quality constant. This was accomplished by using three separate inserts of different internal diameter as described in section 3.2.

The results shown in Figure 4-11 were obtained at the 156 percent theoretical air optimal condition (fuel flow = 0.72 gm/sec; 3-weight-percent test compound in heptane; load = 32 kW) with three velocities: 7.1, 14.1, and

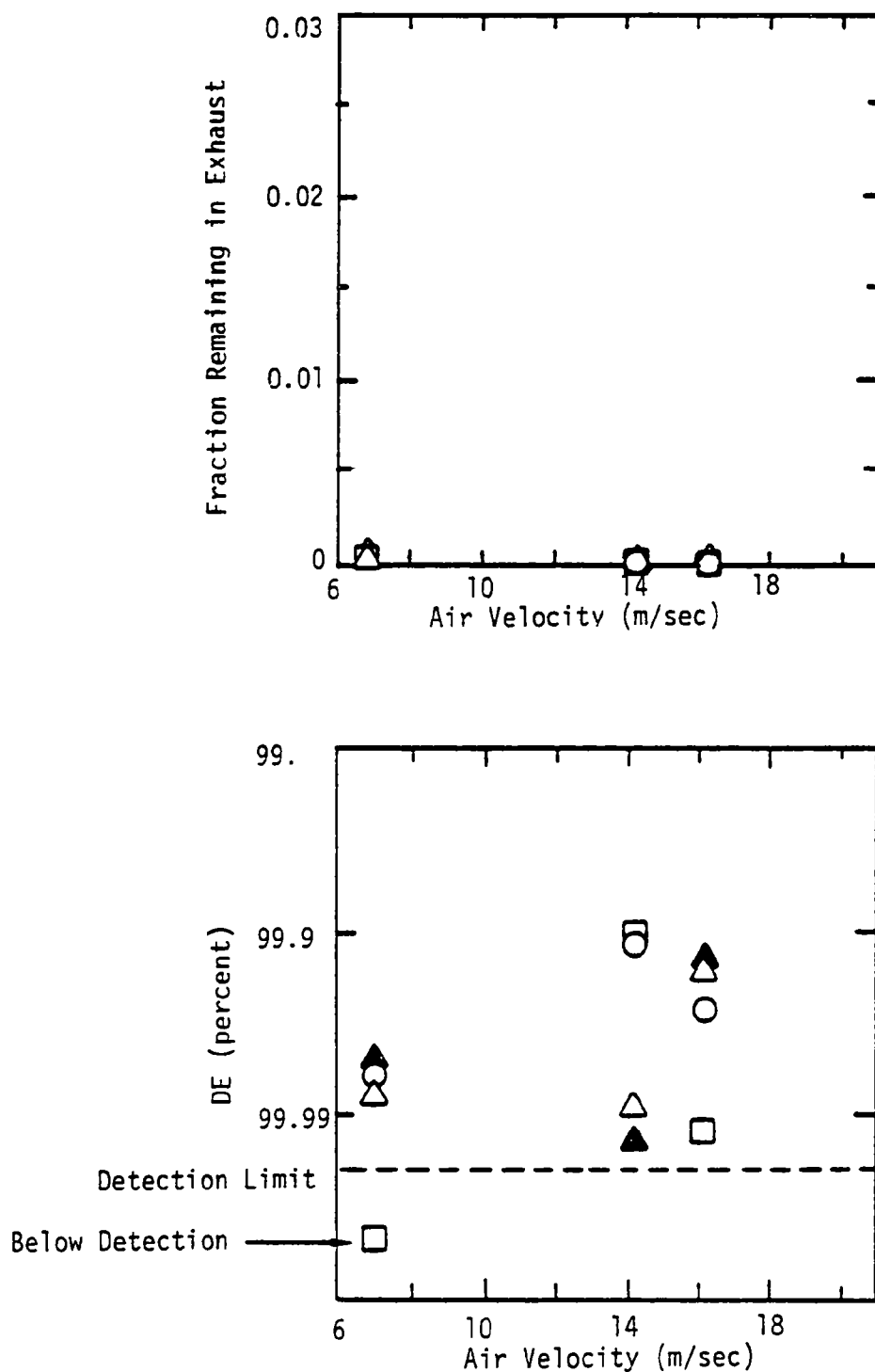


Figure 4-11. Impact of burner air velocity on fraction of test compounds remaining in exhaust of turbulent flow reactor (156 percent theoretical air; 0.72 gm/sec fuel flow; 3-weight-percent equimolar mixture of test compounds in heptane; 22.3 kW load).

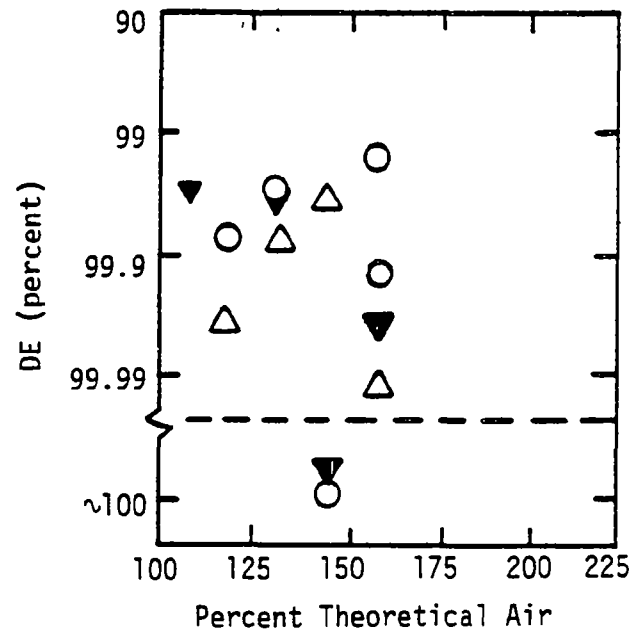
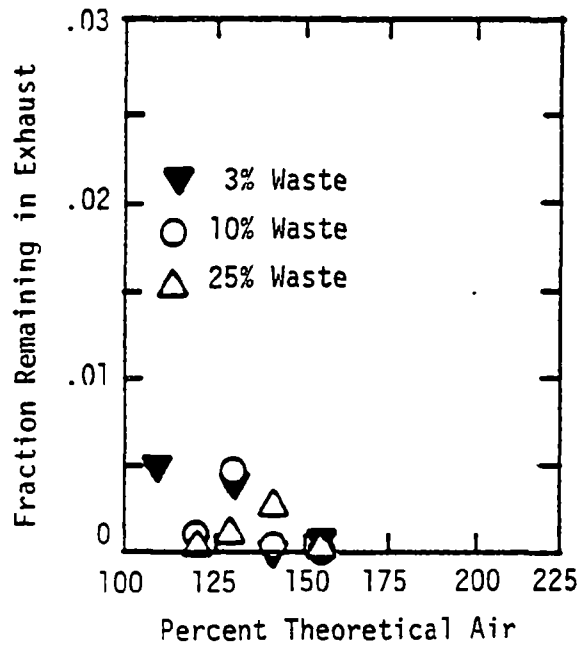
17.2 m/sec. The results are shown as fraction remaining in the exhaust as a function of burner air velocity. The data indicated that the optimal operation of the reactor was relatively insensitive to inlet air velocity over the range investigated (7.1-17.2 m/sec). All of the compounds had DE equal to or greater than 99.9 percent. The rankings from this high-efficiency condition were random, as was expected due to the nature of the escape mechanism for optimal conditions as previously discussed.

#### 4.2.4 Influence of Compound Concentration

In the baseline test experiment described in section 4.2.1, the test compounds constituted only 3 percent by weight of the total feed, the balance being the heptane auxiliary fuel. Hence, the auxiliary fuel determined the thermal environment and as a result, the test compounds each experienced identical thermal histories. In practical liquid injection incinerators, enough auxiliary fuel is added to bring the total heating value up to that necessary for stable combustion and to provide the desired post-flame temperature. As a consequence, the waste can influence and, at elevated levels, control the flame temperature. Also, the presence of significant quantities of waste compound in the fuel could alter the combustion chemistry. Examples of such behavior include the inhibition of flames by halogens (Biordi et al., 1975) which are present in many waste streams, and increased sooting caused by the high aromatic content of certain wastes (Glassman and Yaccorino, 1981).

In the present experiment, the effect of elevated test compound concentration was determined by performing experiments with 10- and 25-weight-percent waste concentration. These results are plotted, along with the baseline 3-percent results, for chloroform, acrylonitrile, benzene, and chlorobenzene in Figure 4-12. The experiments were performed at constant air velocity and variable fuel flow rate and load. Despite almost an order of magnitude change in compound concentration, no consistent variation in fractional destruction was observed. The increased test compound concentration did not result in any significant deterioration of the flame's ability to destroy the test compounds. Rather, the majority of the results showed behavior characteristic of optimal performance (i.e., high DE and random ranking).

### A. CHLOROFORM



### B. BENZENE

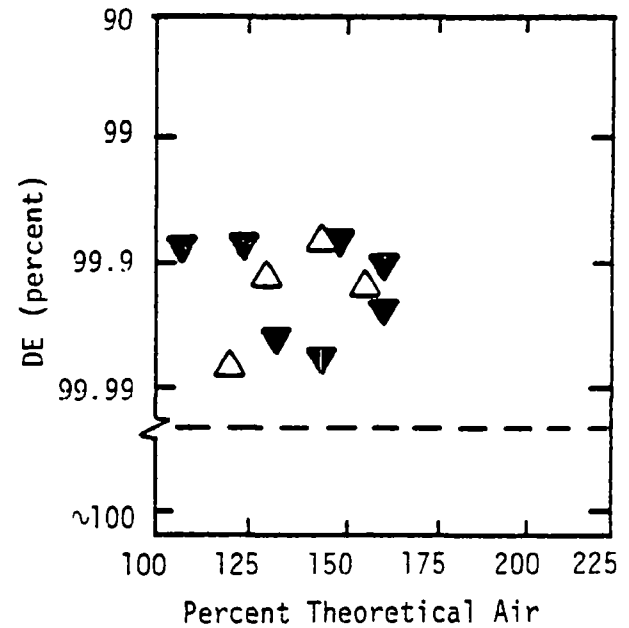
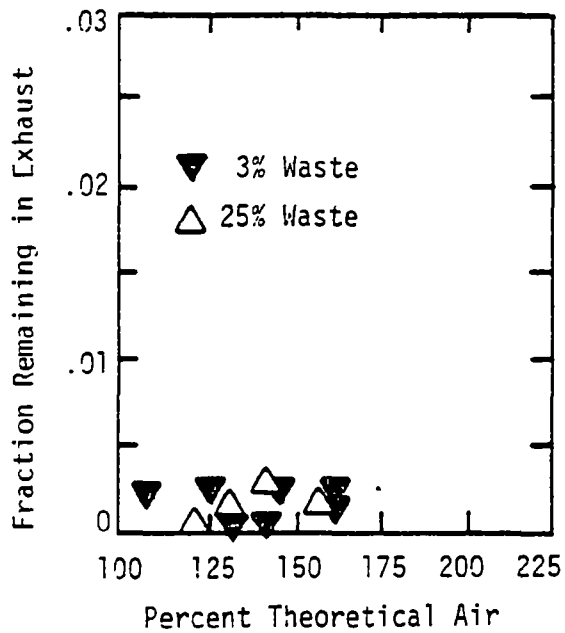
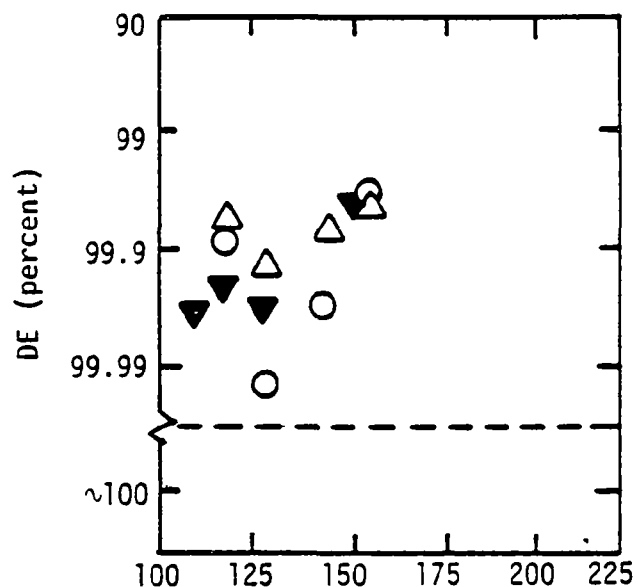
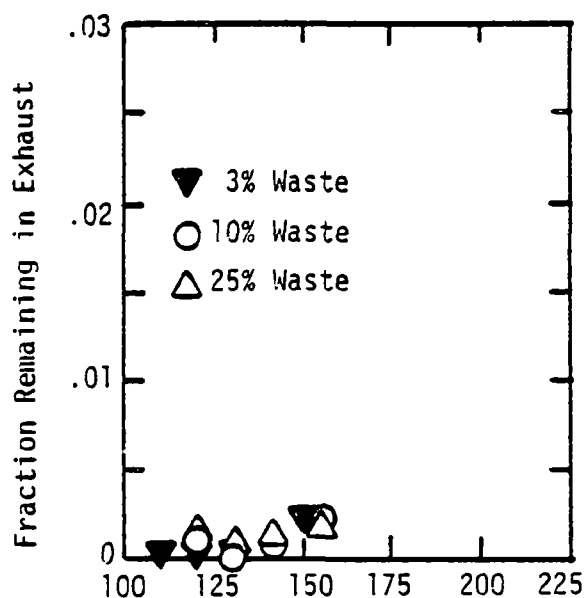


Figure 4-12. Impact of compound concentration on fraction test compound remaining exhaust of turbulent flow reactor (constant air velocity, variable load: 39-26 kW; variable weight concentration of an equimolar mixture of test compounds in heptane).

### C. ACRYLONITRILE



### D. CHLOROBENZENE

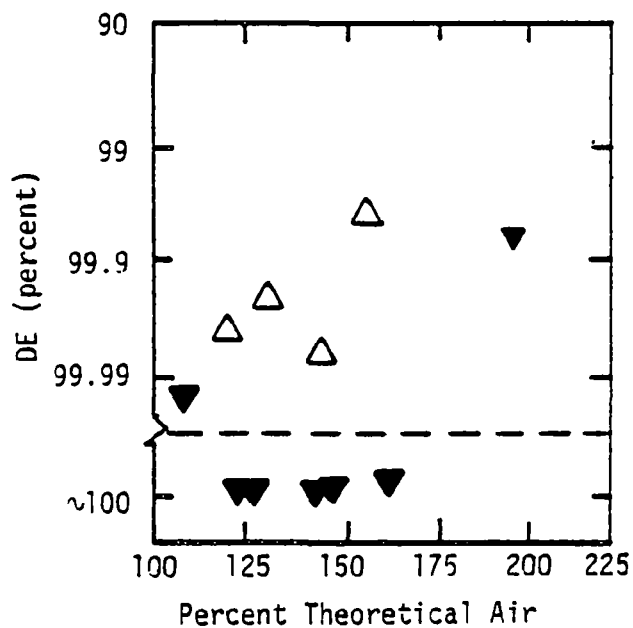
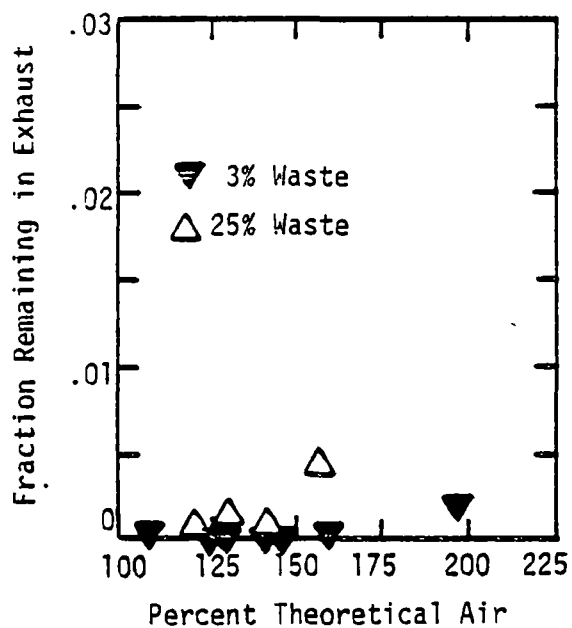


Figure 4-12 (cont.). Impact of compound concentration on fraction test remaining exhaust of turbulent flow reaction (constant air velocity, variable load: 39-26 kPa variable weight concentration of an equimolar mixture of test compounds in heptane).



#### 4.2.5 Effect of Quench Coil

The composition of fuel feed in an incinerator can vary considerably from time to time which can lead to considerable changes in flame shape and size. One problem associated with large changes in flame shape is the potential of flame impingement on a solid surface. The extreme limit of this behavior would be impingement on a cold surface. In the present experiment, heterogeneous quenching by cold-surface impingement was investigated by placing a water-cooled coil directly into the flame.

The data were obtained by repeating the baseline test described in section 4.2.1 in which air velocity was held constant and fuel flow was varied to obtain various firing loads and stoichiometries. A water-cooled quench coil was placed directly into the flame zone. The presence of the coil decreased the overall efficiency of the flame. In Figure 4-13 is shown CO for both the coil-quench conditions and the corresponding quench-free data. The discontinuities in the quench-coil CO data at 156 and 210 percent theoretical air corresponded to points where nozzle size was shifted to prevent changes in atomization quality. At these points slight changes in atomization quality and the positioning of the flame relative to the coils was expected which could influence flame performance. The deviation between the quench and no-quench data was greatest at the previous optimal low-theoretical-air/high-load condition. At this condition the quench coil was fully emersed in the flame. As fuel flow was decreased, the size of the flame became smaller, and eventually the flame separated from the quench coil. At this condition the coil no longer affected the flame zone as confirmed by the virtually identical data for CO above 200 percent theoretical air.

The cooling coil changed what otherwise was an optimum condition into a nonoptimum condition, as indicated by CO measurements. Figure 4-14 shows that this quench-induced nonoptimum condition also resulted in substantially degraded DE performance. The plot demonstrates that measured test compound emissions are considerably elevated over the corresponding non-quenched data (dashed line obtained from data of Figure 4-9). Resolved compound DE data were obtained at two previously optimal conditions, 130 and 156 percent theoretical air. The samples obtained at stoichiometries

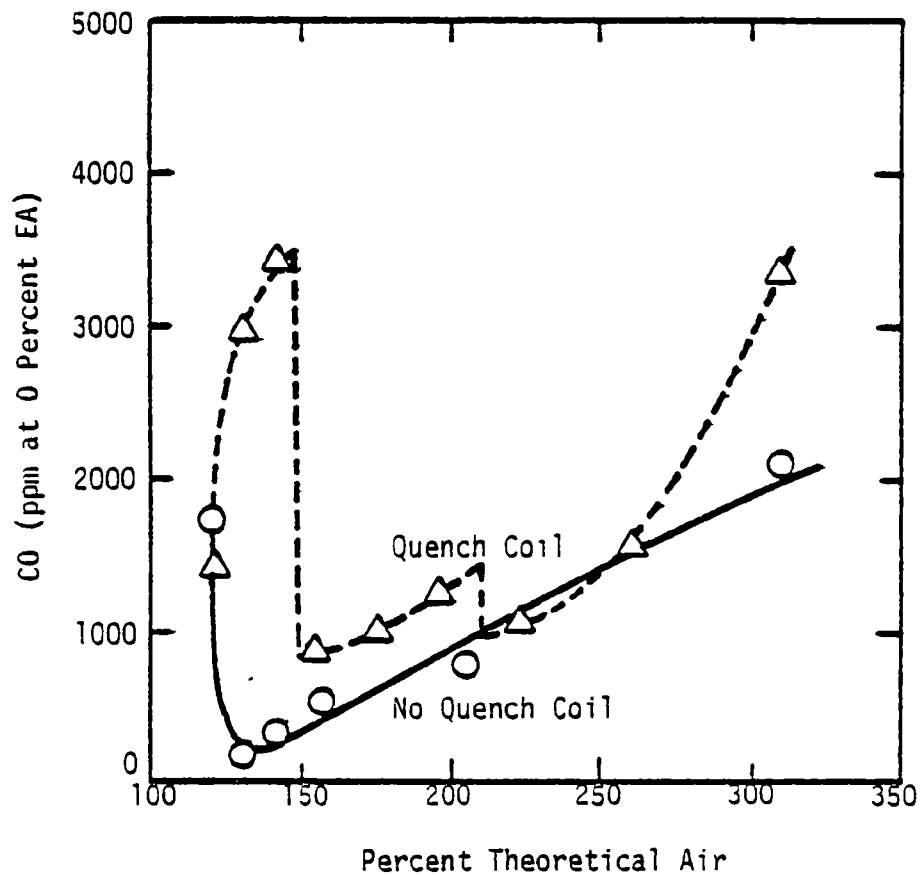


Figure 4-13. Influence of quench-coil on CO in exhaust of turbulent flame reactor as a function of load and theoretical air (constant air velocity, variable load: 42-16 kW; equimolar mixture of compounds added 3 percent by weight to heptane).

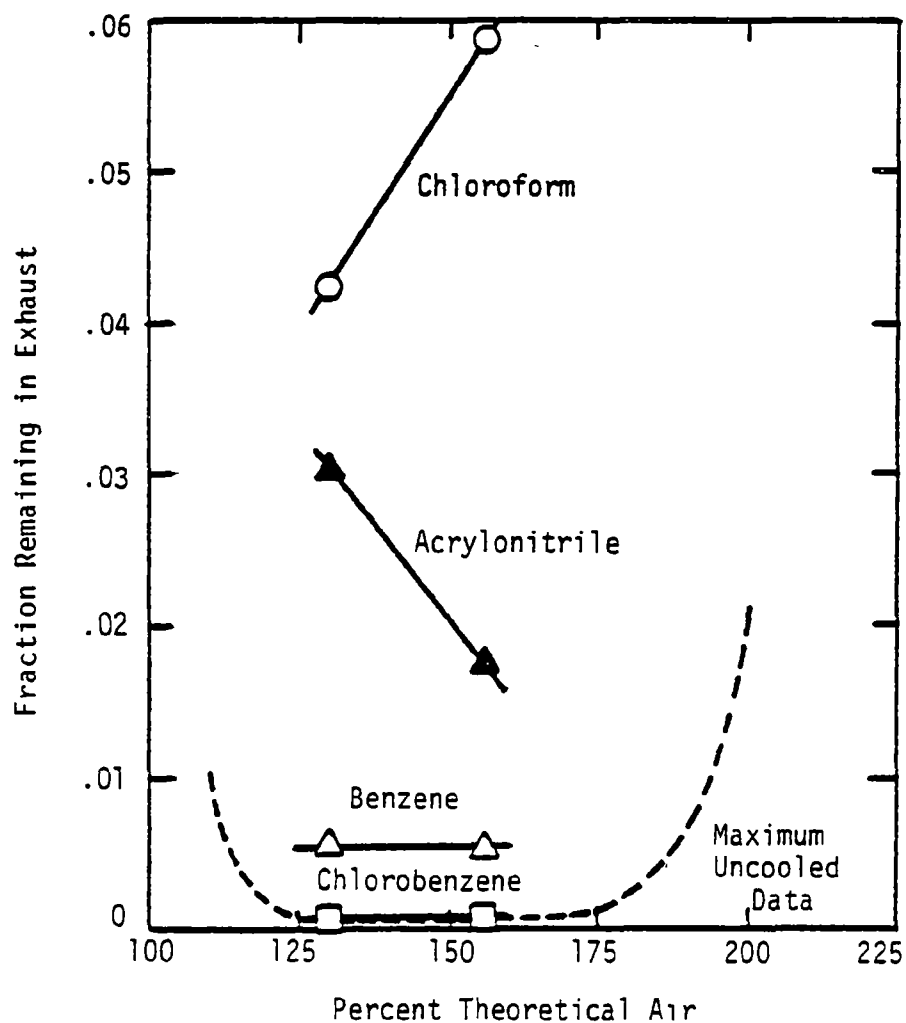


Figure 4-14. Influence of quench-coil on fraction of test compound remaining in exhaust of turbulent flame reactor as a function of load and theoretical air (constant air velocity, variable load: 42-24 kW; equimolar mixture of compounds added 3 percent by weight to heptane).

outside this range had high levels of test compound and other interfering species and the chromatogram peaks could not be resolved. These results, while not quantitative, indicate that DE performance was poorer outside of the 130 to 156 percent theoretical air range than the reported data within the range.

The compound ranking, from most difficult to easiest to destroy, was found to be: chloroform, acrylonitrile, benzene, and chlorobenzene. This ordering was similar to the measured high-excess-air ordering (Figure 4-9; chloroform most difficult, chlorobenzene easiest).

#### 4.2.6 Effect of Nozzle Performance

The pressure-atomized nozzles used in this study function by the breakup of liquid as it is forced through a small orifice under pressure. The atomization quality (droplet size) of the spray is primarily determined by the liquid pressure. These nozzles are designed to operate at liquid pressures in excess of 50 psig. At reduced pressures the mean droplet diameter for the spray increases (Dietrich, 1979) and the ballistic velocity of the individual droplets decreases. For the baseline experiment data presented in Figure 4-9, atomization pressure was held constant by interchanging nozzles of various capacities as the fuel flow was changed. Specific nozzles and corresponding flow rates are identified in Table 4-2.

In the present series of experiments, the CO and DE results for this on-design atomization condition were compared with the results where a single nozzle of relatively large capacity (1.5 gallon/hr) was used. The low atomization pressures used with this large nozzle resulted in off-design atomization performance.

The effect of nozzle performance on CO is shown in Figure 4-15 where CO corrected to 0% O<sub>2</sub> is plotted against percent theoretical air. The "on-design" curve corresponds to the data of Figure 4-9 and was obtained by interchanging nozzles to prevent the atomizing pressure from declining to the point where poor atomization quality is expected. The "off-design" curve was obtained by using the same capacity nozzle through the entire fuel-flow variation. Note that the large-capacity nozzle became "on-design" below 156 percent theoretical air; hence, the two sets of data become identical in this

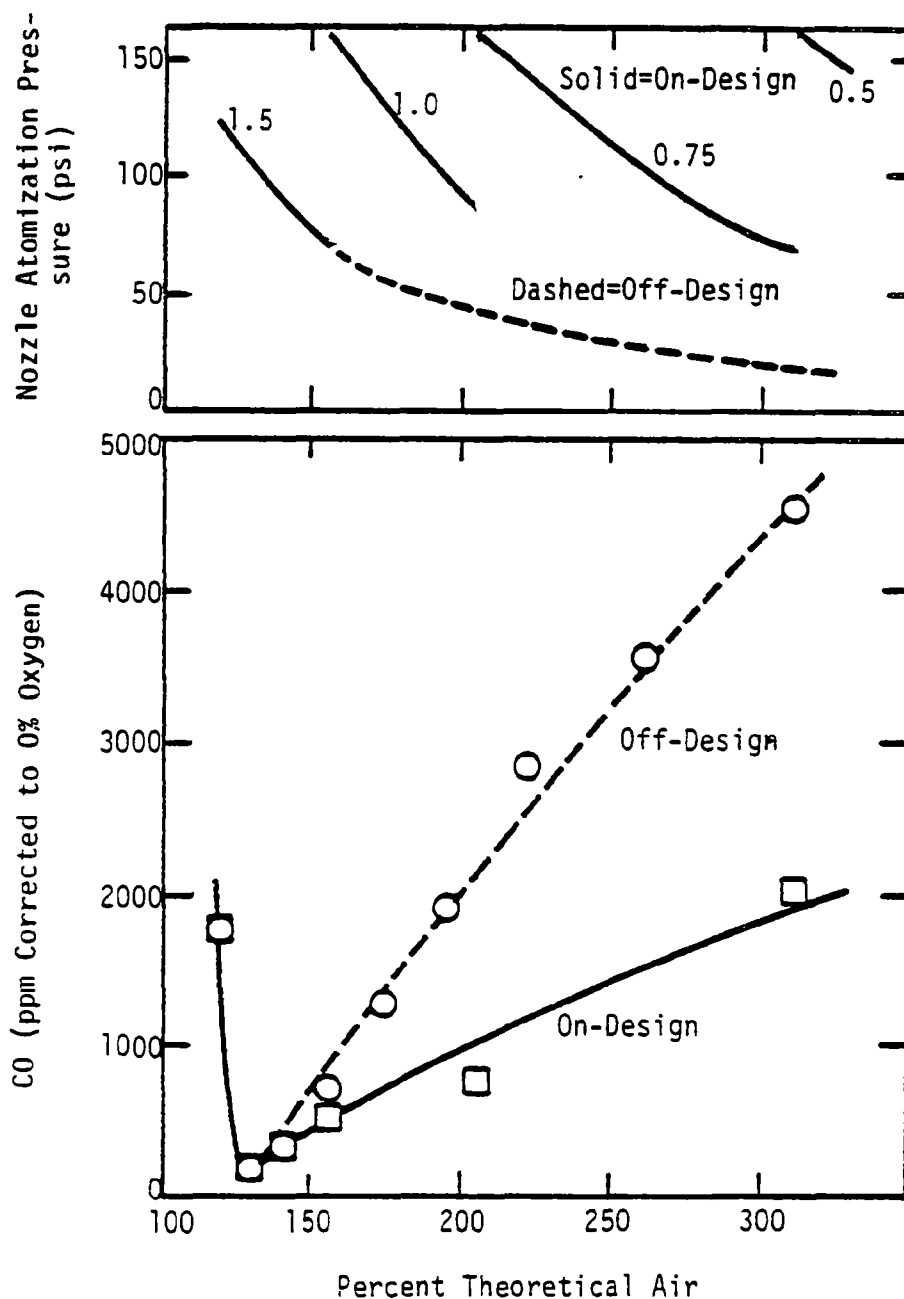


Figure 4-15. Influence of atomization quality on CO in exhaust of turbulent flame reactor as a function of load and theoretical air (constant air velocity, variable load: 42-16 kW; equimolar mixture of compounds added 3 percent by weight to heptane). Also, atomization pressure as a function of theoretical air for each of the nozzles (parameter is nozzle capacity in gal/hr).

region. At the top of the figure the atomizing pressure for the on- and off-design conditions are plotted. As theoretical air was increased (fuel flow decreased), the divergence between the two pressures was reflected in the increased divergence between the on-design and off-design CO plots.

The corresponding DE measurements are shown in Figure 4-16. The DE performance was substantially degraded for 156 percent theoretical air and higher excess air conditions. Chloroform at 310 percent theoretical had a DE of 50 percent, by far the lowest measured in the course of this study. The ranking obtained from these data was (most difficult to easiest to destroy) chloroform, benzene, acrylonitrile, and chlorobenzene. This ranking was similar to the rankings from the baseline experiment (Figure 4-9) and the quench-coil condition (Figure 4-14) in that chlorobenzene was the most easily destroyed compound and chloroform the most difficult.

The poor DE performance probably was caused by either the increase in droplet diameter or the decrease in ballistic velocity associated with low nozzle pressure. Large droplets may not have sufficient time to completely evaporate in the flame, or they may strike the cold wall and escape the flame. The lower droplet velocity could change the flame shape which can affect overall flame efficiency and DE.

#### 4.2.7 Effect of Auxiliary Fuel

In addition to mixing and quenching, the turbulent-flow experiment was designed to consider the effect of auxiliary fuel test compound interactions on the experimental ranking. The turbulent flow tests previously described were performed for a simple aliphatic auxiliary fuel, heptane. The present series was performed with a chemically complex petroleum distillate: No. 2 fuel oil. In these experiments the baseline experimental test shown in Figure 4-9 was repeated with No. 2 fuel oil replacing heptane as the auxiliary fuel. The results are shown in Figure 4-17 as fraction test compound remaining in the exhaust versus burner firing load and theoretical air. The similarities with the corresponding heptane data included a high DE optimal condition between 120 and 150 percent theoretical air, and a ranking in which chloroform was the most and chlorobenzene the least prominent compound. At low-theoretical air/high-load conditions, chlorobenzene became the most promi-

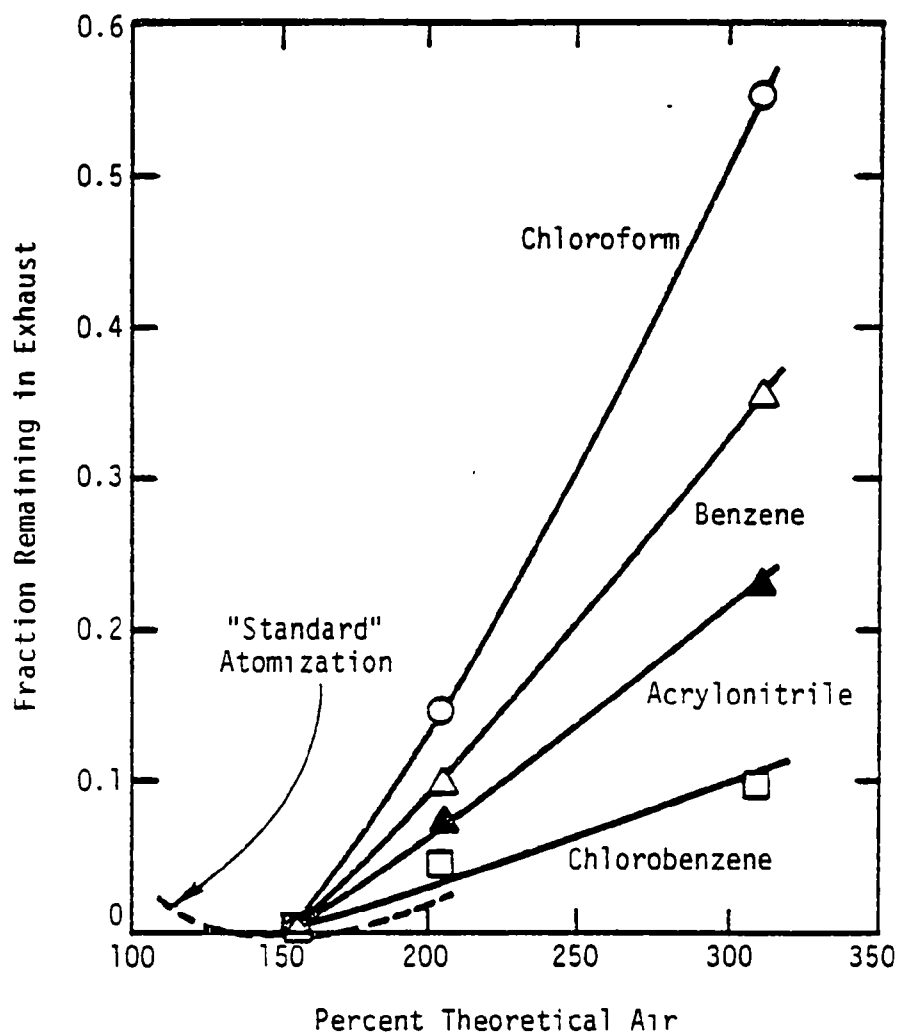


Figure 4-16. Impact of atomizer performance on fraction of test compound remaining in exhaust as a function of percent theoretical air (constant air velocity, variable load: 42-16 kW; equimolar mixture of compounds added 3 percent by weight to heptane).

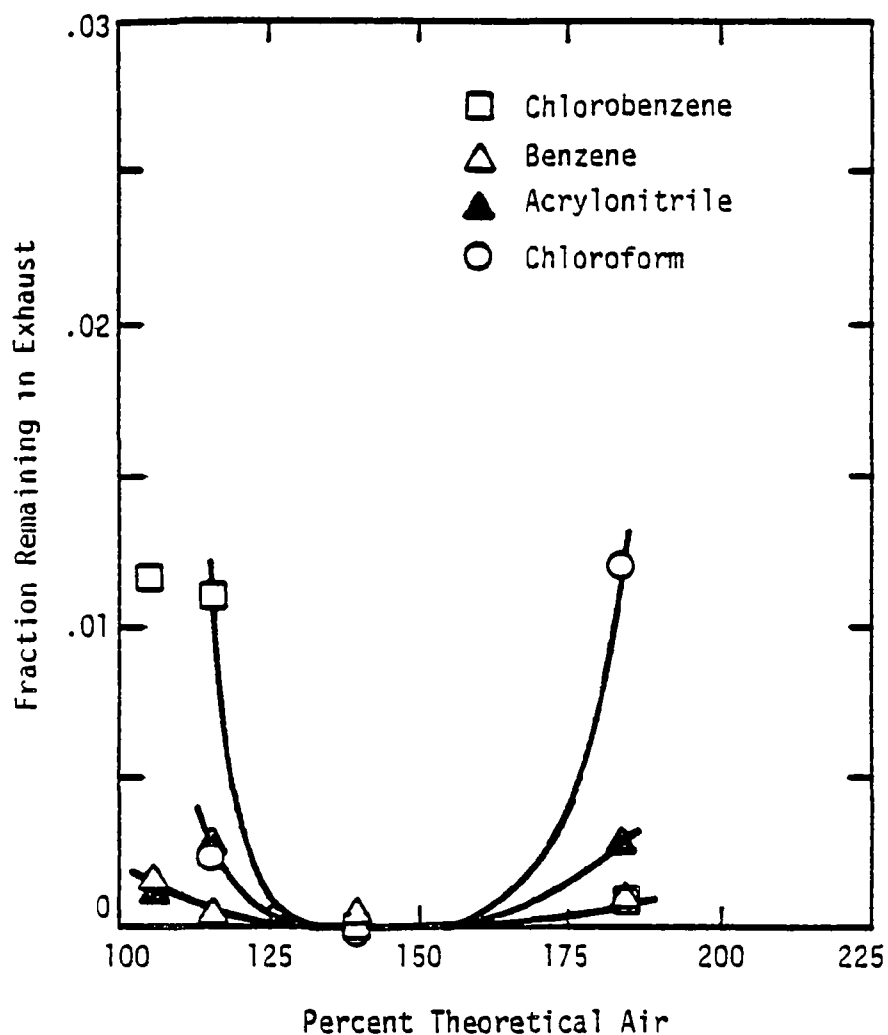


Figure 4-17. Impact of auxiliary fuel type on fraction of test compound remaining in exhaust as a function of percent theoretical air (constant air velocity, variable load: 42-24 kW; equimolar mixture of compounds added 3 percent by weight to No. 2 fuel oil).



nent compound. This differs from the heptane results in which chloroform was also the highest concentration compound at low-theoretical-air conditions.

#### 4.2.8 Turbulent Flow Reactor Data Summary

The following observations were supported by the TFR data:

- Certain experimental conditions can be classified as having optimal flame performance. These conditions can be characterized by low CO and unburned hydrocarbon concentrations and high destruction efficiencies (>99.995 percent). This observation supports the contention that flame efficiency is correlated with DE. Although this observation could be qualified by the presence of an afterburner or a postflame region, this notion suggests that a potential indirect, continuous, real-time monitoring of incinerator performance could be developed by monitoring species such as CO and total hydrocarbons which reflect flame efficiency. However, much careful characterization work is necessary to insure that these potential techniques are not overly conservative and that the response time of the instrument is compatible with the response time of the incinerator.
- Certain flame parameters did not, within the values used for this experiment, significantly deteriorate the performance of the optimum flame. These include burner air velocity, auxiliary fuel type, and high-compound concentration.
- Flame parameters that resulted in degraded DE performance included high theoretical air, low theoretical air, low heat release rates, cold surface impingement, and degraded nozzle performance.
- Any compound differences measured near optimum conditions appeared to be random.
- The rankings observed for non-optimum operation were dependent on experimental conditions, on the cause of the inefficiency (see section 4.3). In particular, the ranking (most difficult to easiest) of chloroform, benzene, acrylonitrile, and chlorobenzene appeared in many cases where quenching phenomena were expected.

## 5.0 SUMMARY OF RANKINGS, CONCLUSIONS, AND RECOMMENDATIONS

### 5.1 Summary and Discussion of Rankings

One of the program objectives was to intercompare the various ranking procedures. The development of these rankings proceeds from the assumption that incinerability is related to the relative thermal stability of the compounds (Cudahy et al., 1981). The thermal stability is either measured directly or inferred from another compound property. The concept of thermal stability is presumed to be universal; that is, it applies equally well to flame and post-flame processes, and to decomposition reactions in dilute and concentrated waste streams. The ranking procedures were developed as a means of estimating the relative thermal stability of waste compounds. The proposed procedures include:

Thermal Decomposition Kinetics. Under this approach the thermal stability is assumed to be related to the dilute phase nonflame thermal decomposition kinetic rate. This is measured in an experimental plug-flow reactor and reported as the temperature required to produce a 99.99 percent DE over a specified residence time ( $T_{99.99}$ ) (Lee et al., 1979, 1982; Duvall and Rubey, 1976, 1977; Dellinger et al., 1982).

Autoignition Temperature (AIT). The AIT is used to determine the tendency of a compound to initiate combustion without the presence of an external ignition source. AIT has been found to correlate with thermal destruction data (Cudahy et al., 1981). The principal advantage to this approach is that AIT data are much more easily and rapidly obtained than thermal decomposition data and a much larger data base is presently available. If thermal stability is assumed to be measured by thermal decomposition kinetics, then AIT is proposed as an approach to estimating thermal stability.

Heat of Combustion. This procedure was initially proposed because 1) increased chlorine substitution tends to yield higher thermal stability, as measured by  $T_{99.99}$ , and 2) heat of combustion tends to decrease with chlorine substitution. This yielded a potential relationship between heat of combustion and  $T_{99.99}$  (Cudahy et al., 1981).

Property Correlation. Attempts have been made to generalize the results of the thermal decomposition experiments so that a ranking similar to the thermal decomposition ranking can be established without performing experiments (Lee et al., 1979; Lee et al., 1982). The approach is to correlate  $T_{99.99}$  with autoignition temperature and other compound specific physical and structural properties. The results have indicated that the strongest correlation is with autoignition temperature.

Susceptibility to Radical Attack. Tsang and Shaub (1981) have assumed that attack on the weakest compound bond by flame radicals is the process controlling destruction. The rankings are established by the grouping of compounds according to the bond most susceptible to radical attack.

Miscellaneous Approaches. These include molar heat of combustion, heat of formation per unit weight, Gibbs free energy per unit weight, ionization potential, flash point, activation energy, and heat of formation of ion per unit weight. Various arguments have been presented as to why each of these can be correlated to  $T_{99.99}$  and, hence thermal stability (Cudahy et al., 1981).

The results of the present study indicate that no single ranking is appropriate to describe the relative compound measurements from the laboratory-scale turbulent spray flame. This implies that the concept of thermal stability ranking is not universal but is condition-dependent.

Both the microspray and the TFR were operated at high-efficiency, high DE conditions, and at conditions which simulated practical incinerator failure modes. The microspray reactor was selected to separate thermal and stoichiometric effects from turbulent mixing effects. In the microspray, high-efficiency DE resulted when the gas temperature was sufficiently high to sustain individual flames around each droplet for conditions where free oxygen was available to the droplet. When insufficient oxygen was available to support droplet flames, high DE occurred when the gas temperature exceeded the level required for nonflame thermal decomposition to become important. Under both the high-efficiency conditions, the DE was too high to be measured (>99.995 percent) and no ranking was determined.

In the TFR, high efficiency resulted in either complete decomposition of the test compounds, or a very high DE with a random ranking. This lack of

ranking appeared to be caused by the random nature of the turbulent flame and only a brief excursion from high-efficiency conditions was necessary to cause a measured DE below 99.99 percent. It should be emphasized that this process is not unique to this experiment and will likely affect the behavior of any large-scale turbulent diffusion flame, such as the flame zone of a liquid injection incinerator.

Under various failure conditions for both the microspray and the TFR, measurable differences between the five test compounds were observed. It was found that the incinerability or ordering of the compounds was dependent on the actual failure condition. For example, chlorobenzene was the most difficult to eliminate in the microspray when the temperature was too low to ignite the droplets, but was the least difficult to eliminate for a variety of failure conditions in the TFR such as poor atomization quality. Figure 5-1 presents a series of bar graphs which were prepared in the manner described in Section 4.1.1, which allows a comparison between incinerability as defined by the various failure modes and the rankings indicated by procedures based upon  $T_{99.99}$ , heat of combustion, the NBS method, and AIT. The bar graph shows the concentrations measured in the experiment normalized so that the most predominant compound shows full scale and the lesser concentrations are expressed as a percentage of that maximum concentration. This approach gives an indication of the measured magnitude of the difference in destruction efficiency between compounds. A comparison of these relative concentration measurements with proposed incinerability ranking techniques demonstrates that none of the proposed techniques agree with the data for all failure conditions. However, some of the ranking procedures were found to be appropriate for specific failure conditions. For example, the nonflame thermal destruction ( $T_{99.99}$ ) and AIT procedures both agreed with the compound concentration measurements when the temperature was below droplet ignition temperature and under oxygen-deficient conditions. Heat of combustion was found to correlate the pure compound data when the microspray was operated below droplet ignition temperature but in sufficient oxygen. In most instances investigated in the TFR under specified failure conditions, chloroform was the most difficult compound to incinerate, and this was anticipated by only one of the four ranking techniques--heat of combustion.

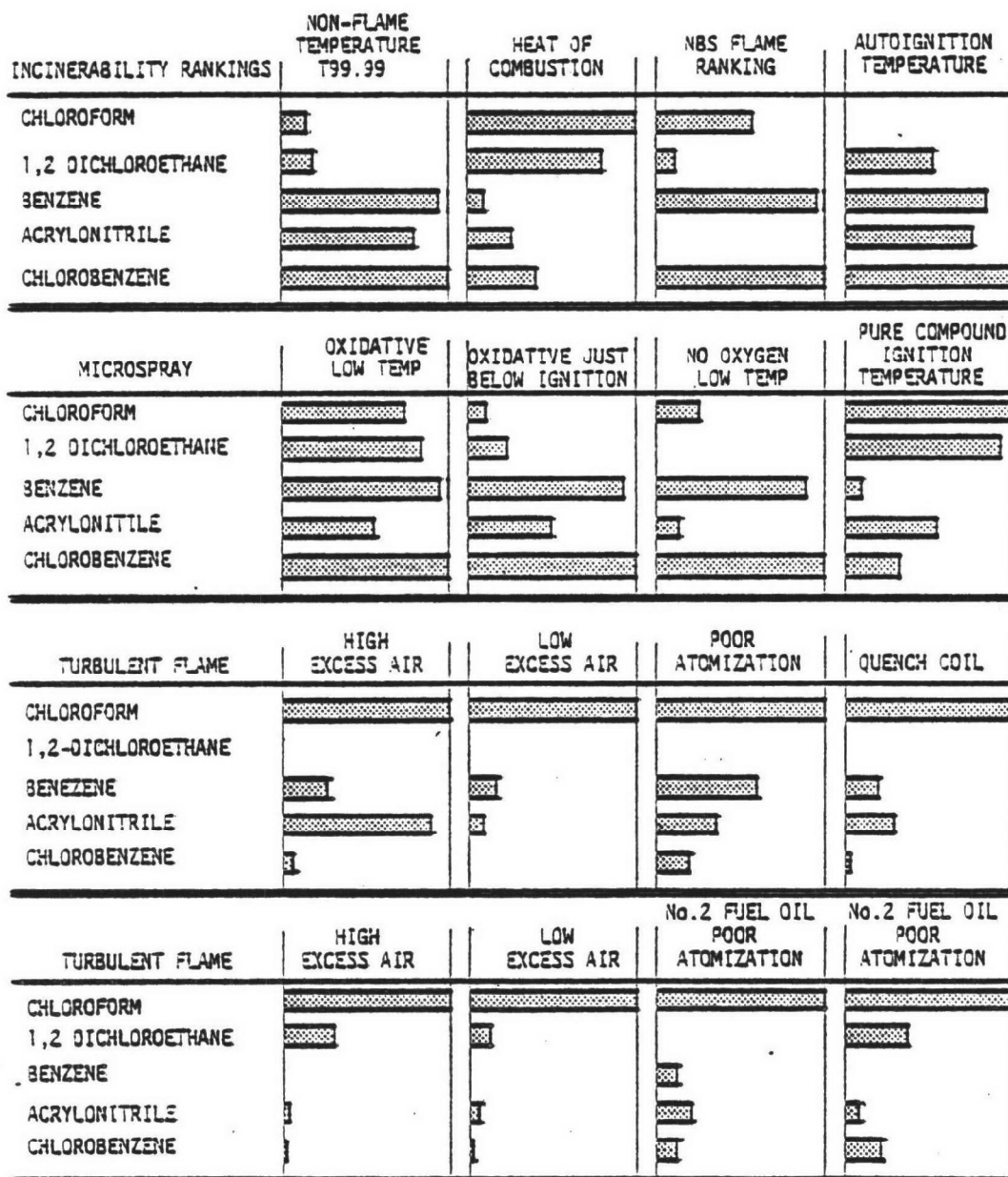


Figure 5-1. Comparison of proposed ranking techniques and relative compound decomposition of compounds under flame failure conditions.

Although measurable differences in the destruction efficiency of the five test compounds were obtained, the differences were not large relative to the extreme differences that can occur in thermal destruction experiments (e.g., at 925 K and 1 sec benzene DE = 20 percent, acrylonitrile DE = 99.995 percent). For the most part the variation in the concentration (between highest and lowest) of the compounds in the exhaust was typically of the order of ten, although larger variations were measured under some circumstances. This suggests that the POHC selection may not be very critical because the differences between compounds are relatively small. If the permit writer selects three compounds based upon two or more ranking techniques, and it is demonstrated that their DRE is greater than 99.99 percent, then it is very unlikely that any other compounds will be destroyed to a lesser degree. Nonetheless, to be assured that the incinerator is quantitatively destroying all compounds requires measurement of the most difficult to destroy compounds under all potential failure conditions.

This study has identified the differences between compound destruction efficiency caused by failure conditions associated with the flame zone. High destruction efficiencies have been demonstrated in the flame alone. However, many incinerators are equipped with post-flame hold-up zones and afterburners in order to achieve additional thermal decomposition of compounds which escape the flame zone. In order for an incinerator to fail to destroy a compound, the material must both escape the flame and the temperature be too low in the post-flame hold-up zone to destroy the compound (less than  $T_{99.99}$ ). The differences in the concentration of compounds in the exhaust of the incinerators is associated with both the flame and nonflame zones. The thermal decomposition which occurs in the post-flame zone can alter the ranking in the exhaust. However, this occurs only if the temperature in the post-flame zone is between the  $T_{99.99}$  of the two compounds. For example, the TFR data indicated that chloroform with a  $T_{99.99}$  of 930 K is the most likely compound to escape the flame and chlorobenzene is the least likely with a  $T_{99.99}$  of 1039 K. If the post-flame zone temperature is less than 930 K, then the flame zone ordering will prevail in the exhaust. If the temperature is greater than 1038 K, then both compounds are quantitatively destroyed if the residence time is greater than 1 second. However, if the temperature is between

930 and 1038 K, then chloroform is destroyed leaving chlorobenzene intact. Hence the postflame rank will prevail if, and only if, the temperature in the postflame is between the two compounds; in this case, a 100 C temperature range. It should be noted that the temperature in the post-flame zone is not uniform and the temperatures referred to above are minimum temperatures for a residence time of one second.

## 5.2 Conclusions

This study represented a first attempt to assess the appropriateness of the various proposed ranking procedures to flame-mode destruction. In these tests the destruction of only five waste compounds was investigated under a variety of conditions which simulated liquid injection incinerator failure modes. The results support three broad conclusions with regard to flame-mode destruction and the resulting incinerability rankings.

Conclusion 1: Flame Destruction of Waste Compounds. Flame destruction of hazardous waste compounds differs from nonflame thermal decomposition due to the addition of processes such as local heat release, finite rate mixing, ignition, free radical attack and high flame temperature thermal decomposition. The experiments have shown that under optimal conditions of mixing, temperature, and stoichiometry flames are capable of destroying hazardous waste compounds to very high efficiencies (greater than 99.995 percent) without the need for high-temperature, long residence-time post-flame zones. Reduced flame destruction efficiency is the result of operation under some failure mode such as poor atomization, poor mixing, flame quenching, etc.

Conclusion 2: Ranking. No single ranking procedure was found to be appropriate for all of the flame-mode failure conditions that were studied. Rankings were dependent on the particular reactor used and on the particular conditions used for each test. This implies that single-parameter ranking procedures cannot a priori be assumed to rank incinerability within a given unit.

Conclusion 3: Turbulent Flame Behavior Correlation. Behavior in the turbulent flow reactor was characterized into two general modes: optimum and nonoptimum. Optimum behavior was characterized by high overall combustion efficiency, which is defined as complete consumption of fuel and fuel

fragments. This condition can be verified easily by low CO and unburned hydrocarbon measurements. Conversely, nonoptimum conditions are defined by incomplete consumption of fuel and fuel fragments, and are indicated by relatively high CO and unburned hydrocarbon exhaust concentrations. The results of this study indicate that a high compound destruction efficiency is characteristic of optimum operation in a turbulent spray flame and the lower destruction efficiency occurs during nonoptimal performance. This correlation between flame efficiency and destruction efficiency offers a potential means of monitoring incinerator performance in a real-time, continuous manner relying on measurements of CO and THC.

### 5.3 Recommendations

This initial study into the nature of the flame-mode incineration process indicates a number of areas where supplemental effort would be valuable.

1. Additional Compounds. The five compounds selected for the present study represent a wide range of values within the proposed ranking systems. However, further testing of an additional group of compounds would allow an evaluation of whether the original five compounds represent the limits of behavior. Additional testing would also be directed toward finding if any subclass of compounds were unexpectedly difficult to incinerate. The TFR results indicated that chloroform was the least incinerable compound for many conditions. This behavior was not initially expected and a number of plausible explanations have subsequently been put forth. Additional compounds should be selected which will test the various possible explanations for the predominance of chloroform in the exhaust.
2. Incinerability Ranking. No one incinerability ranking system appears to predict correctly the relative destruction efficiency of the five compounds tested for all failure conditions investigated. The fact that neither flame reactor yielded a single ranking for all experimental conditions indicates that a single universal ranking is unlikely for the wide variety of incinerator designs in use. Since no single ranking is appropriate, the results of this study suggest that POHCs must be selected by consideration of the actual system.



A system-oriented engineering analysis methodology could be devised which would predict the likely failure conditions associated with each incinerator and the most likely POHC for each failure condition. The results of this study indicate that the POHC for a wide variety of failure conditions could be selected by considering a few rankings of incinerability. Specifically, relative compound destruction data from a number of flame failure conditions correlated with nonflame decomposition data. However, many relative compound effects from the turbulent flame reactor were not correlated with any incinerability ranking (heat of combustion was closest). This suggests that another incinerability ranking is required which considers the specific failure condition associated with a turbulent flame environment. If the dominant mechanism of escape from the turbulent diffusion spray flame is thermal quenching then a susceptibility-to-quench experiment may be required to correlate the data.

3. Further Types of Experimentation. The experiment in this study concentrated on the flame zone. A logical extension would be to consider additional failure modes associated with other portions of the incinerator. Such experiments might examine how rankings are modified by post-flame thermal hold-up zones, afterburners, or scrubbers. These data would more fully determine the limitations of incinerability ranking systems and aid the development of an appropriate incinerability ranking methodology.

## 6.0 REFERENCES

- Badzioch, S., 1967. Thermal Decomposition in Combustion of Pulverized Coal, by N. A. Field, D. W. Gill, B. B. Morgan, and P. G. W. Hawksby. The British Coal Utilization Research Association, Leatherhead, England.
- Baker, R. J., P. Hutchinson, E. E. Khalil, and J. H. Whitelaw, 1975. Measurements of Three Velocity Components in a Model Furnace With and Without Combustion. The 15th Symposium (International) on Combustion, The Combustion Institute, Pittsburgh, PA. p. 553.
- Berglund, R. N. and B. Y. H. Liu, 1973. Generation of Monodisperse Aerosol Standards, Env. Sci. and Tech. 7, 147.
- Biordi, J. C., C. P. Lazzara, and J. F. Papp, 1975. Flame Structure Studies, of  $\text{CH}_3\text{Br}$ --Inhibited Methane Flames. II. Kinetics and Mechanisms. The 15th Symposium (International) on Combustion, The Combustion Institute, Pittsburgh, PA. p. 917.
- Cudahy, 1981. Incinerability, Thermal Oxidation Characteristics and Thermal Oxidation Stability of RCRA Listed Hazardous Wastes. IT Envirosience Corp.
- Dellinger, B., 1982. Personal Communication.
- Dellinger, B., D. S. Duvall, D. L. Hall, and W. A. Rubey, 1982. Laboratory Determinations of High Temperature Decomposition Behavior of Industrial Organic Materials. 75th Annual Meeting of the APCA. New Orleans, LA.
- Dietrich, V. E., 1979. Dropsizes Distribution for Various Types of Nozzles. In Proceedings of the 1st International Conference on Liquid Atomization and Spray Systems. The Fuel Society of Japan, Tokyo, Japan. p. 69.
- Duvall, D. S. and W. A. Rubey, 1976. Laboratory Evaluation of High-Temperature Destruction of Kepone and Related Pesticides. Technical Report UDRI-TR-76-w1, University of Dayton Research Institute. EPA 600/2-76-299.
- Duvall, D. S. and W. A. Rubey, 1977. Laboratory Evaluation of High-Temperature Destruction of Poly-chlorinated Biphenyls and Related Compounds. EPA 600/2-77-228.
- Glassman, I. and P. Yaccarino, 1981. The Temperature Effect in Sooting Diffusion Flames, The 18th Symposium (International) on Combustion, The Combustion Institute, Pittsburgh, PA. p. 1175.
- Kramlich, J. C., G. S. Samuelsen, and W. R. Seeker, 1981. Carbonaceous Particulate Formation from Synthetic Fuel Droplets. Western States Section of the Combustion Institute. Fall Meeting, Tempe, Arizona. WSS/CI-81-52.
- Lee, K. C., J. L. Hansen, and D. C. Macauley, 1979. Predictive Model of the Time/Temperature Requirements for Thermal Destruction of Dilute Organic Vapors. 72nd Annual Meeting of the APCA. Cincinnati, OH.

Lee, K. C., N. Morgan, J. L. Hansen, and G. M. Whipple, 1982. Revised Model for the Prediction of the Time-Temperature Requirements for Thermal Destruction of Dilute Organic Vapors and its Usage for Predicting Compound Destructability. 75th Annual Meeting of the APCA, New Orleans, LA.

Parson, J. S. and S. Mitzner, 1975. Gas Chromatographic Method for Concentration and Analysis of Industrial Organic Pollutants in Environmental Air and Stacks. Env. Sci. Tech., 9, 1053.

Seeker, W. R. and M. P. Heap, 1982. Flame Combustion Processes. Volume II of Final Report for Contract EPA 68-02-2631.

Seeker, W. R., M. P. Heap, and T. J. Tyson, 1981a. Gas Phase Chemistry. Volume I of Final Report for EPA 68-02-2631.

Seeker, W. R., G. S. Samuelsen, M. P. Heap, and J. D. Trolinger, 1981b. The Thermal Decomposition of Pulverized Coal Particles. The 18th Symposium (International) on Combustion. The Combustion Institute, Pittsburgh, PA. p1213.

Semenov, N. N., 1935. Chemical Kinetics and Chain Reactions, Clarendon Press, Oxford, England.

Tsang, W. and W. Shaub, 1981. Chemical Processes in the Incineration of Hazardous Waste. National Bureau of Standards. Paper presented to American Chemical Society Symposium on Detoxification of Hazardous Wastes, New York, NY.

## APPENDIX A

### EXPERIMENTAL FLOW CALIBRATIONS

In this Appendix the techniques used to monitor the reactant flows to the microspray and turbulent flow experiments are discussed. In addition, the flow calibration procedures are described.

#### A.1 Microspray Reactor

Gas flows for the support flat-flame were monitored by Fisher-Porter rotameters. Calibration and use of all rotameters was at a constant 40 psig pressure, as indicated by gauges mounted at each rotameter outlet.

Rotameters were initially calibrated according to the procedures presented in the vendor literature. The air rotameter was of the viscosity compensated design, so calibration depends only on gas density. Air mass flow was obtained by:

$$\dot{m} = S \cdot \dot{m}_{\max} / 100 \quad (\text{A-1})$$

where  $\dot{m}$  = actual mass flow of air (gm/sec)

$S$  = rotameter scale reading (percent of maximum)

$\dot{m}_{\max}$  = mass flow at full scale reading (gm/sec)

The maximum mass flow is calculated from the operating gas density and the rotameter design parameters by:

$$\dot{m}_{\max} = \dot{m}_1 \sqrt{(\rho_f - \rho_2) \rho_2 / (\rho_f - \rho_1) \rho_1} \quad (\text{A-2})$$

where  $\dot{m}_1$  = rotameter maximum mass flow for air at 70 F and 14.7 psia, a published value (gm/sec).

$\rho_f$  = rotameter float density (for the stainless steel floats  $\rho_f = 8.02$  gm/cc).

$\rho_2$  = gas density at the operating condition (gm/cc).

$\rho_1$  = gas density at the standard handbook condition (gm/cc).

Thus, for the air rotameter the calibration condition requires only a density correction that can be calculated from the new pressure, temperature, and

molecular weight. The air calibration was verified by use of a calibrated dry test meter.

The nitrogen and hydrogen rotameters were of spherical float design so that gas viscosity became a calibration variable. These calibration procedures require the use of detailed correction charts and are relatively involved. Details can be found in the vendor literature. The flow characteristics were confirmed by bubble-flow meter measurements.

Liquid flow to the droplet generator was controlled by the pressure placed on the fuel reservoir. This pressure forced liquid through the orifice in the droplet generator. Thus, the pressure-flow relation can be expected to be governed by Bernoulli's equation:

$$\Delta P / \rho = V^2 / 2 \quad (A-3)$$

where  $\Delta P$  = fluid gauge pressure

$\rho$  = fluid density

$V$  = fluid velocity at orifice

This can be arranged to yield

$$\dot{m}_L = CD^2 \sqrt{\rho \Delta P} \quad (A-4)$$

where  $\dot{m}_L$  = liquid flow

$C$  = system constant

$D$  = orifice diameter

Because of manufacturing variations in the orifices and natural wear, the orifice diameter is not known well enough to directly use this equation. Rather, liquid flow was directly measured by timed collection and weighing and the relation was used to extrapolate between measured points and between liquids of differing density.

Dispersion gas flow for the droplet generator was measured by a small, in-line Dwyer rotameter.

## A.2 Turbulent Flow Reactor

Burner air flow was measured by a Barco 3-in. ID venturi.

A magnahelic gauge was used to indicate the pressure drop between the venturi taps. The calibration constant was obtained from the basic flow equations and was found to compare exactly with the manufacturers calibration curve. The calibration was:

$$Q_{air} = 44 \sqrt{\Delta P} \quad (A-5)$$

where  $Q_{air}$  = flow rate of burner air (standard cubic feet per minute).

$\Delta P$  = magnahelic reading (inches water).

A direct calibration check was not possible because of the high air flows. However, an indirect check was performed through burner stoichiometry measurements.

Burner fuel flow was set by the pressure on the fuel delivered to the nozzle. The mechanism governing flow was the same as for the droplet generator: pressurized fuel forced through an orifice. Thus, the controlling equation is identical to equation A-4. Because of manufacturing variations, each nozzle was calibrated at several pressures. The results were well described by Equation A-4, which was subsequently used to interpolate between calibrated points and to extrapolate the calibration to new fuels.

APPENDIX B  
ANALYTICAL TECHNIQUE FOR  
TEST COMPOUNDS

B.1 Introduction:

The Tenax-GC sampling/analysis technique was selected for the measurement of the test compound destruction efficiencies for the following reasons:

1. High Sensitivity: The minimum sensitivity of the technique has been experimentally determined to be about 1.5 ppb, which corresponds to ~99.995% DE for the turbulent flow reactor at nominal operating conditions. Direct grab sample/GC injection techniques are simpler and are more rapidly performed but cannot measure to 99.99 percent DE.
2. Simple Operation/Rapid Turnaround: The principal competing technique, XAD-2, requires chemical extraction of the sample, a concentration step for low concentration samples, and GC analysis. With the Tenax-GC technique the sample cartridge is placed directly in the GC, desorbed and analyzed in a single operation. Thus, sample turnaround can be as low as one hour.

There are two principal limitations on the technique as it is presently employed. First, the compounds can pass through the Tenax with only partial adsorption (volumetric breakthrough). This is a particular problem for compounds with molecular weights below 150. Since all the test compounds fall below this molecular weight limit, breakthrough volumes were carefully checked for each. In general, XAD-2 avoids this problem because of higher compound specific breakthrough volumes. Second, the use of packed columns for separation of test compounds on the GC reduces the resolution of separation. The typical peak width is such that the successful separation of more than five compounds can be difficult due to peak interferences.

The technique, in summary, consists of the adsorption of test compound from a known volume of sample gas onto cooled Tenax. At the conclusion of sampling the Tenax cartridge is placed in the carrier gas line upstream of a packed column. The cartridge is electrically heated and the trapped compounds

are desorbed into the carrier gas. The compounds are trapped at the upstream end of the room temperature packed column. After desorption is complete the column is temperature programmed, and the compounds are separated and analyzed by a flame ionization detector (FID). The system is calibrated in two ways. First, dilute concentrations of test compounds in air are prepared in an 11-liter dilution tank. This gas is sampled and analyzed by the Tenax technique as if it were a normal sample. Second, direct liquid injections of test compounds onto the GC column were performed with a microliter syringe; this bypassed the Tenax. Comparison of the results of the two techniques indicates the presence or absence of systematic calibration errors and indicates if volumetric breakthrough has occurred. The occurrence of volumetric breakthrough was further tested by placing two cartridges in series and determining if any compound appeared on the second cartridge during adsorption.

The following section describes the analytical equipment, the calibration tests, the operating procedures, and miscellaneous verification work.

## B.2 Analytical Equipment:

Sampling and Adsorption: The equipment is illustrated in Figure B-1. Exhaust gas samples were collected from the stack by an uncooled 6.35 mm OD (0.25-in.) stainless steel probe. After leaving the stack the probe was heat-taped and insulated to maintain a 200 C temperature. The sample passed through a filter (47 mm Geman ) in a 200 C oven. The hot sample stream passed through an externally water-cooled Tenax cartridge. The cartridge consists of a 120 mm long by 10 mm ID Pyrex tube packed with  $0.65 \pm 0.02$  grams of Tenax-GC (40-80 mesh). The adsorbant was held in place with small plugs of silianized glass wool. The sample line was connected to the cartridge by Ultra-Torr fittings. The entire cartridge was placed within a heat exchanger that flowed cooling water around the cartridge. The sample subsequently passed through a gas dryer, a rotameter, and a dry test meter. All connections upstream of the cartridge were either 316 stainless steel or 6.35 mm OD (0.25-in.) Teflon.

Desorption and Analysis: This system is based on a Perkin-Elmer Sigma-2 gas chromatograph with a Sigma-10 integrator/data station. The column is a 0.5-long, 3.18-mm OD (1/8-in.) Teflon tube packed with Porapak-Q. The 30 cc/min. carrier gas flow is maintained through the Tenax cartridge, the column,



B-3

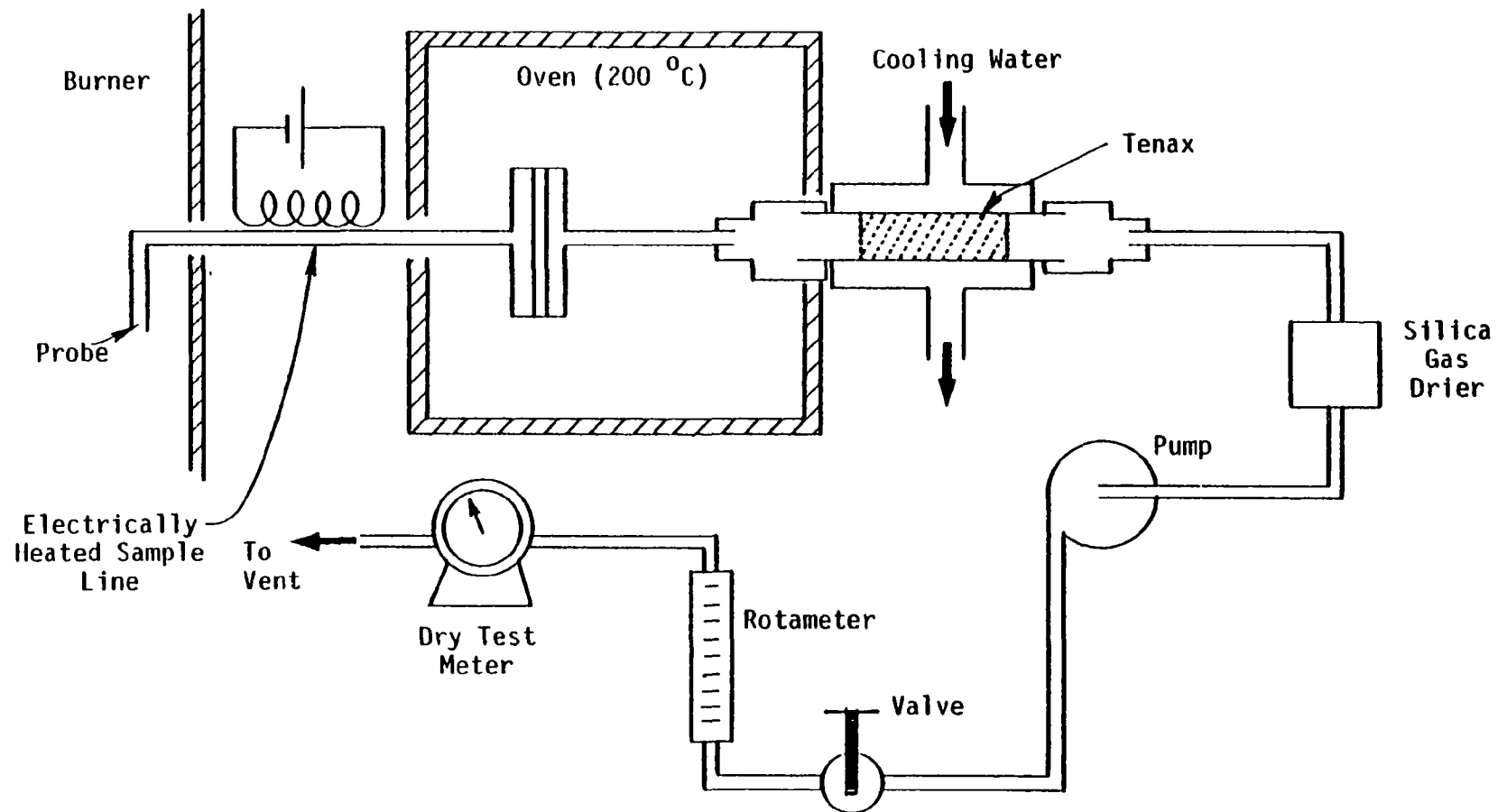


Figure B-1. Sampling and adsorption system.

and the FID, as shown in Figure B-2. The desorber is made from a 58-mm square aluminum block. The dimensions are detailed in Figure 8-3. Eight 500-watt electrical cartridge heaters are imbedded in the block. The voltage to these is controlled by a variable transformer.

### B.3 Operating Procedures:

Prior to use the Tenax cartridges are conditioned under a 20 cc/min. helium flow at 200 C for 45-min. Both before and after sampling the tube ends are covered with celophane and refrigerated.

After the reactor condition has been set the cartridge is placed in the adsorption train, the cooling water started, and the sample flow opened. A sample flow rate of 0.23 liters/min. has been found satisfactory as discussed below. At the conclusion of sampling (2.3-liters or 10-min.) the cartridge is removed and refrigerated.

For analysis, the cartridge is connected into the GC carrier gas line and placed in the desorption block. The block is raised to 120 C and held at this temperature for 5-min. This time and temperature have been found sufficient to quantitatively desorb all of the test compounds. During desorption the GC oven is maintained at room temperature. As the compounds desorb, they are collected at the inlet of the GC column. The compounds do not start to separate at room temperature. If this was not the case, peaks would be broadened by the deposition of newly desorbed compound at the column inlet after separation had started. At the conclusion of the 5-min. desorption time the column was heated to 120 C, held at this temperature for 25 min., and programmed at 5 C/min. to 150 C when samples containing heptane or No. 2 fuel oil were analyzed; or to 180 C for all other cases. Under the present analytical conditions, benzene and 1,2-dichloroethane have nearly identical retention times; because of this, these two compounds were never used in the same experiment. The FID gas flows were 71 cc/min. hydrogen and 442 cc/min. air.

The integrator output record consists of a chromatogram detector signal trace and a table of integrated peak areas. The trace is compared with the tabulated output to insure that the compound peaks are free of interferences, that the baseline boundary conditions were correctly constructed by the

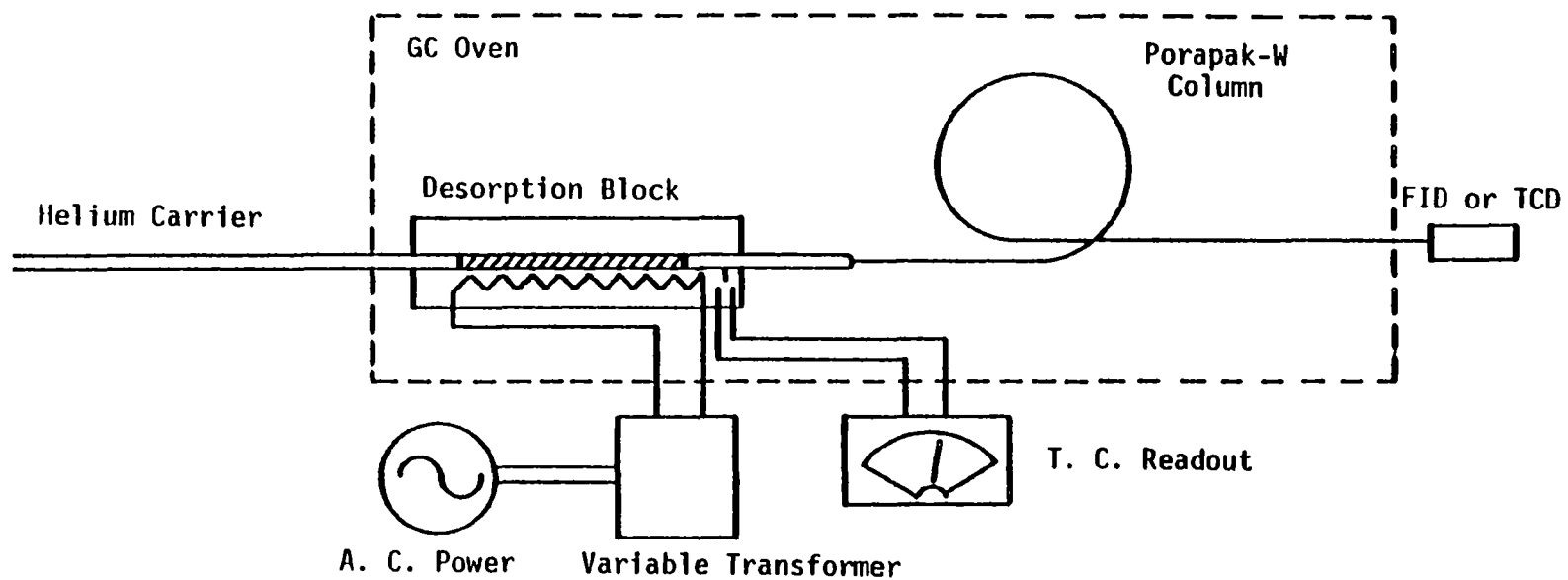


Figure B-2. Desorption and analysis equipment.

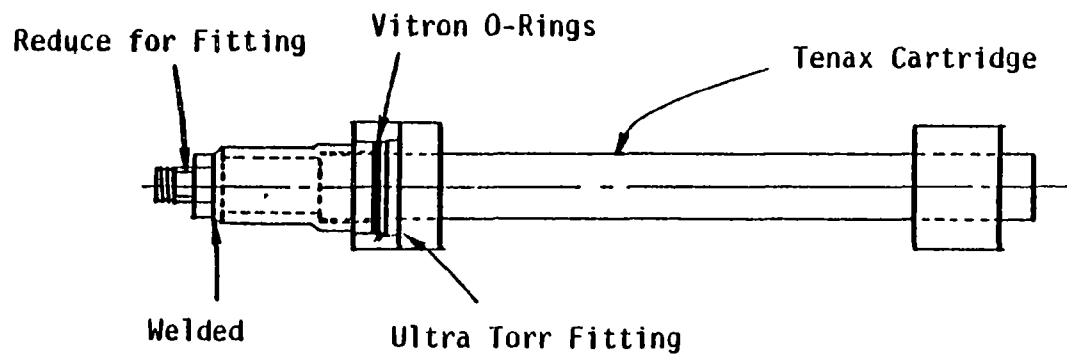
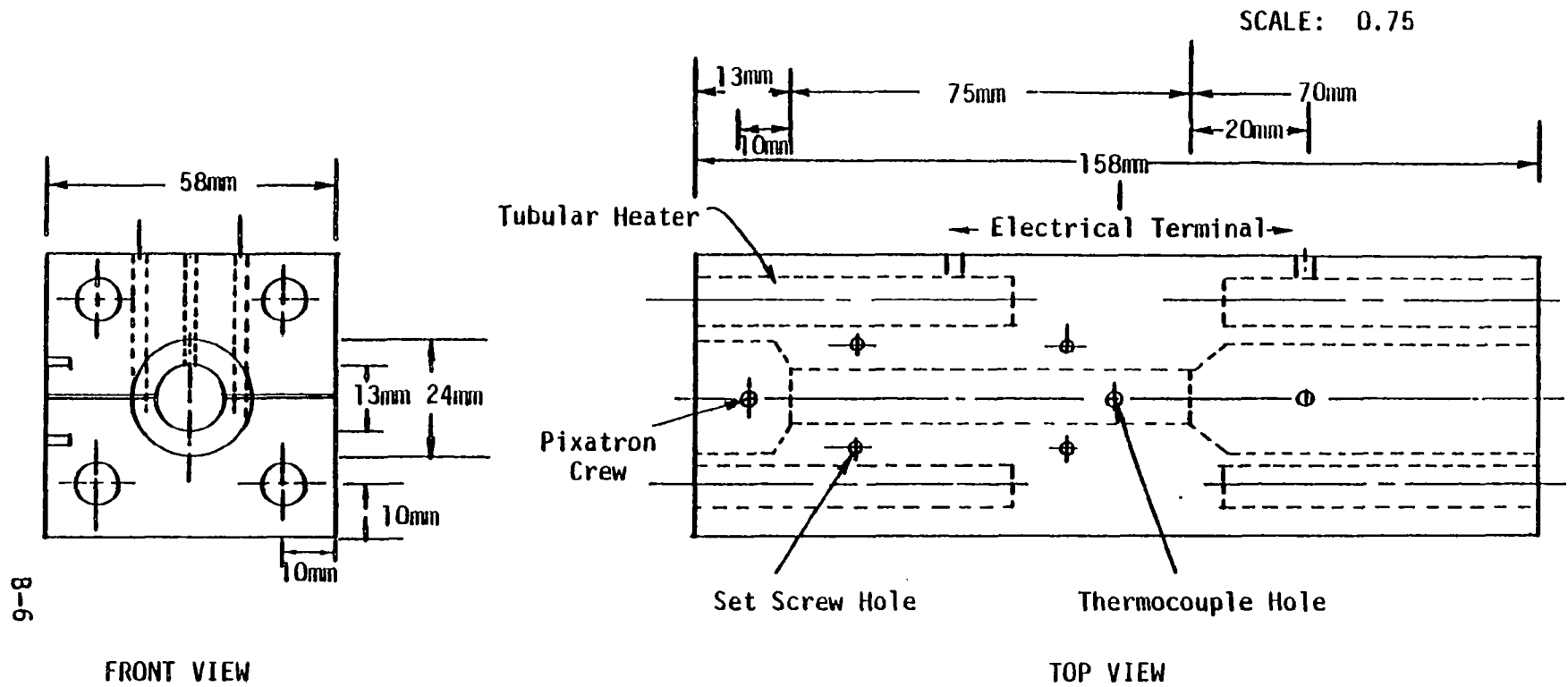


Figure B-3. Cartridge and cartridge heater detail.

integrator, and that the presence of unanticipated peaks could be noted. Integrated peak area values were converted into ppm by use of the calibration curves and destruction efficiencies were calculated using the ppm anticipated from zero destruction operation.

A potential problem with chromatogram interpretation was found in the study. Under some conditions unidentified peaks were found in the chromatograms in addition to those of the waste compounds. This raises the potential that peaks could be misidentified. This problem was aggravated by the fact that waste compound chromatographic retention times were dependent on compound concentration. In response to this problem, a procedure for interpreting chromatograms was developed.

During calibration a plot of liquid volume vs. retention time was prepared for each compound except chlorobenzene. Chlorobenzene was omitted because at its long retention time no potential interfering peaks ever appeared. This plot is shown as Figure B-4; it illustrates that retention time decreased with increasing compound concentrations. The following procedure was used to identify the peaks.

- A tentative peak identity assignment was made on each of the chromatograms.
- The tentative identity assignment was verified through comparison of measured peak area and retention time with Figure B-4.

With this procedure, the misidentification of a peak was possible only if both the area and the retention time of the unknown peak match the values shown in Figure B-4. While misidentification error is still possible, the use of Figure B-4 greatly reduces the likelihood of an actual occurrence.

In practice, few chromatograms caused any difficulty. Certain conditions caused gross flame inefficiency, as indicated by the presence of significant amounts of hydrocarbon fragments. These conditions were also characterized by low DE. Because of the interference between the hydrocarbons and the waste compounds, no quantitative results could be obtained. An example of a chromatogram from which no quantitative data were obtained is presented in Appendix D.

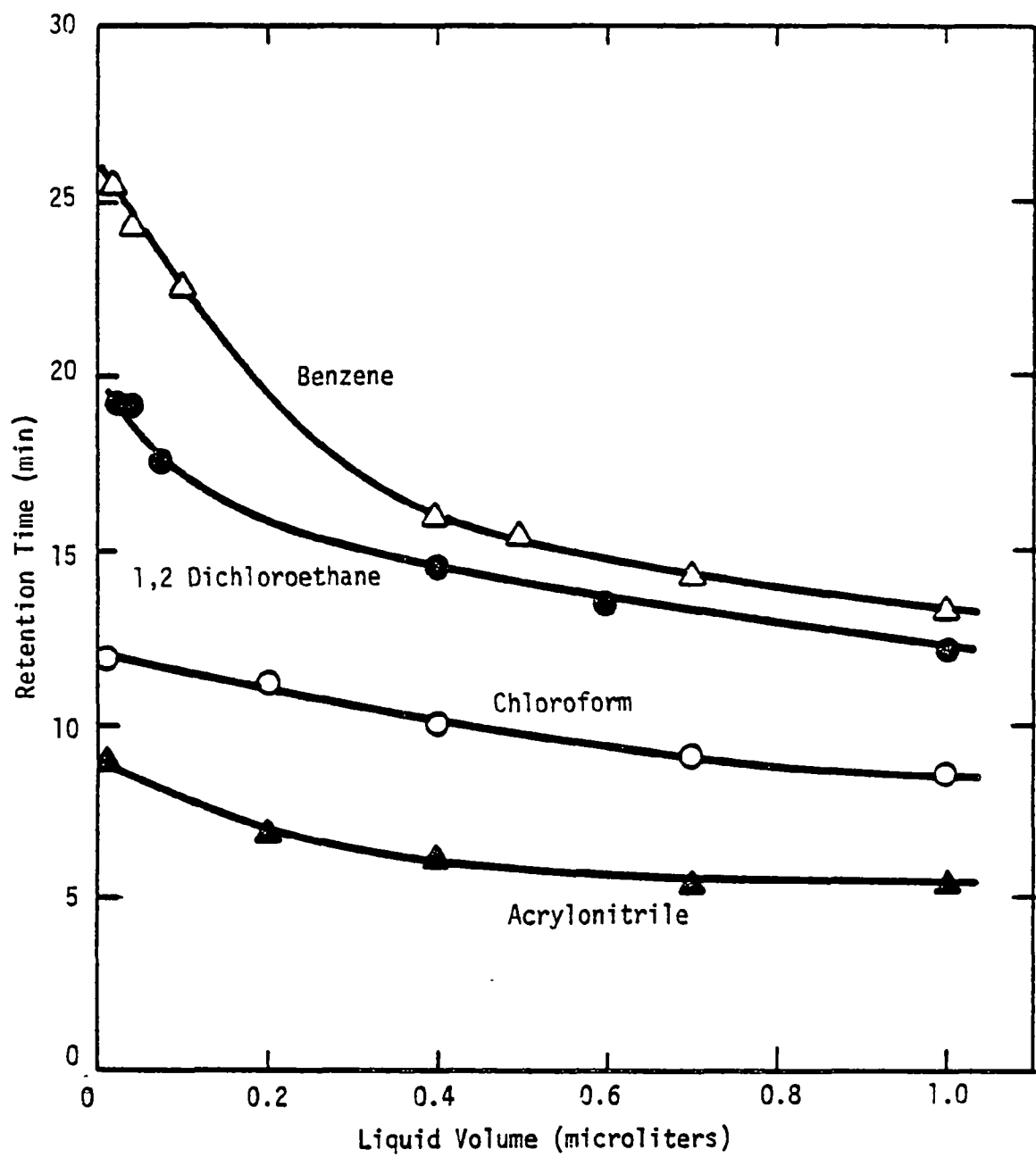


Figure B-4. Relationship between retention time and compound volume. Retention time is based on the time when the column oven first reaches 120°C.

#### B.4 Calibration Techniques:

Test compound calibration was performed by three independent procedures. This was necessary to determine the inherent scatter and reproducibility of the measurement technique, and to locate any systematic errors that appeared in any of the calibration tests. The three techniques were 1) direct syringe injection of test compound onto the GC column; 2) syringe injection of liquid test compound into a Tenax cartridge, followed by routine desorption and analysis; and 3) preparation of known standards in a dilution tank, followed by routine Tenax sampling and analysis of the tank contents.

Direct Column Injection: Liquid samples were withdrawn with a calibrated microliter syringe and directly injected onto the column through the injection septa. Chromatograph conditions were identical to the nominal operation procedure except:

1. The Tenax cartridge desorber was not a part of the system.
2. Rather than follow the prescribed oven temperature programming, an isothermal temperature of 120 C was used (except for chlorobenzene where 180 C was used). The isothermal temperatures increased the speed at which calibrations were performed. The programming is necessary during normal sampling to separate light hydrocarbons from the earliest test compound peaks. Because of the linearity of the FID amplifier, the change in temperature programming does not affect the calibration.

Table B-1 lists the FID mass sensitivity for the various compounds tested, relative to methane.

Syringe Injection Onto Tenax: Liquid test compound samples were directly injected onto packed Tenax cartridges. These were subsequently desorbed and analyzed. The results in the present study were used as an initial, qualitative test for breakthrough volume. After injection, helium was drawn through the cartridge. For some tests a second cartridge was placed behind the first. Breakthrough was detected by the appearance of test compound on the second cartridge and, simultaneously, by the loss of response from the analysis of the first cartridge.

TABLE B-1. MASS SENSITIVITY RELATIVE TO METHANE FOR THE FID

| Compound           | Relative Sensitivity | Compound            | Relative Sensitivity |
|--------------------|----------------------|---------------------|----------------------|
| Acrolein           | 0.54                 | Ethyl Acrylate      | 0.59                 |
| Phenol             | 1.22                 | Hexachlorobenzene   | 0.0                  |
| Benzene            | 1.23                 | Toluene             | 1.09                 |
| Carbon Disulfide   | 0.0                  | Vinyl Chloride      | 0.69                 |
| Acrylonitrile      | 0.59                 | Methyl Ethyl Ketone | 0.68                 |
| 1,2-Dichloroethane | 0.32                 | Chlorobenzene       | 0.77                 |
| Chloroform         | 0.09                 |                     |                      |



Dilution Tank: Dilute samples were prepared by evacuating an 11-liter glass tank and injecting a known amount of sample into the tank as the tank was rapidly repressurized. After repressurization the tank was allowed to equilibrate and the tank pressure and temperature were noted for calculation of the correct dilution factor. A portion of the tank contents are pumped through the Tenax sampling system. The remainder of the calibration test is identical to the normal sampling and analytical procedure.

#### B.4 Calibrations

Figures B-5 through B-11 show the calibration plots for 1,2-dichloroethane, benzene, chlorobenzene, chloroform, acrylonitrile, acrolein, and heptane. These are plotted as microliters liquid vs. integrator peak area. The two plots shown on each graph correspond to the direct injection calibration and the Tenax calibration. The close agreement between the two curves for all compounds except acrolein and heptane indicates that breakthrough volume was not exceeded for these compounds. This was confirmed by the absence of measurable test compound on the second cartridge. Acrolein and heptane both demonstrated significant breakthrough.

#### B.5 Optimization

The Tenax calibration apparatus was used to optimize the response with respect to total sample flow rate. In addition, the breakthrough volume for each of the test compounds was determined.

Flow Rate Optimization: Previous work with Tenax has indicated that maximum breakthrough volume is a function of sample flow rate. Either excessive or too-low flow can result in breakthrough. The experimental sample flow rate was selected for the present study by varying sample flow for a gas containing 45.8 ppm benzene and determining the fraction captured. The results are shown in Figure B-12 and indicate that 0.19 to 0.28 liters/min. sample flow optimizes capture.

Volumetric Breakthrough: The breakthrough of each compound was measured for the standard 0.23 liters/min. flow rate and 10-min. sampling period, and for 3.7 liters total volume. These results are shown in Table B-2 and indicate that only acrylonitrile and chloroform show significant breakthrough at

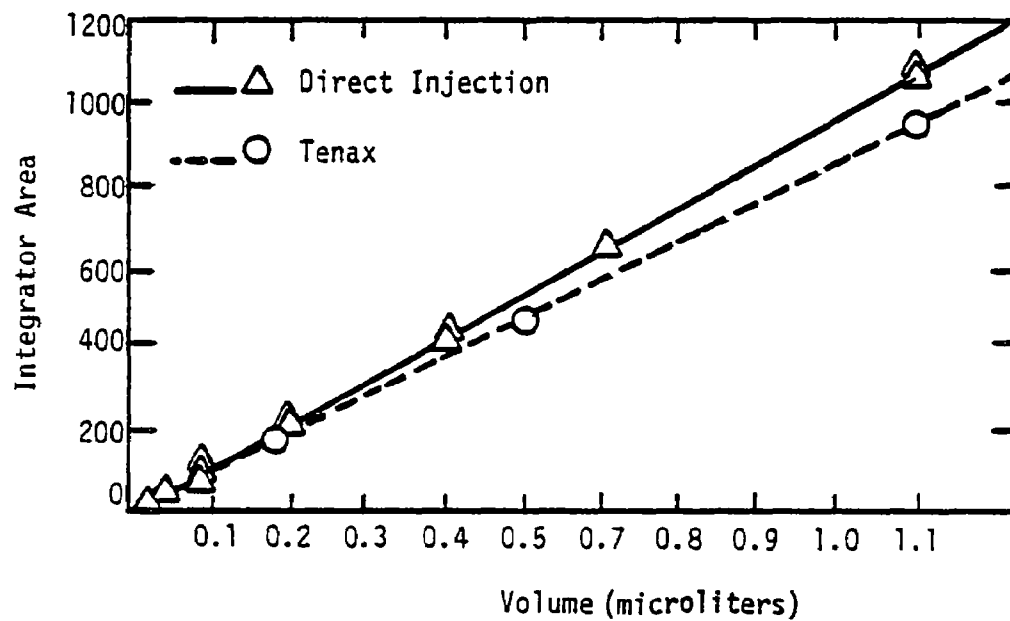


Figure B-5. Calibration curves for 1,2-dichloroethane.

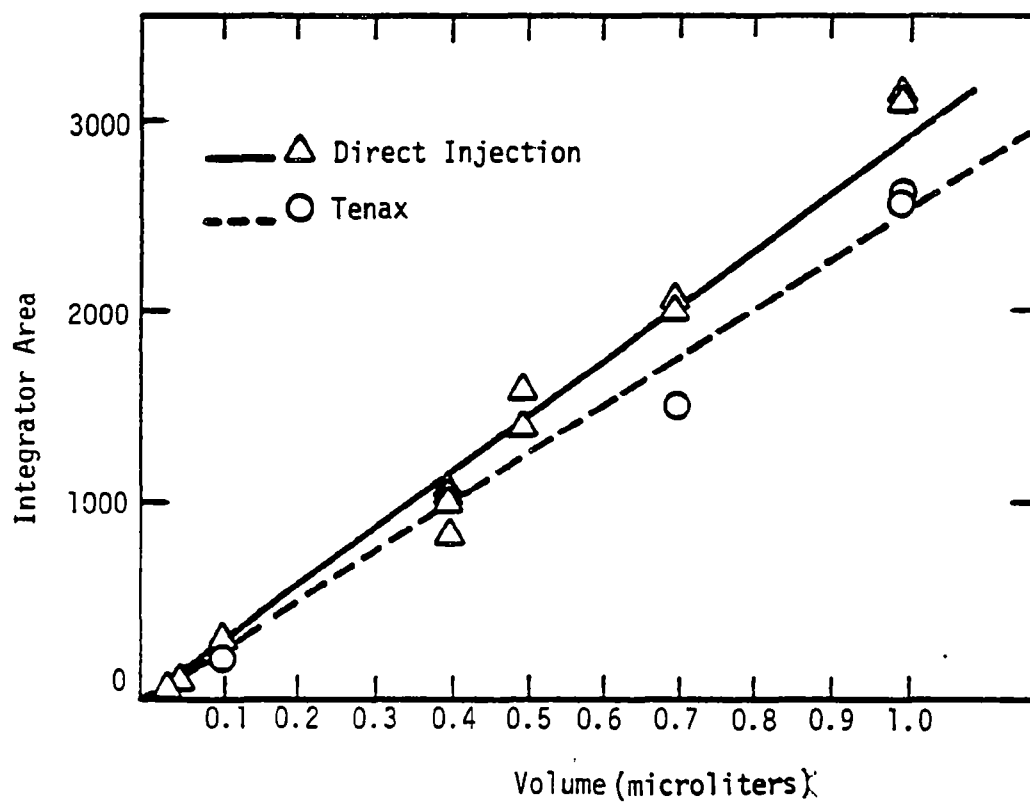


Figure B-6. Calibration curves for benzene.

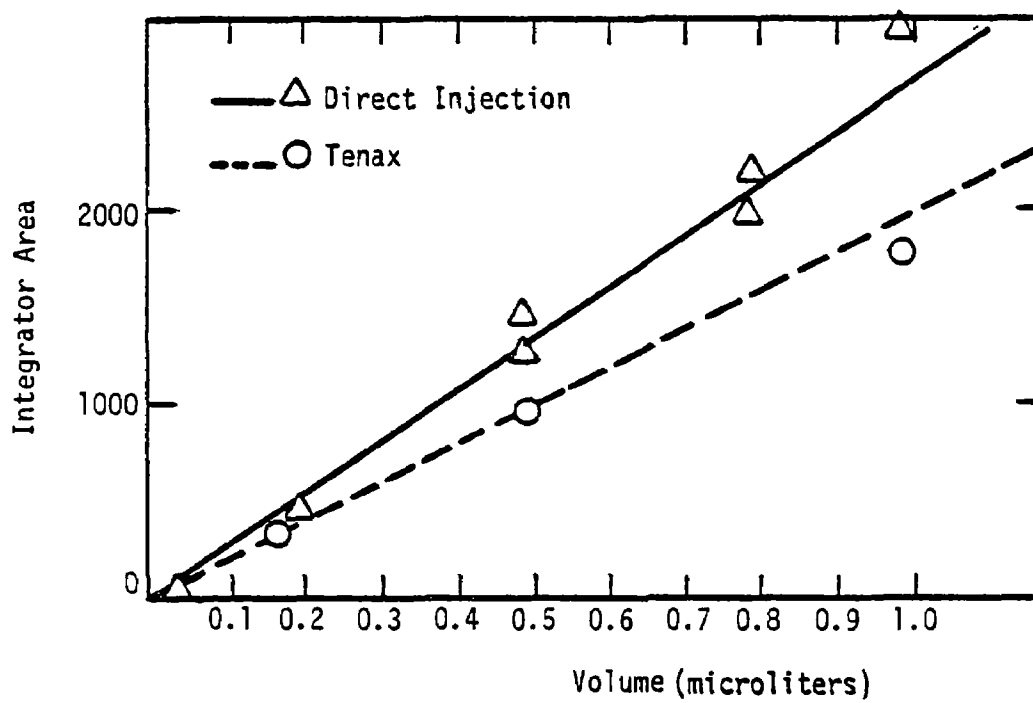


Figure B-7. Calibration curves for chlorobenzene.

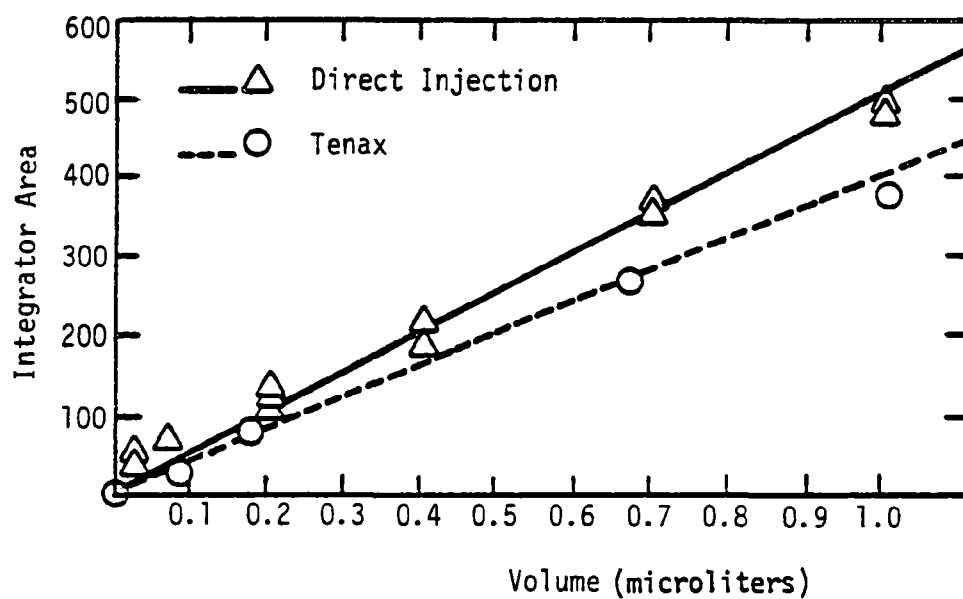


Figure B-8. Calibration curves for chloroform.

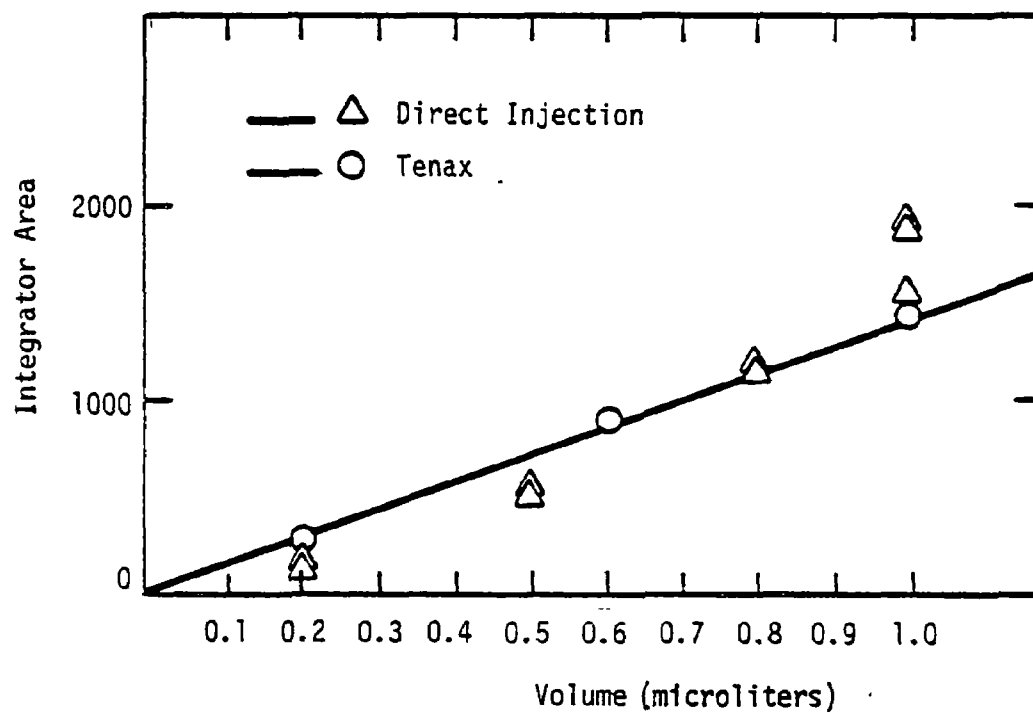


Figure B-9. Calibration curves for acrylonitrile.

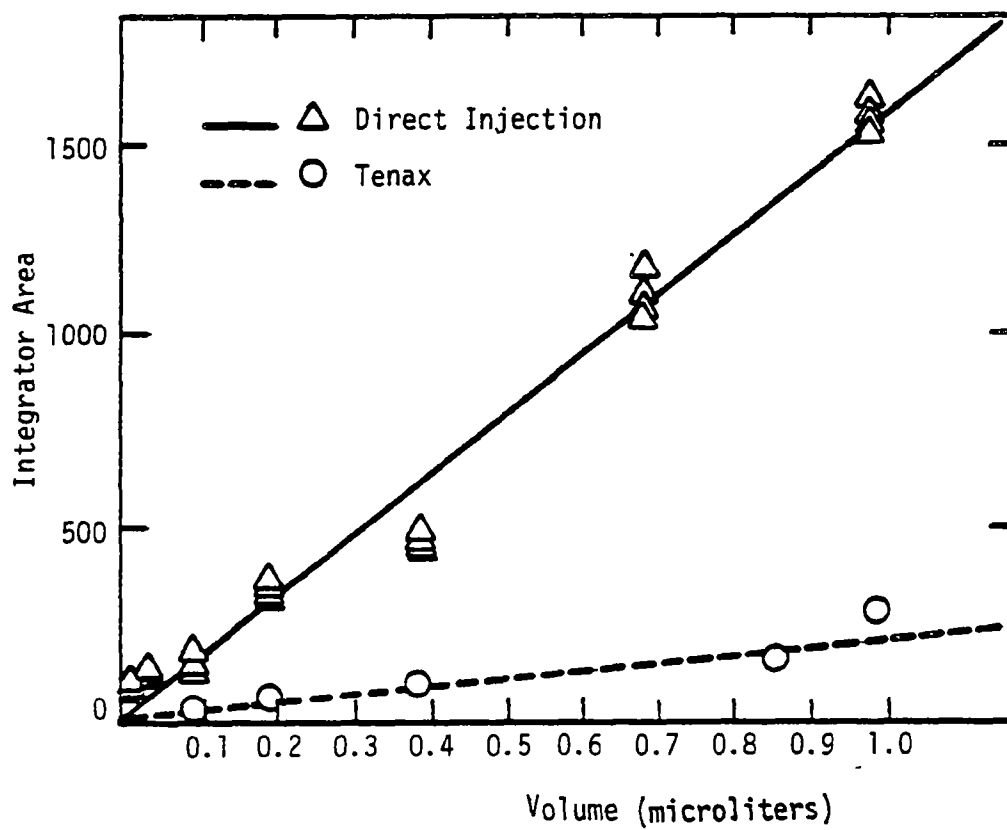


Figure B-10. Calibration curves for acrolein.

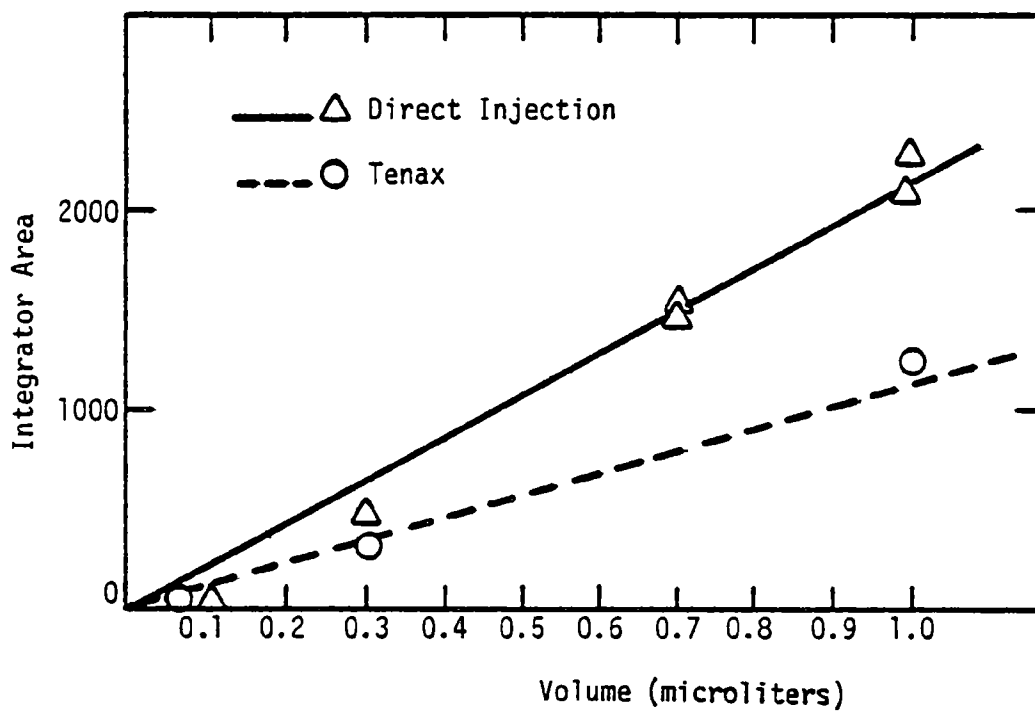


Figure B-11. Calibration curves for heptane.



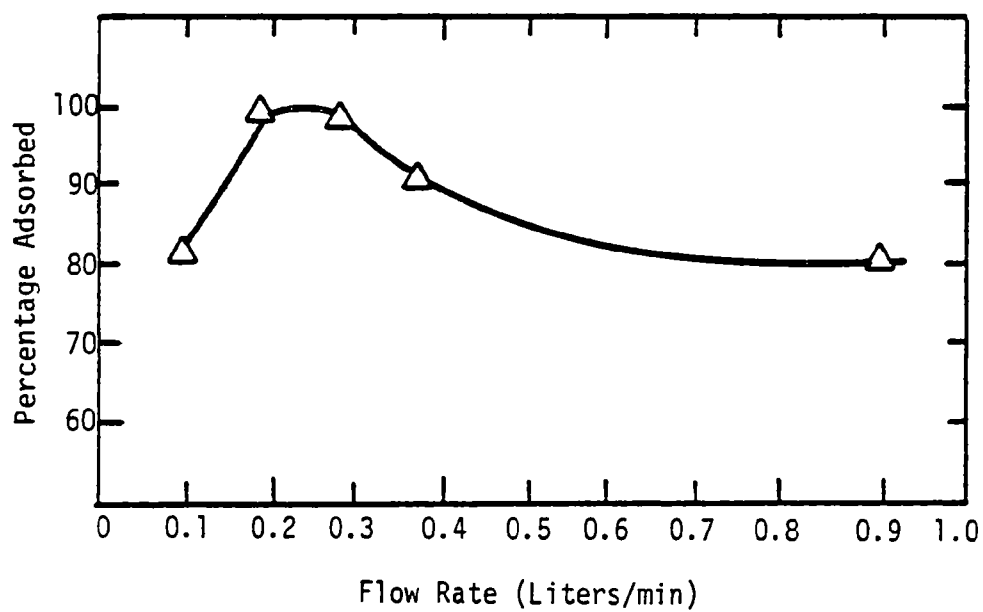


Figure B-12. Adsorption efficiency of a 45.8 ppm benzene stream onto Tenax as a function of flow rate.

TABLE B-2. VOLUMETRIC BREAKTHROUGH MEASUREMENT

| Compound           | Percent Breakthrough |                |
|--------------------|----------------------|----------------|
|                    | V = 3.7 Liters       | V = 2.3 Liters |
| Acrylonitrile      | 17.4                 | 0.4            |
| Benzene            | 0.05                 | 0.0            |
| Chloroform         | 3.40                 | 0.06           |
| Chlorobenzene      | 0.0                  | 0.0            |
| 1,2-Dichloroethane | 0.05                 | 0.0            |

Flow Rate = 0.23 liters/min.

Concentration = 100 ppm

3.7 liters, and at the normal 2.3-liter volume the maximum breakthrough for acrylonitrile was an insignificant 0.4 percent.

Sample Storage: Each GC analysis required about 1.5 hours. Thus, a backlog of unanalyzed samples occasionally accumulated. In no case was a sample held longer than 24 hours before analysis. However, a series of tests were performed to determine if 24 hours was a safe period for storage. A standard gas was prepared and adsorbed onto two cartridges in parallel. The first was analyzed immediately and the second was stored under nominal storage conditions for 24 hours and analyzed. The results, shown in Table B-3, indicate that no significant loss of test compound occurred. The scatter between the two analyses is typical of the measurement technique.

#### B.6 Uncertainty, Accuracy, and Precision

The problem of sample repeatability and precision really involves two questions:

- What is the repeatability of the analytical technique given a time-steady, known concentration to measure?
- What is the time-steadiness of the experiment, assuming a perfect measurement technique?

The first of these questions was addressed by the repeated analysis of known calibration standards. An example of such a series is shown in Table B-4 for benzene. The resulting standard deviation of the relative error is 2.1 percent. Thus, for the measurements to be accepted at the 90 percent confidence interval, the relative error is approximately  $\pm 4.2$  percent. The error for all calibration data as a group indicated an approximate  $\pm 5.0$  percent at the 90 percent confidence interval for the Tenax procedure.

The data indicate that the inherent time unsteadiness of the experimental DE measurements was small under nonoptimum conditions and substantial under optimum conditions. For the optimum conditions the observed time unsteadiness exceeded the  $\pm 5.0$  percent uncertainty associated with the analytical system and, thus, led to the conclusion that optimum DE measurements and rankings were random, time unsteady, and were probably related to the statistical nature of a turbulent flame. However, none of these optimum data

TABLE B-3. SAMPLE STORAGE STABILITY

| Compound           | Analysis           |                         |
|--------------------|--------------------|-------------------------|
|                    | Immediate<br>(ppm) | After 24<br>Hours (ppm) |
| Acrylonitrile      | 16.7               | 18.2                    |
| Chloroform         | 16.2               | 14.5                    |
| 1,2-Dichloroethane | 16.2               | 16.9                    |
| Chlorobenzene      | 8.77               | 9.5                     |

Table B-4 Calibration Repeatability Data for Benzene

| Response (peak area) |          | Relative<br>Error |
|----------------------|----------|-------------------|
| Expected             | Obtained |                   |
| 1141                 | 1101     | .0350             |
| 1141                 | 1126     | .0131             |
| 1470                 | 1399     | .0483             |
| 1470                 | 1451     | .0129             |
| 2129                 | 2090     | .0183             |
| 2129                 | 2138     | -.0042            |
| 3118                 | 3146     | -.00898           |
| 3118                 | 3153     | -.0112            |
| 3118                 | 3136     | -.0058            |

were used to establish the ranking presented in this study.

For nonoptimum conditions, the DE measurements and rankings were repeatable. One example of a direct repeat is found in Figure 1-4. The two data sets shown in the neighborhood of 150 percent theoretical air are a direct repeat at identical experimental conditions. They were separated by a small amount during plotting for clarity. This repeat demonstrates that nonoptimum rankings were repeatable.

A further means of evaluating the repeatability of nonoptimum rankings is to compare the rankings for different data points within identical failure condition. For example, Figure 1-6 shows data for off-design nozzle operation. Both sets of rankings (210 and 315 percent theoretical air) show the same ranking for this failure condition. Figure 1-7 demonstrates another example in which the rankings from two individual data sets agree for the failure condition caused by the quench coil.

It was recognized that an unqualified presentation of a ranking list was unsatisfactory in that it fails to delineate the quantitative "closeness" of compounds ranked consecutively. Thus, the rankings were summarized in bar graph form, of which Figure 1-8 is an example. These figures give a quantitative indication of both the ranking order, and the relative spread separating the compounds. The analytical uncertainty in the ranking figures has been found to be  $\pm 5$  percent. The repeatability of the experimental conditions was not statistically established, although the limited direct repeat data indicate that approximately a  $\pm 10$  percent confidence interval can be placed on each of the bar graphs.

## APPENDIX C

### THERMAL DECOMPOSITION MODEL

The model was designed to account for behavior in the Microspray Reactor that resulted from the simultaneous evaporation of test compound droplets, and the thermal destruction of the vapor.

Droplet evaporation is governed by the rate of heat transfer to the droplet. The rate of heat flow to a sphere is:

$$q = hA_D (T_\infty - T_{BP}) \quad (A-1)$$

where  $q$  = heat flow, cal/sec,

$h$  = heat transfer coefficient, cal/cm<sup>2</sup>-sec-K,

$A_D$  = droplet surface area =  $\pi D_D^2/4$  where  $D_D$   
is the droplet diameter, cm.

$T_\infty$  = free stream temperature specified from microspray thermocouple measurements, K.

$T_{BP}$  = boiling point of the droplet liquid.

Thus, the evaporation rate for an individual droplet is Equation (A-1) divided by the latent heat of vaporization, and the evaporation rate per unit volume can be obtained by multiplying by the number of droplets per cubic centimeter:

$$Q = \frac{nh\pi D_D^2 (T_\infty - T_{BP})}{4H} \quad (A-2)$$

where  $Q$  = the evaporation rate, gm/cm<sup>3</sup> - sec

$n$  = droplets/cm<sup>3</sup>

$H$  = latent heat of vaporization, cal/gm.

The heat transfer coefficient is related to the droplet Nusselt number by:

$$h = Nu k_H / D_D \quad (A-3)$$

where  $Nu$  = Droplet Nusselt number  $\cong 2$

$K_H$  = gas film heat transfer coefficient, cal/cm-sec-K.

This is substituted into Equation (A-4) to yield:

$$Q = \frac{nk_H\pi D_D (T_\infty - T_{BP})}{2H} \quad (A-4)$$

The reaction equation is essentially a conservation equation for vapor phase compound that relates the source term from vaporization and the sink term due to reaction to the change in concentration as the gas moves through the burner. The equation is

$$V \frac{dC}{dx} = Q - kC \quad (A-5)$$

where  $V$  = gas velocity, cm/sec

$C$  = vapor concentration of compound, gm/cm<sup>3</sup>

$k$  = reaction rate coefficient, sec<sup>-1</sup>.

Substituting Equation (A-4) into (A-5) and dividing by  $V$ , the equation can be cast into the functional form:

$$\frac{dC}{dx} = F(C,x) \quad (A-6)$$

A companion equation for droplet evaporation can be obtained from (A-4):

$$\frac{dC_1}{dx} = Q = G(x) \quad (A-7)$$

where  $C_1$  = the equivalent concentration of unevaporated material, gm/cm<sup>3</sup>,

$F, G$  are the functional forms defined by Equations (A-5) and (A-4), respectively.

Equations (A-6) and (A-7) are numerically integrated subject to the following constraints:

1. Initial conditions:  $C(0) = 0$

$C_1(0)$  = equivalent inlet spray concentration.



2. Constants:  $n$  = estimated from experimentally observed spray shape.  
 $k_H$ ,  $H$ ,  $T_{BP}$ ,  $V$  are assumed constant.  
 $T_\infty$  = a known function of  $X$  determined from thermocouple measurements in the absence of spray.  
 $k$  = evaluated from thermal decomposition data and the local value of  $T_\infty$ .

3. Droplet diameter: This is related to  $C_1$  through:

$$D_D = \left[ \frac{6C_1}{\rho \pi} \right]^{1/3}$$

4. When  $C_1$  reached zero (all liquid evaporated) the problem was reduced to integration of (A-5) with  $Q = 0$ .

The specific model output was a profile of fraction feed evaporated and fraction feed reacted as a function of  $X$ . The model was used to examine the effect of droplet diameter, temperature profile, and compound type on stack gas concentration. An example of output is shown in Figure C-1. The following points are noted:

- The droplets are completely evaporated by one-cm into the reactor.
- Because of the declining temperature the reaction essentially ceases after about 20 cm so that the reaction extent is unchanged over the final 80 cm of the reactor.
- The exit concentration (at 100 cm = 0.77) was identified by the entrance plane or gas flame temperature (900 K) when these results were plotted as a single point on Figure 3-5.

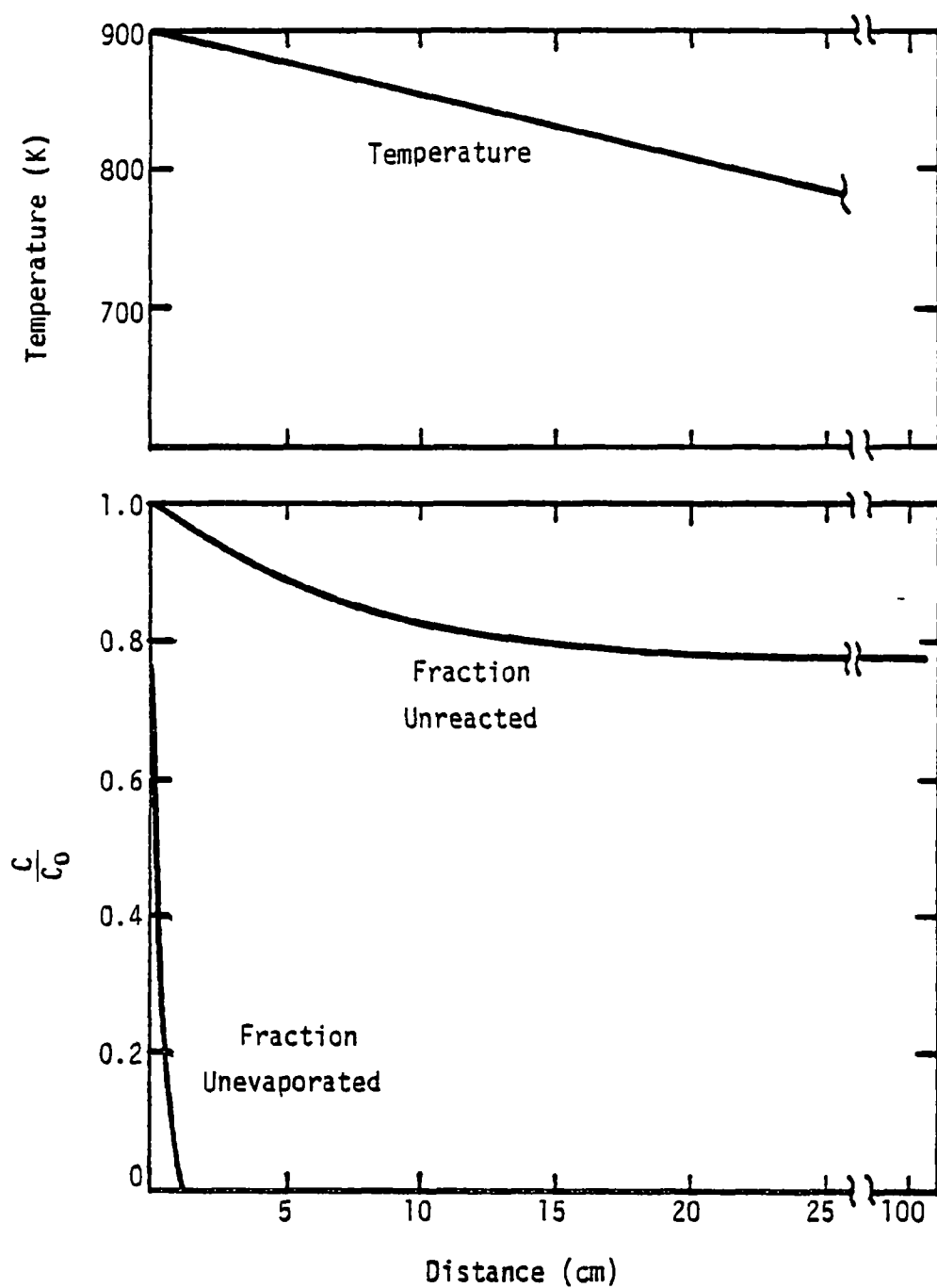


Figure C-1. Typical model output.

## APPENDIX D

### RAW DATA

This section presents the raw test compound data and describes the procedure for converting the raw data into destruction efficiencies for the two experiments.

#### D.1 Sample Chromatograms

A selection of chromatograms typical of various microspray and turbulent slow reactor conditions are presented below. Figure D-1 shows a relatively high efficiency microspray condition with few identifiable peaks. The numbers printed next to each peak are the retention times in minutes. A typical moderate efficiency microspray condition is shown in Figure D-2. A chromatogram typical of high-efficiency turbulent flow reactor operation is shown in Figure D-3. Few peaks are present and only one peak, associated with a fuel fragment at 45.18 min. is measurable. Figures D-4 and D-5 show chromatograms for moderate DE heptane fueled turbulent flow reactor data in which the test compound mixture contained benzene and 1,2-dichloroethane, respectively. A low-DE turbulent flow chromatogram is shown in Figure D-6. At very low efficiency operating conditions significant quantities of fuel and fuel fragments are released by the flame in addition to the test compounds. These conditions can result in an uninterpretable chromatogram, as shown in Figure D-7.

#### D.2 Calculation Procedures

Chromatogram peak areas were related to moles for each compound by use of the calibration figures in Appendix B. This number is converted into mole fraction based on dry gas by:

$$\text{Mole Fraction (dry)} = \frac{(\text{moles compound}) (24.63 \text{ liters/mole})}{(\text{sample volume} - \text{liters})} \quad (\text{D.1})$$

The mole fraction water in the wet combustion gas is estimated from a

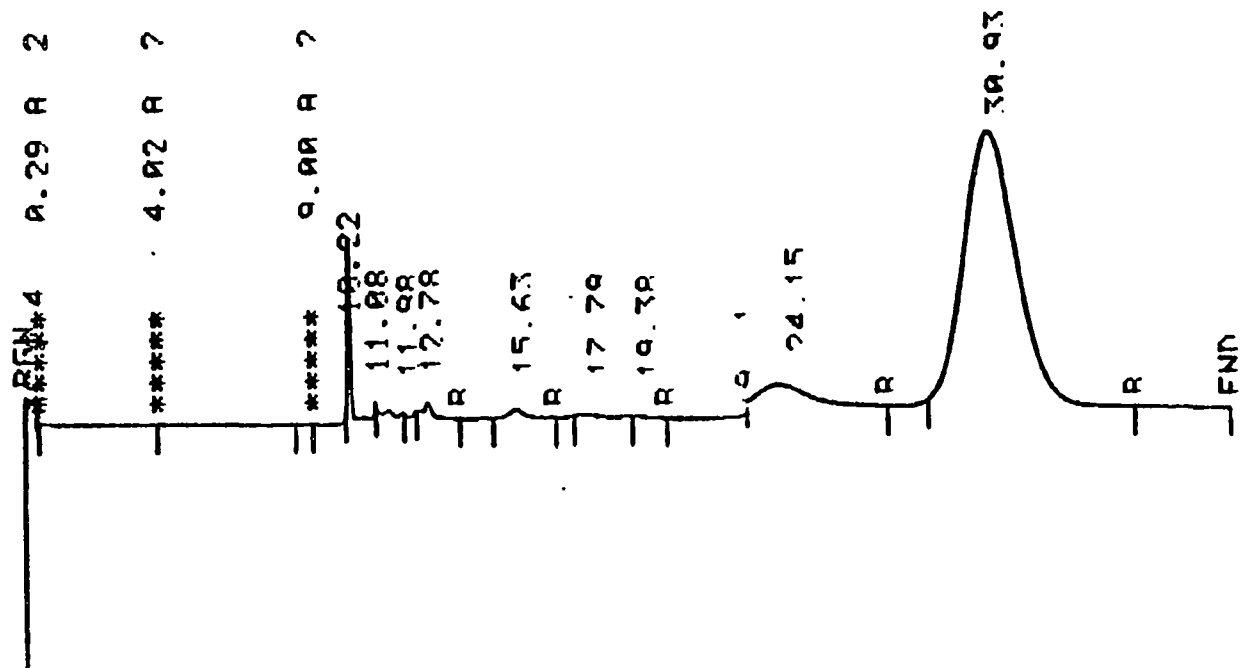


Figure D-1. Chromatogram for a high-DE microspray condition.

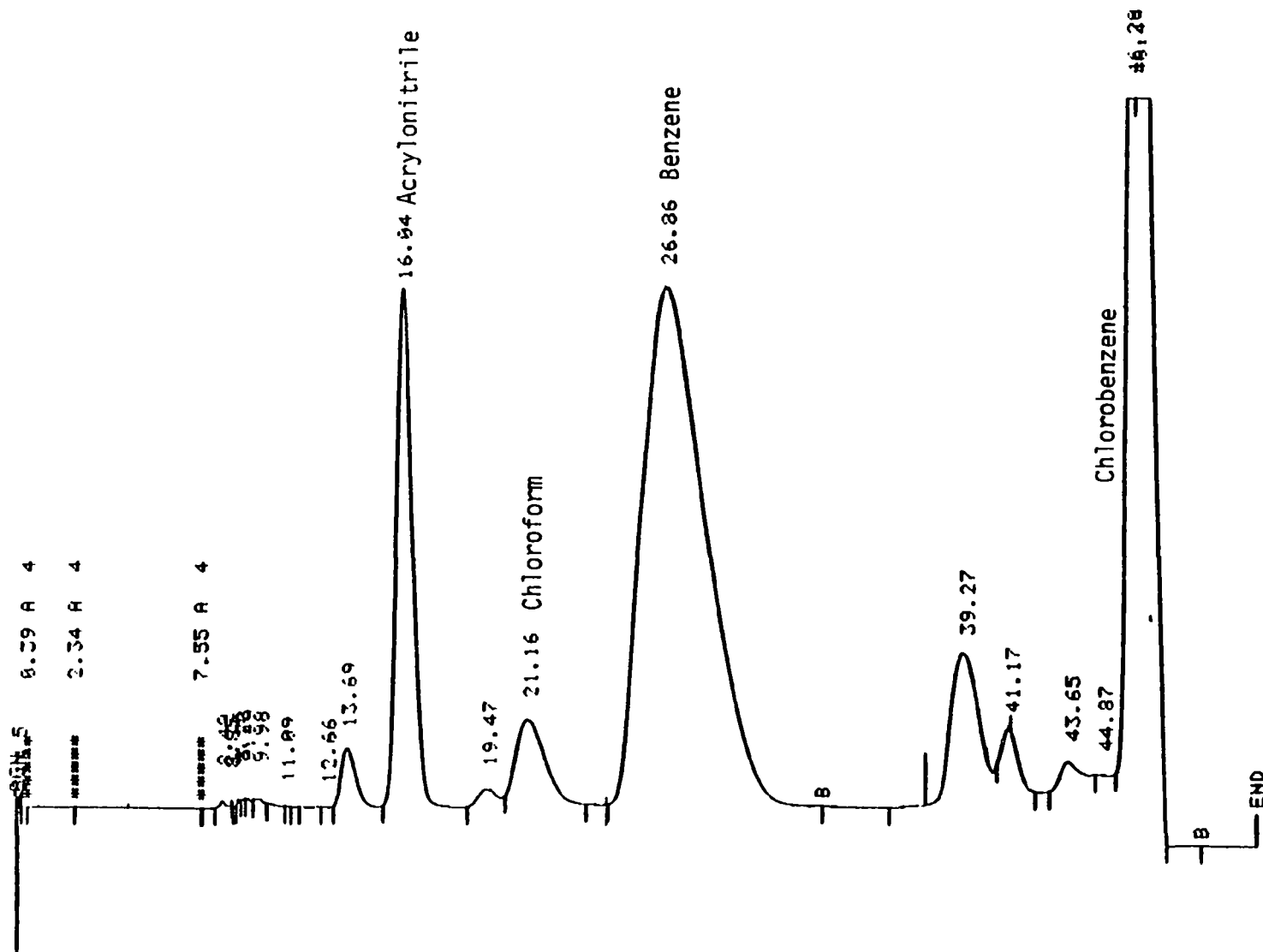


Figure D-2. Chromatogram for moderate-DE microspray condition.

D-4

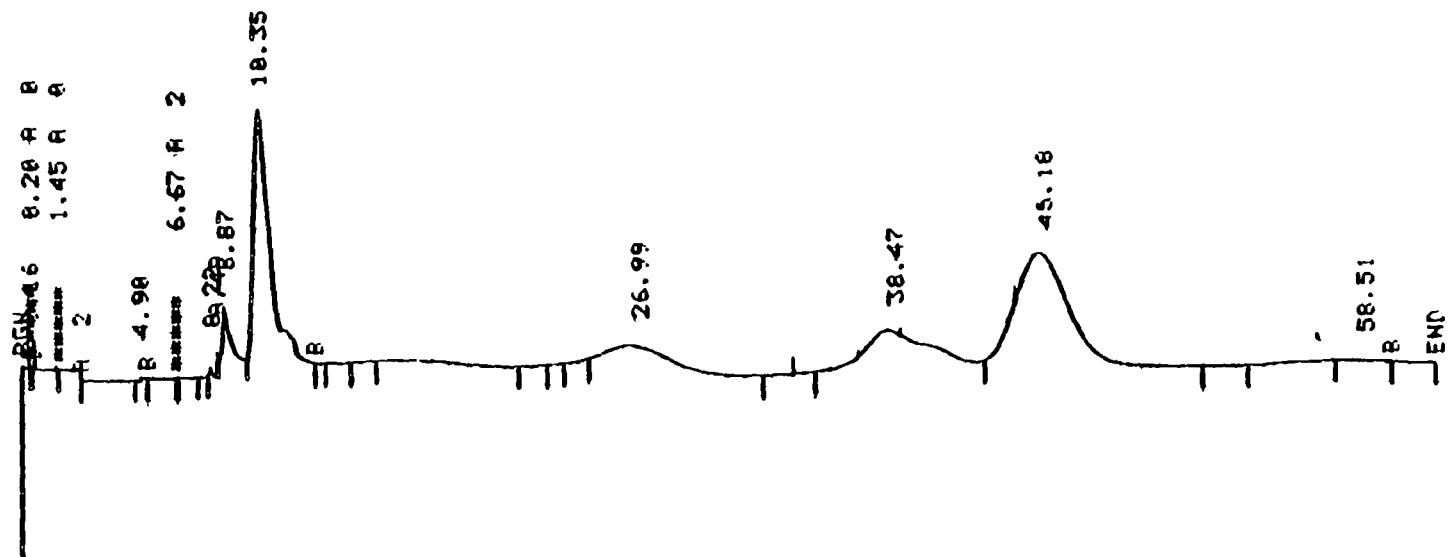


Figure D-3. Chromatogram for a high-DE turbulent flow reactor condition.

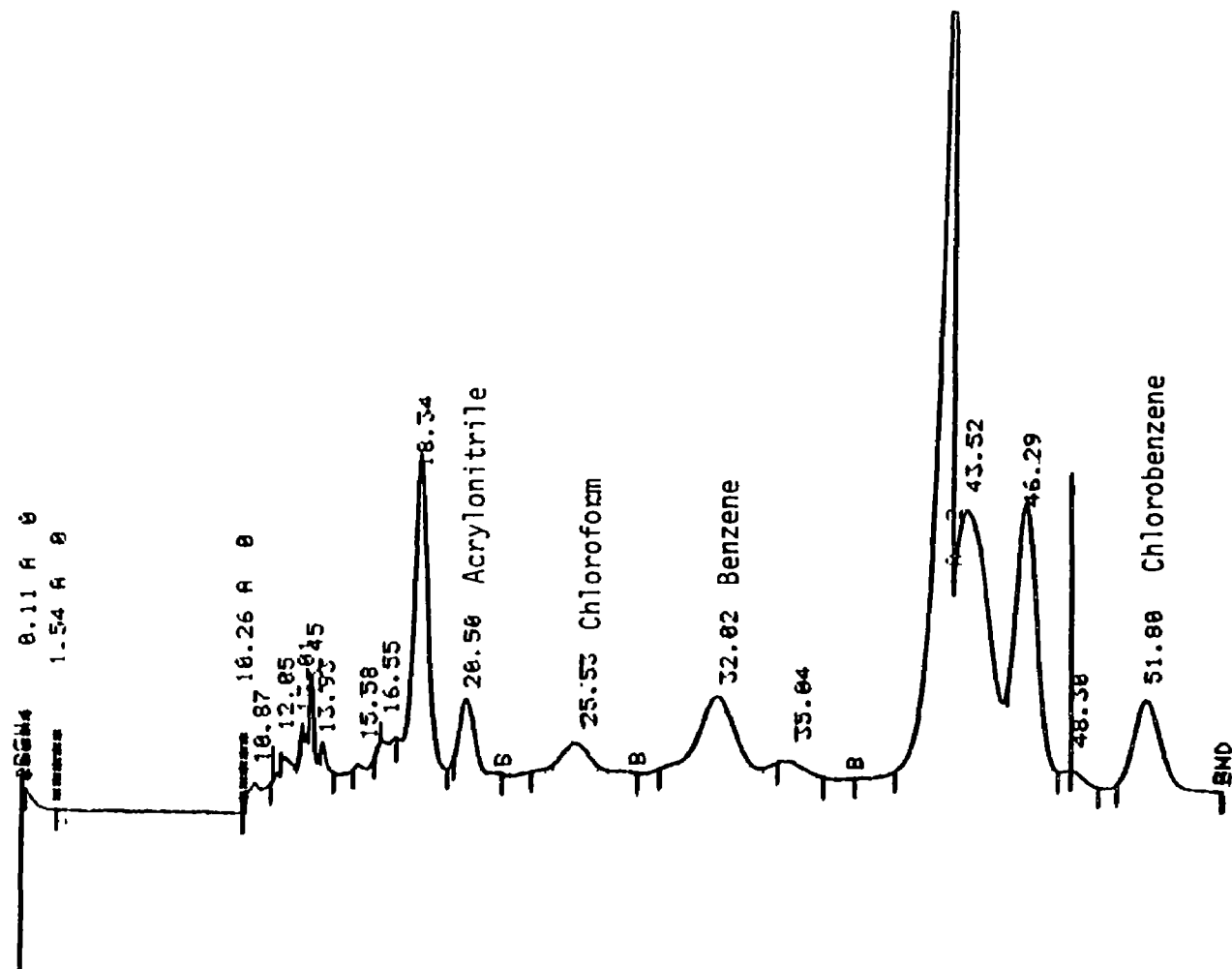


Figure D-4. Chromatogram for moderate-DE heptane-fueled turbulent flow reactor condition.

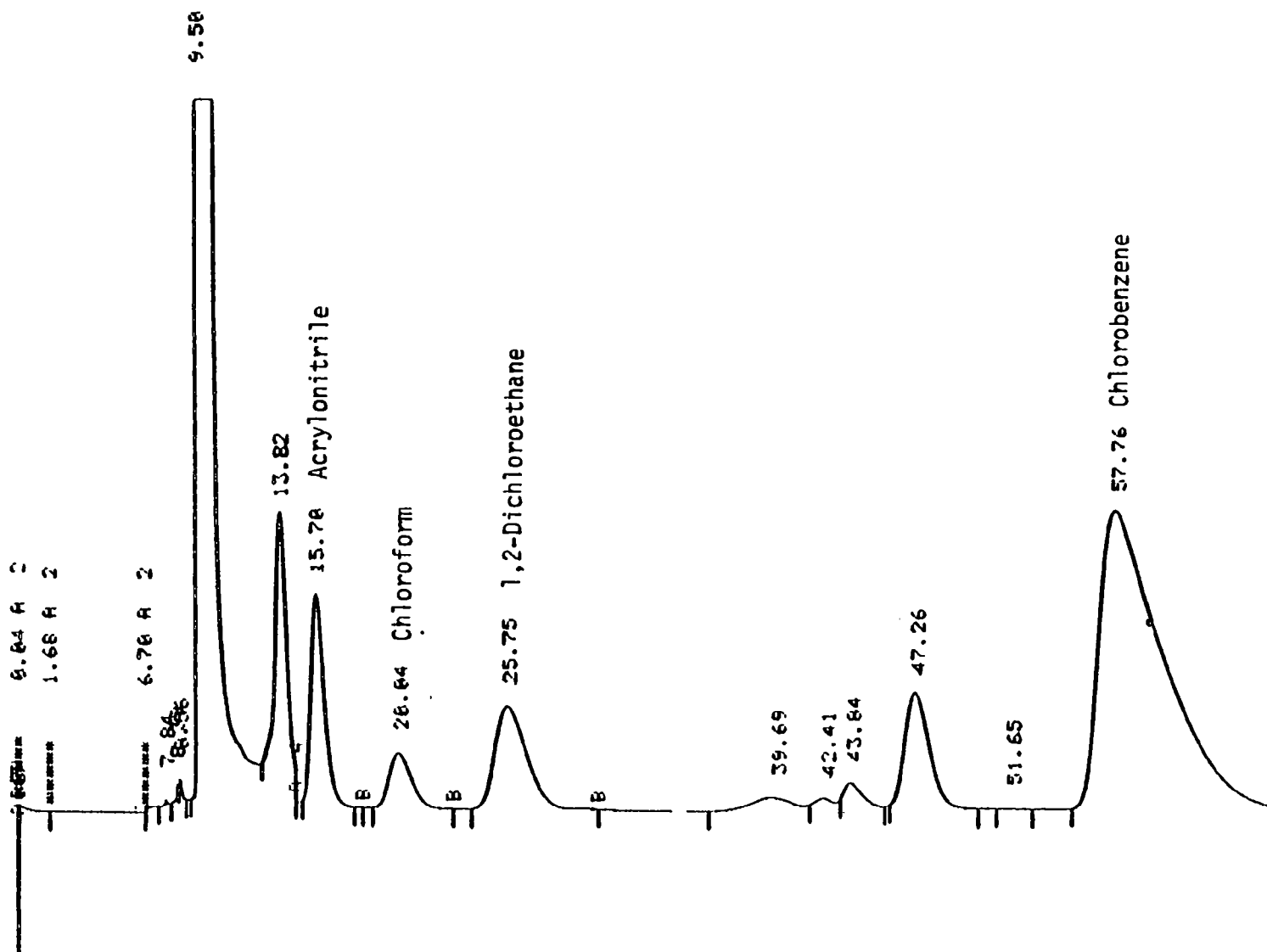


Figure D-5. Chromatogram for moderate-DE No. 2 oil-fired turbulent flow reactor condition.



L-0

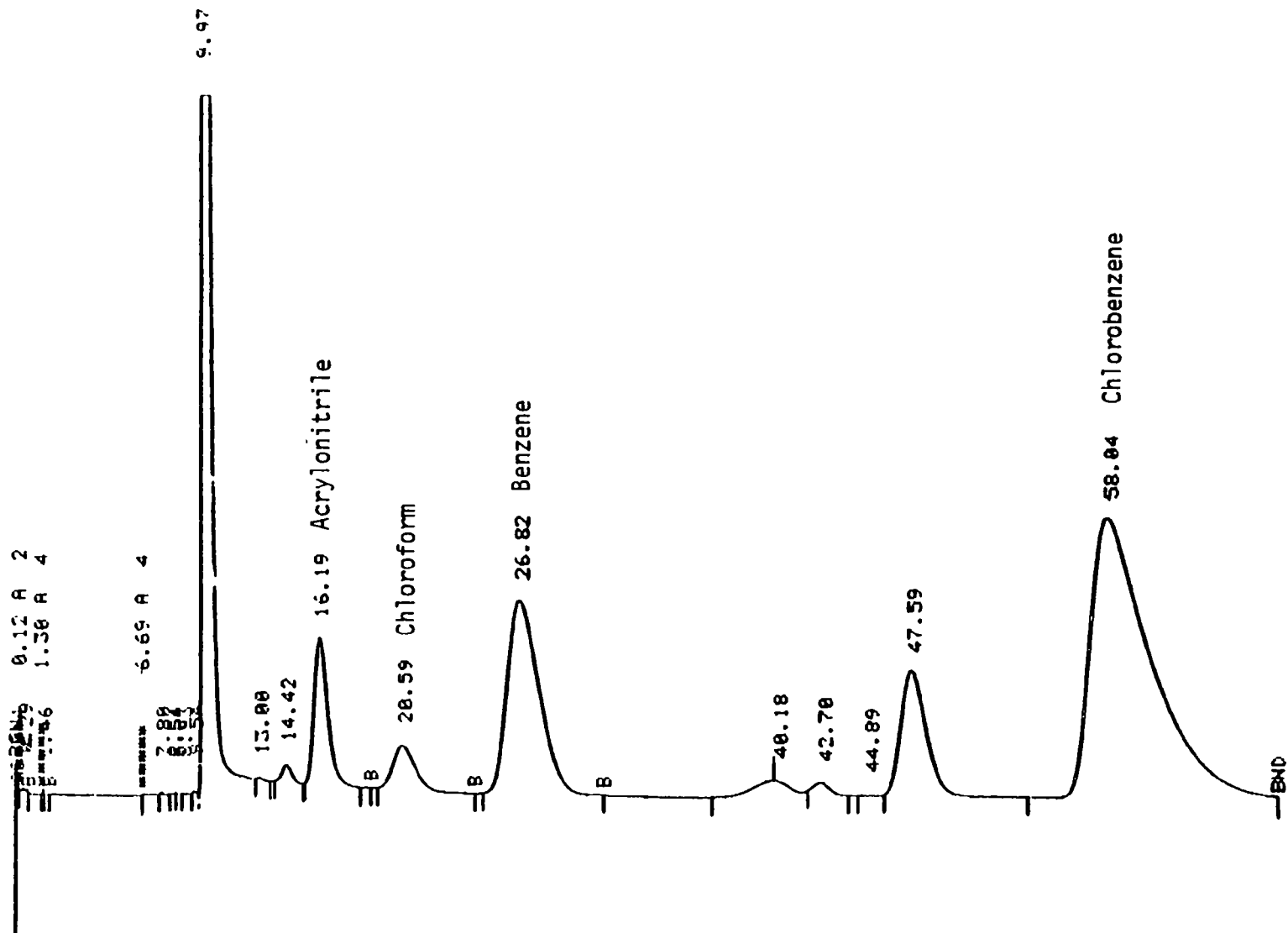


Figure D-6. Chromatogram showing a poor-DE turbulent flow reactor condition.

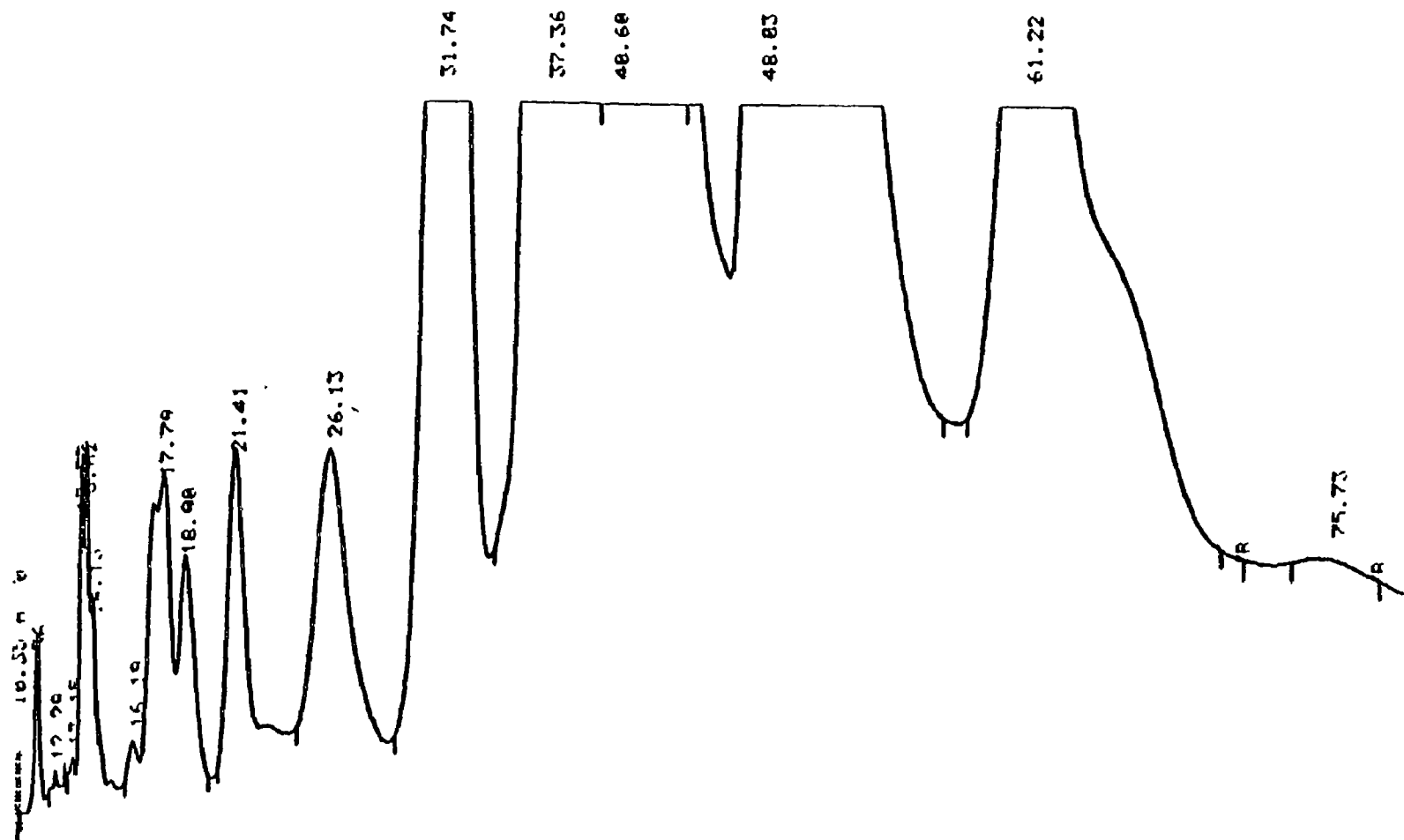


Figure D-7. Chromatogram showing very low efficiency turbulent flow reactor operation with significant fuel fragments present.

complete combustion model and the dry mole fractions are corrected to burner (wet) mole fractions by:

$$\text{Burner Mole Fraction} = (\text{Dry Mole Fraction}) - (1 - \text{Water Mole Fraction}) \quad (\text{D.2})$$

The mole fraction of compound that would be present at the burner exit if efficiency were zero is calculated by:

$$\frac{\text{Zero Efficiency Mole Fraction}}{\text{Mole Fraction}} = \frac{(\text{Fuel Flow}) (\text{Moles Compound/Mass Fuel})}{\text{Total Reactor Molar Flow}} \quad (\text{D.3})$$

The (Moles Compound/Mass Fuel) is calculated from the fuel mixture composition and the (Total Reactor Molar Flow) is calculated from the fuel flow, the air flow, and the complete combustion model. The fraction unreacted compound is the ratio of Equation D-2 and D-3.